

NBER WORKING PAPER SERIES

DIGITAL MEDIA MERGERS:
THEORY AND APPLICATION TO FACEBOOK-INSTAGRAM

Justin Katz
Hunt Allcott

Working Paper 34028
<http://www.nber.org/papers/w34028>

NATIONAL BUREAU OF ECONOMIC RESEARCH
1050 Massachusetts Avenue
Cambridge, MA 02138
July 2025

We thank Guy Aridor, Susan Athey, Emilio Calvano, Francesco Decarolis, Matt Gentzkow, Brett Gordon, Hong Jin, Garrett Johnson, Brian O’Kelley, Ariel Pakes, Marc Rysman, Carl Shapiro, Nils Wernerfelt, and seminar participants at the Knight-Georgetown Institute’s DMA and Beyond Conference, the 2024 NBER Winter Digitization meeting, the 2024 NBER Summer Institute IO meeting, Ofcom, Stanford-Berkeley IOFest, and UC San Diego for helpful comments. We are grateful for the research assistance of Levi Kiefer, Zimei Xia, Aava Farhadi, and Jenna Bowsher. We thank Ariel Azia, Lewis Jennings, Devendra Wagh, and Dionisis Kintos at Similarweb for providing Facebook and Instagram ad load statistics. Similarweb’s website is www.similarweb.com. Replication files are available from allcott.stanford.edu/research. Disclosures: Allcott and Katz were both previously employed by Microsoft Research, Allcott has previously done consulting on matters related to social media (but not related to FTC v. Meta), and Allcott is one of the (unpaid) researchers on Meta’s 2020 Facebook and Instagram Election Study. Neither author has any consulting work or other conflict of interest related to the topic of this paper. Katz acknowledges funding support from The Institute of Consumer Money Management (ICMM) Pre-doctoral Fellowship on Consumer Financial Management, awarded through the National Bureau of Economic Research. The views expressed herein are those of the authors and do not necessarily reflect the views of the National Bureau of Economic Research.

NBER working papers are circulated for discussion and comment purposes. They have not been peer-reviewed or been subject to the review by the NBER Board of Directors that accompanies official NBER publications.

© 2025 by Justin Katz and Hunt Allcott. All rights reserved. Short sections of text, not to exceed two paragraphs, may be quoted without explicit permission provided that full credit, including © notice, is given to the source.

Digital Media Mergers: Theory and Application to Facebook-Instagram
Justin Katz and Hunt Allcott
NBER Working Paper No. 34028
July 2025
JEL No. D12, L1, L4, L86

ABSTRACT

We present a new model of competition between digital media platforms with targeted advertising. The model adds new insights around how user heterogeneity and overlap, along with user and advertiser substitution patterns, determine equilibrium ad load. We apply the model to evaluate the proposed separation of Facebook and Instagram. We estimate structural parameters using evidence on diminishing returns to advertising from a new randomized experiment and information on user overlap, diversion ratios, and price elasticity from earlier experiments. In counterfactual simulations, a Facebook-Instagram separation increases ad loads, transferring surplus from platforms and users to advertisers, with limited total surplus effects.

Justin Katz
Harvard University
jkatz@g.harvard.edu

Hunt Allcott
Stanford University
and NBER
allcott@stanford.edu

It is hard to overstate the importance of quality and price for users and advertisers in digital markets. According to one estimate, there are now 5.6 billion internet users worldwide, averaging 6.6 hours online each day (Kemp 2025). About 63 percent of the \$770 billion yearly global advertising budget is spent online (Dentsu 2024). Given this importance, there is significant concern about digital platforms’ market power and how this might affect outcomes for users and advertisers (Stigler Center 2019; CMA 2020; Scott Morton and Dinielli 2020).

Facebook and Instagram are one key example of this discussion. In 2020, the U.S. Federal Trade Commission (FTC) sued Meta for antitrust violations, arguing that the company had illegally monopolized the “personal social networking” market and requesting that Instagram and WhatsApp be divested to restore competition. As the case went on trial in spring 2025, the FTC and Meta disagreed over market definition, the extent of Meta’s market power, and how divesting Instagram might affect user experiences and ad prices. The FTC (2021) argued that the relevant market effectively included only Facebook, Instagram, and Snapchat, while Meta (2021a) replied that “The FTC’s fictional market ignores the competitive reality: Facebook competes vigorously with TikTok, iMessage, Twitter, Snapchat, LinkedIn, YouTube, and countless others to help people share, connect, communicate or simply be entertained.” An FTC expert argued that merging Facebook and Instagram had increased ad load (Hemphill 2025), while a Meta expert argued that again separating the platforms would increase ad load (Benedict 2025).

In this paper, we consider an important subset of these issues. In theory, how do mergers or separations of digital media platforms affect advertising loads and total surplus? In the context of Facebook and Instagram, what are the key empirical facts that govern these potential effects? Quantitatively, how might separating Facebook and Instagram affect market outcomes and welfare?

We begin with a model of digital media as a two-sided market. While the model nicely applies to the Facebook-Instagram case, it is generally useful for understanding platform competition with targeted advertising. Heterogeneous users and advertisers continuously allocate their time and ad spending between two platforms (e.g., Facebook and Instagram) and non-strategic outside options. The platforms set advertising load, accounting for how higher ad load decreases both user time on platform and equilibrium ad prices. Ad markets clear at the user level, with user-specific prices.

The model includes familiar forces from the two-sided market literature (e.g., Rochet and Tirole 2003; Anderson and Coate 2005; Rysman 2009). When the two platforms are managed jointly, the monopolist internalizes how ad load affects prices but not how ads reduce user surplus, so profit-maximizing ad load can be either above or below the social optimum depending on users’ ad aversion and advertisers’ demand elasticity. When the two platforms are separated, they compete for both users and advertisers, so ad loads can increase or decrease depending on which side of the market is more competitive. The magnitude of the separation effect depends on the share of users that “multi-home” (i.e., use both platforms) and how much they use each platform.

When users and advertisers both multi-home, separating the platforms can cause “inefficient duplication”: if advertising has diminishing returns but the separated platforms can’t coordinate ad targeting, they may inefficiently impress the same user with duplicate ads from a given advertiser,

resulting in lower ad click-through rates. A series of recent papers have emphasized the importance of inefficient duplication in ad markets (Anderson et al. 2012; Ambrus, Calvano, and Reisinger 2016; Anderson, Foros, and Kind 2018; Athey, Calvano, and Gans 2018; Gentzkow et al. 2024). In our model, when the two platforms separate, there is a “business stealing” incentive for platforms to reduce inefficient duplication by expanding ad load to target lower-value users the other platform is less likely to target. While separated platforms’ ad load choices would otherwise be strategic substitutes, business stealing can make ad load strategic complements.

The model highlights that merging or separating digital platforms such as Facebook and Instagram has theoretically ambiguous effects on equilibrium ad load and total surplus. However, these effects depend on a specific set of empirical parameters: user overlap and time use distributions, the user-side diversion ratio, users’ demand slope and ad aversion, the extent of diminishing returns to duplicate impressions, and advertisers’ price elasticity. In the rest of the paper, we focus on the Facebook-Instagram case, presenting empirical evidence on the key parameters that we then use to estimate the model and carry out counterfactual simulations to resolve the theoretical ambiguities.

We collect the empirical evidence from a rich array of new and existing sources, mostly focused on 2020, the year the FTC filed its lawsuit. First, nationally representative survey data from the 2020 National Public Opinion Reference Survey (Pew Research Center 2020) show that adult Instagram users were more likely to use Facebook than vice-versa. In our model, Instagram’s higher share of multi-homers means that separation would have larger effects on Instagram’s ad load and prices.

We then report diversion ratios that we construct using earlier results from the 2020 Facebook and Instagram Election Study (“FIES”) (Allcott et al. 2024, 2025; Allcott, Kiefer, and Tangkitvanich 2025). FIES included two randomized experiments with nationally representative samples of Facebook and Instagram users, in which randomly selected treatment groups were paid to deactivate their accounts for six weeks. A subset of participants agreed to install software to record their smartphone time use.

If the FTC’s “personal social networking” market definition were correct, users would primarily substitute between Facebook, Instagram, and Snapchat. In reality, the estimated diversion ratio from Facebook to Instagram is a precisely estimated 0.054, and the estimated diversion ratio from Instagram to Facebook is statistically zero, although the confidence interval admits a diversion ratio as large as 0.29. Strikingly, users substitute more to web browsers and other non-social media apps than to social media apps such as Snapchat, Twitter, and YouTube, although there is statistically significant substitution from Instagram to TikTok.

We then reanalyze data from the Digital Addiction (“DA”) experiment implemented by Allcott, Gentzkow, and Song (2022). DA was a randomized experiment with Facebook and Instagram users in which a randomly selected treatment group was paid to reduce time spent on (but not necessarily deactivate) Facebook, Instagram, and other social media apps for three weeks. The DA results imply that time use is very price elastic: about 40 percent of Facebook and Instagram use is worth less than \$2.50 per hour to users. In our model, this means that any ad load increases would cause

relatively small consumer surplus losses.

We also import the [Brynjolfsson et al. \(2024\)](#) estimate that on average, users’ time on platform is very inelastic to ad load. In our model, this inelasticity and the limited diversion between Facebook and Instagram imply that separation would not generate much additional incentive to reduce ad load to attract users. Instead, separation would induce the platforms to compete harder for advertisers, by increasing ad load and thus reducing ad prices.

Finally, to measure advertiser-side diminishing returns, we ran a new experiment with Facebook and Instagram ads to estimate the effect of duplicated ad campaigns on ad click-through rates. We generated 120 separate user audiences averaging about 1,300 users each and targeted them with week-long ad campaigns for 15 popular products. We randomized whether the audiences were targeted with either one or two identical campaigns. Click-through rates on the duplicated campaigns averaged 28 percent lower than on the non-duplicated campaigns. In our model, this means that separation without coordinated ad delivery could generate a material “business stealing” incentive to increase ad load, and that duplication could cause meaningful inefficiencies.

We use these empirical moments to estimate the model’s structural parameters. We impose a quadratic functional form on users’ utility from time on the two platforms, and we identify the ad disutility, price responses, platform substitution, and distribution of utility intercepts from the observed ad and price elasticities, diversion ratios, and time use distribution. We identify advertisers’ aggregate price elasticity from the platform’s first-order condition, in the spirit of how [Berry, Levinsohn, and Pakes \(1995\)](#) identify marginal costs from a Nash-Bertrand pricing assumption. Drawing intuition from the inverse elasticity markup rule, because user time is not very elastic to ads, Meta has a low marginal opportunity cost of ad load, and it thus sets ad load on a less elastic place on its advertising demand curve.

We use the estimated model to simulate the effects of separating Facebook and Instagram. Driven by the empirical results that the user diversion ratio is low and user time is relatively inelastic to ads, the model predicts that separation would induce more competition for advertisers than for users. This would increase ad load, reducing ad prices. Since a larger share of Instagram users are multi-homers, separation increases modeled ad load more on Instagram.

The modeled effects of separation depend substantially on inefficient duplication. In a scenario where the separated platforms independently set ad load but can coordinate ad delivery to avoid duplication, advertiser surplus would increase by 11 percent. In an alternative scenario where the platforms can’t avoid duplication and predict the same user-specific click-through rates, the “business stealing” effect drives ad load higher and ad prices lower. Advertiser surplus would increase by 15 percent, but duplication loss generates substantial inefficiency. In either scenario, user surplus decreases slightly as ad load increases, the platforms’ profits decrease as ad prices drop, and total surplus decreases slightly as ad load moves away from the social optimum. In either scenario, the sum of user and advertiser surplus decreases slightly. Thus, in our model, the FTC’s proposed separation remedy is not beneficial—it just transfers surplus from Meta and its users to advertisers while introducing inefficient duplication.

Strikingly, the total surplus generated by Facebook and Instagram changes by at most about one percent across all modeled scenarios, because total surplus is dominated by consumer surplus, which changes little with ad load. The importance of consumer surplus is consistent with findings from [Brynjolfsson, Collis, and Eggers \(2019\)](#) and [Allcott, Braghieri, Eichmeyer, and Gentzkow \(2020\)](#) that users are willing to pay considerable amounts to continue using the platforms.

There are several important caveats. First, we consider only one margin through which competition affects welfare: equilibrium ad loads and prices in an otherwise static market. The FTC ([2021](#)), [Scott Morton and Dinielli \(2020\)](#), and others point to important additional potential effects of digital media mergers and separations, including entry of competing social media platforms and the existing platforms’ incentives to improve user experience and privacy practices. Second, other than coordinated ad targeting, we do not consider other merger-specific efficiencies, such as sharing features and ad systems across platforms. If Instagram were separated without access to Meta’s targeting and attribution technologies, ad targeting would likely become much worse, harming both users and advertisers. Third, we do not model any harms to users from social media addiction ([Allcott, Gentzkow, and Song 2022](#)). If separation increases ad load, the decreased time use would presumably reduce such harms. Fourth, even within the context of our model, our empirical calibrations are imperfect. For example, our user diversion ratios are identified from only six weeks of deactivation, although we discuss several reasons why diversion ratios might not be that much different over a longer period. As another example, our estimate of advertisers’ price elasticity from the platform’s first order condition depends on our structural assumptions.

Our work builds on several important literatures. First, we extend theoretical literatures on platform competition in general (e.g., [Rochet and Tirole 2003, 2006](#); [Rysman 2009](#); [Armstrong 2006](#); [Weyl 2010](#)) and specifically in media markets (e.g., [Anderson and Coate 2005](#); [Bergemann and Bonatti 2011](#); [Anderson and De Palma 2012](#); [Prat and Valletti 2022](#); [Anderson and Peitz 2023](#); [Chen 2024](#)). Second, we extend research focusing on the effects of multi-homing in advertising markets, including duplication and incremental pricing (e.g., [Ambrus, Calvano, and Reisinger 2016](#); [Anderson, Foros, and Kind 2018](#); [Athey, Calvano, and Gans 2018](#); [Zubánov 2021](#); [Gentzkow et al. 2024](#)). Third, we build on other work studying media industry mergers and separations (e.g., [Berry and Waldfogel 2001](#); [Chandra and Collard-Wexler 2009](#); [Fan 2013](#); [Gentzkow, Shapiro, and Sinkinson 2014](#); [Jeziorski 2014](#); [Benzell and Collis 2022](#)). Fourth, the FIES experiment we leverage is related to other work on estimating diversion ratios from product availability experiments in social media ([Aridor 2025](#)) and other markets ([Goldfarb 2006](#); [Conlon and Mortimer 2013, 2021](#); [Conlon, Mortimer, and Sarkis 2021](#)).

Our primary contribution is to develop an empirically tractable model of digital media mergers or separations and apply it to a policy-relevant context with a compelling array of data. Our model’s key forces are consistent with earlier theoretical work, including [Anderson and Coate \(2005\)](#), [Ambrus, Calvano, and Reisinger \(2016\)](#), [Athey, Calvano, and Gans \(2018\)](#), and others mentioned above. However, advertising market models with multi-homing consumers can easily lose tractability, so prior work has made assumptions that may be undesirable in some applications,

such as no user substitution between platforms (e.g., [Ambrus, Calvano, and Reisinger 2016](#)) or effectively homogeneous time use within a platform (e.g., [Anderson, Foros, and Kind 2018](#); [Athey, Calvano, and Gans 2018](#)). In [Athey, Calvano, and Gans \(2018\)](#), the model delivers results such as discontinuous reaction functions and mixed strategy equilibria that are hard to map to realistic market conditions. In contrast, our model is explicitly designed to be empirically implemented, accommodating empirically realistic estimates of user heterogeneity, substitution patterns, and other parameters in computationally tractable pure strategy equilibria.

We also provide a new empirical estimate of the return to duplicate ad campaigns. Despite the important role of inefficient duplication in ad market models, to our knowledge there are no direct experimental estimates in the literature. [Gentzkow, Shapiro, and Sinkinson \(2014\)](#) identify diminishing returns in a structural model in a historical newspaper context. [Lewis \(2010\)](#), [Johnson, Lewis, and Reiley \(2016\)](#), and [Meta \(2016\)](#) estimate the effect of ad campaign frequency on performance. Our experiment is designed to identify a related but different parameter, which is the return to duplicating ad campaigns with standard frequencies.

Sections 1–6, respectively, present the model, experimental designs, model-free empirical evidence, structural estimation, counterfactual simulations, and conclusion.

1 Model

1.1 Setup

There are two digital media platforms indexed by j . The platforms choose ad load α_j (in ads per unit time on platform) to maximize profits. Bold typeface indicates vectors—e.g., $\boldsymbol{\alpha}$ is the vector of ad loads on each platform. Platform j ’s profit is ad revenue minus ad cost: $\Pi_j(\alpha_j) = R_j(\boldsymbol{\alpha}) - \alpha_j c_j$. Marginal costs c_j could represent the actual incremental cost of serving more ads (for example, customer service for advertisers), dynamic incentives to restrict ad load (for example, to gain market share and benefit from network effects), and in our structural estimation, any other reasons why the platforms’ theoretical first-order conditions don’t otherwise match the data.¹

There are N total users indexed by i . Users choose time on each platform T_{ij} and numeraire consumption n_i to maximize utility $U_i(\mathbf{T}_i, n_i; \boldsymbol{\alpha})$. We assume that U_i is quasilinear in n_i , so changes in U_i correspond to changes in consumer surplus. We assume that users’ utility or disutility from ad load accounts for expected consumer surplus from any purchases of advertised products, so we do not need to separately account for consumer surplus in advertisers’ product markets. We let $T_{ij}(\boldsymbol{\alpha})$ denote utility-maximizing time use as a function of ad load. There are two user types: “single-homers” on platform j exogenously have $T_{i,-j}(\boldsymbol{\alpha}) \equiv 0$, while “multi-homers” may have positive use on both platforms.

There are A advertisers indexed by a . Ad clicks generate value π_a for advertisers. For example,

¹This reduced-form approach to representing dynamic incentives in a static model is similar to [Wollmann \(2018\)](#), who analyzes investment decisions based on hurdle rates in a model of static Bertrand-Nash competition. Our theory also can capture network effects through the effect of ad load on users’ time on platform.

π_a might equal a product’s markup times users’ purchase probability after clicking on an ad. The model is isomorphic if we redefine “clicks” as some other advertising result (such as impressions or purchases) or redefine “advertisers” as independent ad campaigns run by the same firm. Advertisers choose the quantity of clicks q_a to purchase from the platforms to maximize profits $\Pi_a(q_a)$.

The targeted advertising technology is as follows. An ad “campaign” involves m impressions of advertiser a ’s ads to each targeted user, where m is the platform’s assessment of the optimal number of impressions per user.² Define ω_{ia} as platform’s prediction of user i ’s probability of clicking on each ad impression during advertiser a ’s first ad campaign, which we call the “click-through rate” (CTR). We assume that both platforms have the same targeting technology (even if separated), so ω_{ia} is the same on both platforms. (We relax that assumption in Appendix A.3.) The click-through rate after the first campaign is $(1 - \zeta_i) \cdot \omega_{ia}$, where ζ_i captures diminishing returns to additional impressions.

As described below, there is a separate ad market for each user, with equilibrium price per impression p_i . The predicted cost per click is thus p_i/ω_{ia} , and the predicted value per impression is thus $\omega_{ia}\pi_a$ for the first campaign and $(1 - \zeta_i) \cdot \omega_{ia}\pi_a$ for any subsequent campaign. For user i , define $H_i(x) \in [0, 1]$ as the cumulative density function (CDF) of $\omega_{ia}\pi_a$ across advertisers.

The platform’s contract offer to advertisers is to serve ads to the $\mathcal{U}_a(q)$ users with the lowest predicted cost per click and charge the cost $C_a(q) = \sum_{i \in \mathcal{U}_a(q)} m \cdot p_i$. Advertisers know $C_a(q)$ when choosing q .

We impose three assumptions that substantially simplify the analysis.

Assumption 1. Independent click-through rates: $\omega_{ia} \perp \omega_{ia'}, \forall (a, a'); \omega_{ia} \perp T_{ij}(\alpha), \forall (a, j);$ and $\omega_{ia} \perp \zeta_i, \forall a$.

Assumption 2. Identical uniform values per impression: $H_i(x) = H(x) = \frac{x}{\eta} - \eta_0, \forall i$.

Assumption 3. Bounded profits per impression: $(1 - \zeta_i) \cdot \eta \cdot (1 + \eta_0) \leq p_i^m, \forall i$, where p_i^m is the merged equilibrium price when platforms are constrained to serve at most one campaign to user i from advertiser a .

Assumption 1 states that click-through rates are independent across advertisers and independent of both time on platform and diminishing returns. This rules out the possibility that some users are more or less valuable on average across advertisers. This assumption could be weakened by modeling distinct user types, such as high- or low-income people. Assumptions 1 and 2 together imply that a given change in α has the same effect on all $C_a(q)$, and Assumption 2 facilitates straightforward demand aggregation across individual users.

Assumption 3 implies that predicted value per impression for the second campaign is weakly below the market clearing price if the merged platform never showed duplicated impressions, since $\eta \cdot$

²Assuming the same m for all users is isomorphic to assuming heterogeneous impressions m_i with $m_i \perp \omega_{ia}\pi_a, \forall (i, a)$, and $m \equiv E_i[m_i]$. We also show in Appendix A.1 that equilibrium prices are identical with heterogeneous m_i and an alternative assumption where m_i is increasing in profits per impression and decreasing in prices, with a specific functional form.

$(1 + \eta_0)$ is the maximum value per impression given Assumption 2. Thus, in the merged equilibrium, the platform never shows a given campaign to a user a second time, since it is weakly more profitable to show the first campaign from the marginal advertiser.

1.2 Merged and Separated Equilibria

We now describe two equilibria. In the “merged equilibrium,” the two platforms set ad load to maximize joint profits, and advertisers buy ads from the one merged entity. In this equilibrium, the platforms have “coordinated ad delivery,” meaning that each user’s available ad slots are allocated optimally across both platforms, and there is thus one ad price p_i for each user. In the “separated equilibrium,” the two platforms independently set ad load to maximize their own profits, and advertisers buy ads separately from each platform. We compare two types of separated equilibria: with “uncoordinated ad delivery,” meaning that each user’s available ad slots are allocated optimally within each platform but not necessarily across platforms, and coordinated ad delivery. Uncoordinated delivery can lead to different ad prices p_{ij} as well as inefficient duplication, where both platforms target the same ad campaign at the same user.

1.2.1 Merged Equilibrium

Advertisers choose the quantity of clicks to purchase from the merged firm. Advertiser profits equal the value of clicks net of advertising costs:

$$\Pi_a^m(q) = \pi_a \cdot q - C_a(q). \quad (1)$$

Maximizing profits gives

$$\pi_a = C'_a(q_a) \quad (2)$$

In words, advertisers purchase ads until the marginal cost per click equals the value per click.

Ad markets clear at the user level:

$$\overbrace{\boldsymbol{\alpha} \cdot \mathbf{T}_i(\boldsymbol{\alpha})}^{\text{supply}} = \overbrace{\sum_a m \cdot \mathbf{1}[i \in \mathcal{U}_a(q_a)]}^{\text{demand}} = \sum_a m \cdot \mathbf{1}[p_i \leq \pi_a \omega_{ia}] = Am \cdot (1 - H_i(p_i)). \quad (3)$$

Rearranging equation (3) and substituting the functional form for $H_i(x)$ from Assumption 2 gives equilibrium price

$$p_i = \eta \cdot \left(1 + \eta_0 - \frac{\boldsymbol{\alpha} \cdot \mathbf{T}_i(\boldsymbol{\alpha})}{Am} \right). \quad (4)$$

This equation shows that equilibrium prices are increasing in ad demand (the number of advertisers A and campaign size m) and decreasing in ad supply (ad load $\boldsymbol{\alpha}$ and time on platform \mathbf{T}_i). We assume that η and η_0 are such that we always have an interior equilibrium.

1.2.2 Separated Equilibrium

In the separated equilibrium, advertisers choose the number of clicks q_j to purchase from each of the two platforms. With uncoordinated ad delivery, each platform's ability to deliver q_j clicks depends on the number of impressions that are duplicated on the other platform. Many duplicated clicks and more strongly diminishing returns means that a platform will get fewer clicks per impression. Define $O_a(q_1, q_2)$ as the “duplication function”: the number of duplicated clicks purchased, as a (weakly increasing) function of the number of clicks purchased on each platform. Now, q_j clicks cost $C_{aj}(q_j; O_a(\mathbf{q}))$, and advertiser profits are

$$\Pi_a^s(q_1, q_2) = \pi_a \cdot (q_1 + q_2) - \sum_j C_{aj}(q_j; O_a(\mathbf{q})). \quad (5)$$

To derive advertisers' first-order condition, define i^* as the marginal user impressed by advertiser a on platform j . Further define “marginal duplication” O'_{aj} as the derivative of O_a with respect to q_j . This is the probability that the impression on user i^* is duplicated on the other platform. Then define $\tilde{C}'_{aj} = p_{i^*a}/\omega_{i^*a}$ as the expected cost per click for a hypothetical unduplicated impression on the marginal user. Finally, define ζ_j as the time-use weighed average of ζ_i on platform j for multi-homing users. (ζ_j depends on α , but we suppress that notation.)

With probability O'_{aj} , the impression on the marginal user i^* is duplicated, and the predicted click-through rate is $(1 - \zeta_j) \cdot \omega_{i^*a}$.³ With probability $(1 - O'_{aj})$, the impression is not duplicated. Thus, the expected marginal CTR is $O'_{aj} \cdot (1 - \zeta_j) \cdot \omega_{i^*a} + (1 - O'_{aj}) \cdot \omega_{i^*a} = (1 - \zeta_j O'_{aj}) \cdot \omega_{i^*a}$, and the expected marginal cost per click is $\tilde{C}'_{aj}(q_j) / (1 - \zeta_j O'_{aj})$.

Using this result, maximizing profits gives

$$\pi_a = C'_{aj}(q_{aj}; O_a(\mathbf{q})) = \frac{\tilde{C}'_{aj}(q_j)}{1 - \zeta_j O'_{aj}}. \quad (6)$$

In words, advertisers purchase ads until the duplication-adjusted marginal cost per click equals the value per click. As marginal duplication O' increases, platforms must deliver more ad impressions for each click, raising advertising costs.

With uncoordinated ad delivery, the user-level market clearing condition is analogous to the merged case, except that markets now clear separately on each platform j :

$$\overbrace{\alpha_j \cdot T_{ij}(\alpha)}^{\text{supply}} = \overbrace{\sum_a m \cdot \mathbf{1}[p_{ij} \leq \pi_a \omega_{ia} \cdot (1 - \zeta_j \cdot O'_{aj})]}^{\text{demand}} = Am \cdot \left(1 - H_i\left(\frac{p_{ij}}{1 - \zeta_j O'_{aj}}\right)\right). \quad (7)$$

Rearranging equation (7) and again substituting the functional form for $H_i(x)$ gives equilibrium

³The marginal CTR can be multiplied ζ_j by rather than ζ_{i^*} because $\zeta_i \perp \omega_{ia}$, per Assumption 1.

price

$$p_{ij} = \eta \cdot \left(1 + \eta_0 - \frac{\alpha_j T_{ij}(\boldsymbol{\alpha})}{Am} \right) \cdot (1 - \zeta_j O'_{aj}). \quad (8)$$

This equation shows that equilibrium prices are discounted by the expected “duplication loss” $\zeta_j O'_{aj}$.

Let \mathcal{U}_j be the set of users on platform j , and $N_j = |\mathcal{U}_j|$ indicate their number. We show in Appendix A.2 that the marginal duplication function evaluated at equilibrium ad demand is

$$O'_{aj} = \frac{\sum_{i \in \mathcal{U}_j} \mathbf{1}[\alpha_j T_{ij}(\boldsymbol{\alpha}) \leq \alpha_{-j} T_{i,-j}(\boldsymbol{\alpha})]}{N_j} \in [0, 1]. \quad (9)$$

This equation shows that marginal duplication depends on several forces. First, marginal duplication decreases as time use decreases on platform $-j$ relative to j . In the extreme where $T_{i,-j}(\boldsymbol{\alpha}) = 0$, meaning that all of j ’s users are single-homers, the indicator in the numerator is always zero. Second, holding constant multi-homers’ average time use, marginal duplication decreases as the covariance between T_{ij} and $T_{i,-j}$ decreases. Intuitively, if time use and other factors are homogeneous across platforms, then all users would see duplicated impressions in equilibrium, but duplication decreases if users heterogeneously spend more of their time on either j or $-j$. Third, marginal duplication decreases as platform j increases ad load relative to $-j$. Intuitively, as platform j increases ad slots, it increasingly serves ads to marginal users who are not valuable enough to be impressed on the other platform.

With coordinated ad delivery, the ad market clears jointly across the two platforms. Thus, the ad market clearing condition and equation for price p_i are as written earlier for the merged equilibrium.

1.3 Equilibrium Ad Load

We now solve for ad load in the social optimum, merged equilibrium, and separated equilibrium. Derivations are in Appendix A.

1.3.1 Social Optimum

The social planner maximizes the sum of consumer, advertiser, and platform surplus. The social planner uses competitive equilibrium prices for allocating ad load because the platform’s contract allocates ads to highest-value advertisers. Platform revenue cancels because it is a transfer from advertisers to the platform, giving

$$W = \sum_i U_i^*(\mathbf{T}(\boldsymbol{\alpha}), n; \boldsymbol{\alpha}) + \sum_i Am \cdot \int_{x=p_i(\boldsymbol{\alpha})}^{(\pi\omega)^{\max}} x dH(x) - \boldsymbol{\alpha} \cdot \mathbf{c}. \quad (10)$$

The first-order condition for ad load equates marginal consumer surplus losses with marginal advertiser benefits net of c_j . Solving for socially optimal ad load gives

$$\alpha_j^o = \frac{\sum_i \left[\frac{\partial U_i^*(\cdot; \alpha)}{\partial \alpha_j} + p_i(\alpha) \cdot \left(T_{ij}(\alpha) + \alpha_{-j}^o \frac{\partial T_{i,-j}(\alpha)}{\partial \alpha_j} \right) \right] - c_j}{-\sum_i p_i(\alpha) \cdot \frac{\partial T_{ij}(\alpha)}{\partial \alpha_j}}. \quad (11)$$

The first term in the numerator ($\frac{\partial U^*}{\partial \alpha}$) is negative, capturing that socially optimal ad load is lower when users dislike ads more. The remaining terms other than c_j capture the marginal benefit of ad load to advertisers. This marginal benefit equals the equilibrium ad price p_i (which depends on values per click π_a and captures advertisers' marginal value of impressions) times several terms capturing the change in the quantity of ad slots. The term T_{ij} captures the mechanical effect that when user time on platform is higher, more ad load per unit time generates more ad slots. The final term in the numerator captures how ad load on platform j affects user time (and thus ad slots) on the other platform, depending on whether the platforms are substitutes for users (implying $\frac{\partial T_{-j}}{\partial \alpha_j} > 0$) or complements (implying $\frac{\partial T_{-j}}{\partial \alpha_j} < 0$). The denominator, which is positive, captures how socially optimal ad load is lower when $\frac{\partial T_j}{\partial \alpha_j}$ is larger, i.e. when higher ad load causes more decrease in time on platform (and thus ad slots).

A corner solution is also possible, i.e. socially optimal ad load can be zero. This happens if the consumer surplus loss from the first ad is higher than the advertiser value for that ad, i.e. if $\sum_i \frac{\partial U_i^*(\cdot; \mathbf{0})}{\partial \alpha_j} > \sum_i p_i(\mathbf{0}) \cdot T_{ij}(\mathbf{0})$.

1.3.2 Merged Equilibrium

The merged firm maximizes profit

$$\Pi^m(\alpha) = \sum_i \overbrace{\alpha \cdot T_i(\alpha)}^{\text{ad supply}} \cdot p_i - \alpha \cdot c. \quad (12)$$

The first-order condition for ad load equates the marginal revenue loss from lower ad prices on all slots sold with the marginal net revenue gain from offering additional slots. Solving for revenue-maximizing ad load gives

$$\alpha_j^m = \frac{\sum_i \left[\frac{\partial p_i}{\partial \alpha_j} \cdot \alpha \cdot T_i(\alpha) + p_i(\alpha) \cdot \left(T_{ij}(\alpha) + \alpha_{-j}^m \cdot \frac{\partial T_{i,-j}(\alpha)}{\partial \alpha_j} \right) \right] - c_j}{-\sum_i p_i(\alpha) \cdot \frac{\partial T_{ij}(\alpha)}{\partial \alpha_j}}. \quad (13)$$

The first term in the numerator is negative, capturing that revenue-maximizing ad load is lower when advertisers are more price responsive. The remaining terms are the same as in equation (11). This is because of advertisers' optimization from equation (2), which equates their marginal benefit from ads (which the social planner considers) with their willingness to pay for those ads (which the platform considers).

Comparing the first terms in the numerators of equations (11) and (13) shows the distortion in the merged equilibrium relative to the social optimum: socially optimal ad load will exceed the merged equilibrium level if $\sum_i \frac{\partial U_i^*(\cdot; \alpha)}{\partial \alpha_j} \geq \sum_i \frac{\partial p_i}{\partial \alpha_j} \cdot \alpha \cdot T_i(\alpha)$. As highlighted in [Anderson and Coate](#)

(2005), the social planner restricts ad load to avoid consumer harm, while the platform restricts ad load to increase ad prices. To see this more clearly, define $\gamma_{ij} > 0$ as the marginal disutility from an additional ad, and temporarily assume $\partial \mathbf{T}_i / \partial \boldsymbol{\alpha} = \mathbf{0}$ to isolate the most relevant forces in our empirical application. Then socially optimal ad load exceeds the merged equilibrium level if

$$\sum_i \gamma_{ij} T_{ij} \leq \sum_i T_{ij} \cdot \left(\frac{\eta}{Am} \boldsymbol{\alpha} \cdot \mathbf{T}_i \right). \quad (14)$$

Socially optimal ad load will be relatively higher if the ad disutility γ_j is small. Merged equilibrium ad load will be relatively higher if time use \mathbf{T}_i is small, because higher ad load reduces prices on a smaller number of inframarginal impressions. Holding average time use fixed, relative merged equilibrium ad load decreases with time use variance, because platform profits depend more heavily on ad prices for heavy users, whose ad prices are more sensitive to changes in ad load.

1.3.3 Separated Equilibrium

The separated platforms maximize profit

$$\Pi_j^s(\alpha_j) = \sum_i \overbrace{\alpha_j \cdot T_{ij}(\boldsymbol{\alpha})}^{\text{ad supply}} \cdot p_{ij} - \alpha_j c_j. \quad (15)$$

Solving for revenue-maximizing ad load gives

$$\alpha_j^s = \frac{\sum_{i \in \mathcal{U}_j} \left[\frac{\partial p_{ij}}{\partial \alpha_j} \cdot \alpha_j \cdot T_{ij}(\boldsymbol{\alpha}) + p_{ij}(\boldsymbol{\alpha}) \cdot T_{ij}(\boldsymbol{\alpha}) \right] - c_j}{-\sum_{i \in \mathcal{U}_j} p_{ij}(\boldsymbol{\alpha}) \cdot \frac{\partial T_{ij}(\boldsymbol{\alpha})}{\partial \alpha_j}}. \quad (16)$$

Comparing this to equation (13) shows that the merged platforms internalize two effects that the separated platforms ignore. The difference between the first terms in the numerators shows that the merged platforms internalize how ad load affects ad prices on the other platform. Since higher ad load decreases prices, this effect reduces ad load in the merged equilibrium relative to the separated equilibrium. We call this the “advertiser-side Cournot effect.” The last term in the numerator of equation (13) is not present in equation (16), showing that the merged platforms internalize how ad load affects time spent (and thus ad slots) on the other platform. If the platforms are substitutes ($\frac{\partial T_{-j}}{\partial \alpha_j} > 0$), this effect increases ad load in the merged equilibrium. If the platforms are complements ($\frac{\partial T_{-j}}{\partial \alpha_j} < 0$), this effect reduces ad load in the merged equilibrium. We call this the “user-side substitution effect.”

These two effects are familiar from the early two-sided markets literature (e.g., [Rochet and Tirole 2003](#); [Anderson and Coate 2005](#); [Rysman 2009](#)). However, in our model with user preference heterogeneity, the magnitudes of these effects are governed by the amount of user overlap. If all users are single-homers, then the merged and separated equilibria are the same: changes in platform j ’s ad load don’t affect ad prices or time use for any of the other platform’s users. All else equal, the more multi-homers there are, the more different the two equilibria become. Multi-homers’ average

time on platform also matters. The first term in the numerator of equation (13) shows that even if there are many multi-homers, higher ad load on platform j doesn't affect platform $-j$'s revenue much if multi-homers' $T_{i,-j}$ is small.

Moreover, equilibrium ad load depends on the full time use distribution, not just the mean. Both terms in the numerator of equation (16) include products of time on platform T_{ij} with price, which also depends on T_{ij} . Thus, holding constant the average T_{ij} , an increase in the variance of T_{ij} will also affect the equilibrium.

Coordinated versus uncoordinated ad delivery. The differences between the merged and separated equilibria described so far apply with either coordinated or uncoordinated ad delivery. With coordinated ad delivery, equations (15) and (16) would just have one user-specific ad price p_i instead of p_{ij} . See Appendix Section A.6.3 for details.

With uncoordinated ad delivery, duplication loss affects the ad price p_{ij} and its derivative $\frac{\partial p_{ij}}{\partial \alpha_j}$. Equation (8) showed that p_{ij} is discounted by the expected duplication loss $\zeta_j O'_{aj}$. To most clearly see the effects on $\frac{\partial p_{ij}}{\partial \alpha_j}$, we differentiate equation (8) while momentarily assuming $\partial \zeta_j / \partial \alpha \approx 0$, giving

$$\frac{\partial p_{ij}}{\partial \alpha_j} \approx - (1 - \zeta_j O'_{aj}) \cdot \frac{\eta \cdot \left(T_{ij} + \alpha_j \frac{\partial T_{ij}(\alpha)}{\partial \alpha_j} \right)}{Am} - \frac{p_{ij} \zeta_j}{(1 - \zeta_j O'_{aj})} \frac{\partial O'_{aj}}{\partial \alpha_j}. \quad (17)$$

The first term shows how increasing ad load reduces price by increasing the number of ad slots, both directly and indirectly by changing user time on platform. This force also exists in the merged equilibrium. Like the prices p_{ij} , this term is also discounted by the expected duplication loss $\zeta_j O'_{aj}$.

The second term is specific to the separated equilibrium with uncoordinated ad delivery. As described in Section 1.2.2, marginal duplication is decreasing in ad load (i.e., $\frac{\partial O'_{aj}}{\partial \alpha_j} < 0$), as the additional ad slots increasingly serve ads to marginal users who are not impressed on the other platform. In equilibrium, this lower duplication probability reduces the cost per click, depending on the magnitude of diminishing returns ζ_j . This provides an additional incentive for the separated platforms to increase ad load. We call this the “business stealing effect.”

Both terms show that duplication loss lowers the opportunity cost of higher ad load, the first by reducing return to duplicated ads, and the second by allowing higher ad load to directly reduce duplication loss. These forces are related to the “business sharing” effect in Ambrus, Calvano, and Reisinger (2016) in that they increase ad load in the separated equilibrium. Our two forces are not separately present in Ambrus, Calvano, and Reisinger (2016), principally because our model is tailored to institutional features of targeted ad markets with user-level ad prices. In our model, the payoff from higher ad load depends on marginal duplication, which itself depends on ad load. In Ambrus, Calvano, and Reisinger (2016), the payoff from higher ad load depends only on average duplication, since marginal impressions are implicitly randomly shown across users.⁴ For similar reasons, our model's forces are distinct from the version of “business stealing” present in

⁴Ambrus, Calvano, and Reisinger (2016) also analyze joint versus separated ownership of two platforms. That analysis is again related, but non-nested, with ours. They consider the case where both the merged and separated equilibrium feature duplication loss, whereas we always assume no duplication loss in the merged equilibrium.

the [Athey, Calvano, and Gans 2018](#) model of one-sided media market competition with duplication loss, where platforms increase ad load to increase the single-homer share of *advertisers* who have higher incremental value to platforms.⁵

The extent of diminishing returns ζ_j matters for several reasons. First, it affects the equilibrium α by governing the magnitude of the business stealing effect. Second, it governs the welfare effects of separation by mechanically determining the loss from duplicated impressions.

1.3.4 Discussion

In reality, Meta and other digital media platforms can set user-specific ad load ([Hemphill 2025](#)). The model applies directly to that case, with the profit-maximizing ad loads derived above holding for each user or user type.

In deriving marginal duplication in equation (9), we assume that both platforms predict the same click-through rate ω_{ia} for each user. In practice, the two platforms might predict different ω_{ia} , perhaps using different data or targeting systems. This would reduce average duplication O_a . However, Appendix A.3 shows that *marginal* duplication could either increase or decrease with different predicted ω_{ia} , and thus the change in separated equilibrium ad load is ambiguous.

In Appendix A.4, we show that in the separated equilibrium, the platforms’ optimal ad loads can be strategic substitutes or strategic complements, depending on the strength of two forces. First, advertisers view ad slots on each platform as substitutes, so platforms reduce ad load in response to an increase by their rival. This is a standard Cournot game force that in isolation would make ad load choices strategic substitutes. The strength of this force depends on user overlap: a platform responds more to its rival’s actions when more users multi-home and thus can be reached by advertisers on the other platform.

Second, as described above, with uncoordinated ad delivery there is a business stealing incentive to increase ad load. This force allows for strategic complementarity in ad load, as shown formally in Proposition 1 in Appendix A.4. Intuitively, an increase in a platform’s ad load reduces the rival platform’s advertising demand by increasing the average duplication probability. Depending on the time use distribution, this may reduce the rival platform’s *marginal* duplication probability, which would increase the rival’s optimal ad load.⁶

The equations above show how ad load in the merged equilibrium could be larger or smaller than the social optimum, and that separating the platforms could move ad load either closer to or further from the social optimum. The relationships between these equilibria are governed by a specific set

⁵[Athey, Calvano, and Gans 2018](#) implicitly refer to this force as a form of entry deterrence, rather than “entry accommodation,” in the market for single-homing advertisers.

⁶The version of “business stealing” in the [Athey, Calvano, and Gans \(2018\)](#) model of one-sided media market competition with duplication loss also implies scope for strategic complementarity, as shown in their Figure 2. As described in the previous section, the reason for strategic complementarity is slightly different due to our focus on targeted ads. We build on their work by putting a similar effect in a two-sided market model of targeted ads and allowing for heterogeneous time use conditional on homing status. Unlike [Athey, Calvano, and Gans \(2018\)](#), our model’s heterogeneous time use gives continuous reaction functions that (i) allow us to more clearly characterize duplication loss as a force that can lead to strategic complementarity or non-monotonic reaction functions and (ii) can be more realistically taken to data.

of parameters: user overlap, the mean and distribution of time on platform, user-side diversion ratios, users’ disutility from ads, the extent of diminishing returns to duplicate impressions, and advertisers’ price elasticity. In the rest of the paper, we estimate these parameters and then use the estimated model to evaluate counterfactuals.

2 Experimental Designs

Section 1 described how a set of parameters govern the effects of merging or separating digital platforms. In this section, we present experimental designs and data for a survey and several randomized experiments that we use to estimate these parameters.

2.1 National Public Opinion Reference Survey

To estimate user overlap between Facebook and Instagram, we use microdata from the National Public Opinion Reference Survey ([Pew Research Center 2020](#)), henceforth the “NPORS.” It is particularly important to measure app use overlap in a nationally representative sample instead of an online opt-in sample, because the latter might naturally be selected on internet use. NPORS overcomes this potential issue because it is a high-quality probability sample, where potential respondents are randomly selected from the U.S. adult population using address-based sampling and can respond on paper, online, or over the phone. The survey question we use asks, “Please indicate whether or not you ever use the following websites or apps,” with a list of possible responses including Facebook, Instagram, and six other apps.

To correspond to the timing of the experiments described below, we use the 2020 survey, which has 3,607 valid responses to the question we use. We use the study’s nationally representative sample weights.

2.2 Facebook and Instagram Election Study

To estimate diversion ratios and the joint distribution on time on platform, we use results from the U.S. 2020 Facebook and Instagram Election Study, henceforth the “FIES.” The microdata can only be used to study the role of social media in elections, so we did not use the microdata for this paper. Instead, we adapt results reported in a replication study by [Allcott, Kiefer, and Tangkitvanich \(2025\)](#), which are similar to results from [Allcott et al. \(2024\)](#) and [Allcott et al. \(2025\)](#).

The FIES included two parallel randomized experiments, one that paid Facebook users to deactivate Facebook, and another that paid Instagram users to deactivate Instagram. We say that Facebook and Instagram, respectively, are the “focal platform” in each experiment. To recruit participants, Meta placed survey invitations at the top of the news feeds for stratified random samples of Facebook and Instagram users. Participants were also invited to an optional “passive tracking sample” in which mobile app use would be recorded.

A randomly selected Control group was offered \$25 if they did not log into their focal platform for the one week between September 23 and the end of the day on September 29, 2020. A randomly selected Deactivation group was offered \$150 if they did not log into their focal platform for the six weeks between September 23 and the end of the day on November 3, the day of the election. The “treatment period” is the additional five weeks from September 30 to November 3 when the Deactivation group was being paid to avoid logging in, while the Control group was not.

The app use analyses in [Allcott, Kiefer, and Tangkitvanich \(2025\)](#) include the 3,729 Facebook users and 2,700 Instagram users who consented to passive tracking and have valid app use data. The FIES data include weights that make the sample representative of Facebook and Instagram users on a set of variables including baseline focal app use measured in Meta’s internal data. [Allcott, Kiefer, and Tangkitvanich \(2025\)](#) then adjust those weights so that the reweighted passive tracking samples match the NPORS on the share of users that are multi-homers.

2.3 Digital Addiction Experiment

To estimate the price elasticity of time on platform, we use microdata from the Digital Addiction experiment ([Allcott, Gentzkow, and Song 2022](#)), henceforth “DA.” Participants were recruited using Facebook and Instagram ads. All participants consented to have their mobile app use recorded. Baseline data were collected during a 20-day “baseline period” from April 13 through May 2, 2020.

A randomly selected “Bonus group” was offered a “Screen Time Bonus” to reduce their use of five social media apps (Facebook, Instagram, Twitter, Snapchat, and YouTube) plus web browsers during a 20-day “bonus period” from May 25 through June 13. The structure of the bonus was essentially equivalent to a price of \$2.50 per hour for using those apps during the 20-day period.

We analyze the 783 participants in the Bonus and Control groups who were not randomly selected to receive additional experimental screen time limit functionality. From that group, we construct two partially overlapping samples of 670 “Facebook users” and 541 “Instagram users,” who ever used the respective mobile app before the bonus period began on May 25. We do not construct sample weights for this analysis.

2.4 Ad Duplication Experiment

To estimate how duplicated social media ad impressions affect click-through rates due to diminishing returns, we ran a new experiment on Facebook and Instagram. An ideal experiment would randomly vary, for a representative sample of users and ad campaigns, whether users are exposed to a campaign once or twice. We cannot implement this exact experiment from outside Meta, but we used Meta’s Ads Manager functionalities to approximate it quite closely, by targeting user audiences with either single or duplicated ad campaigns.

In our experiment, we served ads for 15 popular products across five popular categories. To choose the categories, we began with the top six categories for digital ad spending from the [Sensor-Tower \(2024\)](#) Digital Market Index: shopping, consumer packaged goods, media and entertainment,

health and wellness, food and dining, and financial services. We excluded the latter category because Meta restricts financial services ads, giving five product categories. Within each category, we used online sources to identify three major advertisers along with each advertiser’s most popular product. For consumer packaged goods, for example, the products were Tide Pods, Dove Deep Moisture body wash, and Nescafe Clasico coffee. We created a new Facebook page for each category that ran ads recommending the top three products as our “product picks.”⁷

For each of the 15 products, we ran eight initial ad campaigns for a different product in the same category from February 4 to 11, 2025. The users Meta targeted for these initial campaigns gave us eight similarly sized, non-overlapping audiences per product. We then randomly assigned each audience to be re-targeted by a follow-up campaign in one of eight treatment conditions from a 2x2x2 matrix, varying (i) the number of campaigns (one or two) targeting the audience; (ii) the daily budget (high or low); and (iii) the ad objective (maximizing clicks or reach). We ran these follow-up campaigns from February 24 to March 3, 2025. Appendix B provides more details on product selection, ad creatives, and implementation.

Eight user audiences for each of 15 products generated a total of 120 audiences. Half of those were assigned duplicated campaigns, while the other half had non-duplicated campaigns, for a total of 180 follow-up campaigns. An implementation error affected three campaigns, giving a possible sample of 177 campaigns. To limit the role of outliers, for our primary analyses in Section 3.5 we also winsorize low CTRs at the 10th percentile and drop an additional trio of campaigns where the two duplicate campaigns had less than 50 percent audience overlap, giving a “primary sample” of 174 campaigns.

3 Model-Free Empirical Evidence

The model in Section 1 highlighted key parameters that govern the effects of merging or separating digital media platforms. We now present evidence on several of those parameters.

3.1 User Overlap

Table 1 presents data on Facebook and Instagram adult user overlap from the NPORS. The first row shows that among the population of US adults that used Facebook or Instagram in 2020, about 93 percent used Facebook and 59 percent used Instagram. The second row cuts the same data differently. Of Facebook users, 56 percent used Instagram, making them “multi-homers” in our analysis, and the remaining 44 percent were Facebook single-homers. Of Instagram users, 88 percent used Facebook, and the remaining 12 percent were Instagram single-homers.

In the model from Section 1, more user overlap magnifies the advertiser-side Cournot, user-side substitution, and business stealing effects. The fact that more Instagram users are multi-homers means that if the platforms were separated, these forces would be stronger for Instagram than Facebook.

⁷Meta’s terms of use allow third parties to advertise product recommendations.

One caveat is that like our other data, the NPORS does not include youth under 18, a population that is less likely to use Facebook. However, youth are only a small part of the advertising market and thus less important for our overall conclusions.

3.2 Time Use Distribution

Figure 1 presents the distribution of Facebook and Instagram mobile app time use in the FIES Control groups during the last four weeks of the treatment period, when the Deactivation groups were paid to be deactivated but the Control groups were not. To construct this figure, we combine the separate Facebook and Instagram time use distributions reported by Allcott, Kiefer, and Tangkitvanich (2025), up-weighting the Facebook sample such that the relative numbers of Facebook and Instagram users match the NPORS data. The center of the figure is a heat map of the joint time use distribution for multi-homers. The histograms at the top and right present the marginal distributions of Facebook and Instagram use, respectively.

In these data, the average Facebook user spent 42 minutes per day on the app. Daily use was similar for single-homers and multi-homers, with averages of 43 and 41 minutes per day, respectively. The average Instagram user spent 14 minutes per day on the app. Single-homers spent more time on the app than multi-homers, with averages of 16 and 13 minutes per day, respectively. The distributions are skewed, with a smaller number of heavy users.

In the model from Section 1, the fact that the average multi-homer spends more time on Facebook than Instagram has several implications for the separated versus merged equilibria. First, all else equal, the “advertiser-side Cournot” effect is larger for Instagram: in the merged equilibrium, Instagram has a larger incentive than Facebook to restrain ad load to keep ad prices high on the other platform. Second, in the separated equilibrium, marginal duplication would be lower on Facebook: more time on Facebook means that users are served ads with lower click-through rates that are not duplicated on Instagram. Thus, duplication loss would decrease ad prices less on Facebook than Instagram if separated.

Figure 1 also shows that time use variance is higher on Facebook. The standard deviations of the marginal distributions are 31 and 15 minutes per day on Facebook and Instagram, respectively. As discussed in Section 1, higher time use variance induces the platform—but not the social planner—to reduce ad load.

Section 1 also discussed the importance of time use correlation within multi-homers. On one extreme with perfect positive correlation, all the mass in the heat map in Figure 1 would be on an upward-sloping 45-degree line. On the other extreme with perfect negative correlation, all the mass would be on a downward-sloping line. In reality, Facebook and Instagram use are slightly positively correlated, with a correlation coefficient of 0.02. As described in Section 1, this makes marginal duplication higher than it would be with negative correlation, but lower than it would be with a more positive correlation. This discussion highlights the value of high-quality time use data and a model that can accommodate realistic time use distributions instead of, for example, assuming that users are homogeneous.

We highlight three caveats. First, these time use data include mobile app use only. Instagram use has long been almost entirely on mobile (Comscore 2014). However, Kemp (2020) reports that 2.7 percent of users accessed Facebook only via computer in 2020, 29 percent used both phones and computers, and 68 percent used only mobile phone. Thus, mobile time use somewhat understates total Facebook time use.

Second, these time use data cover a specific four-week period in fall 2020, and this period was after the Control group had been paid to deactivate for a week.⁸ Figures 2 and 3 (introduced below) suggest that this week of deactivation may have initially reduced Control group time use slightly relative to what it would have been otherwise, but average use over the final four weeks of the five-week treatment period is roughly similar to the levels before and after the experiment.

Third, the market intelligence company eMarketer (2025) estimated that daily time use averages in 2020 for Facebook and Instagram monthly active users were 33 and 29 minutes, respectively—a much smaller difference than the FIES data suggest. While the FIES sampling and weighting approaches should in theory deliver the most credible publicly available time use estimates, we will present alternative estimates and counterfactual simulations that match the eMarketer (2025) averages.

3.3 Diversion Ratios

The diversion ratios between Facebook and Instagram can be calculated from the effects of deactivation payments in the FIES experiment. To illustrate the calculation, Figures 2 and 3 present daily Facebook and Instagram use around the FIES experiment. The dark grey shading indicates the week (from September 23–29) when both Deactivation and Control groups were being paid to deactivate. The light grey shading indicates the five week treatment period (from September 30–November 3) when only the Deactivation group was being paid to deactivate.

Panel (a) of each figure presents use of the focal platform. In both figures, Control group use decreased substantially from September 23–29 before returning close to its original level, while Deactivation group use stayed depressed over the additional five-week treatment period.⁹ Panel (b) of each figure presents use of the other platform. In both figures, Deactivation group use of the other platform increased slightly over the treatment period, but by much less than focal platform use decreased. This means that the diversion ratios are small.

To describe substitution patterns, Allcott, Kiefer, and Tangkitvanich (2025) use an instrumental variables estimator to estimate the effects of deactivation on time use. Define T_{ij0} and T_{ijd} as participant i 's use of platform j during the baseline and deactivation treatment periods, respectively, and define $\nu_{s(i)}$ as a vector of randomization stratum indicators. Further define D_i as a deactivation group indicator, and define \tilde{D}_i as a measure of compliance with deactivation, with $\tilde{D}_i = 1$ corresponding to zero focal platform use during the treatment period and $\tilde{D}_i = 0$ corresponding to

⁸There are generally only a few days of baseline app use data before deactivation began on September 23.

⁹The Deactivation and Control groups appear to have slightly different baseline averages, but any imbalance should not affect the diversion ratio estimates because equation (18) controls for baseline use.

Control group average use. The estimating equation is

$$T_{i,-j,d} = \tau_{-j}^{Dj} \tilde{D}_i + \beta T_{i,-j,0} + \nu_{s(i)} + \epsilon_{ij}, \quad (18)$$

instrumenting for \tilde{D}_i with the deactivation group indicator D_i . τ_j^{Dj} and τ_{-j}^{Dj} , respectively, are the local average treatment effects (LATEs) of fully deactivating j on use of j and $-j$, for people induced to deactivate by the \$150 payment. Appendix Figure A2 presents these LATEs.

The (local average) diversion ratio is the ratio of LATEs on the other platform versus the focal platform: $\delta_{-j}^j = -\tau_{-j}^{Dj} / \tau_j^{Dj}$. By definition, the diversion ratio is positive if j and $-j$ are substitutes, and negative if they are complements. We calculate standard errors via the Delta method, assuming zero covariance between τ_j^{Dj} and τ_{-j}^{Dj} .

Figure 4 presents the estimated diversion ratios δ_j^{-j} from Facebook and Instagram to each other and to ten other apps or categories. The diversion ratios from Instagram appear less precisely estimated because average Instagram use is smaller, which decreases the diversion ratio’s denominator. Roughly consistent with the graphical evidence discussed above, the estimated diversion ratio from Facebook to Instagram is $\hat{\delta}_I^F \approx 0.054$. In other words, reducing Facebook use by one minute increases Instagram use by 0.054 minutes. The estimated diversion ratio from Instagram to Facebook is $\hat{\delta}_F^I \approx 0.096$. This is not statistically distinguishable from zero; the upper bound of the 95 percent confidence interval is about 0.29.

The estimated diversion ratios to other apps are economically significant, although only moderately precise. For Facebook users, two categories (web browsers and “all other apps”) have more positive diversion ratio point estimates than Instagram. For Instagram users, YouTube, TikTok, new apps, web browsers, and “all other apps” have more positive diversion ratio point estimates than Facebook. The bottom row shows that when defining $-j$ as total screen time (on all apps combined, including Facebook and Instagram), the estimated diversion ratios are statistically zero. This means that the data cannot reject that all Facebook or Instagram use is substituted to other apps on the phone, although the estimates are imprecise, especially for Instagram. Diversion ratio estimates for heavy baseline users are slightly more precise but qualitatively similar; see Appendix Figure A4.

This evidence does not support the Federal Trade Commission’s market definition in *FTC v. Meta*. If the appropriate market definition from the user’s perspective included only “personal social networking services,” which the FTC (2021) defined primarily as Facebook, Instagram, and Snapchat, the diversion ratios from Facebook or Instagram to the other two apps would be much higher. In reality, the data imply that Facebook and Instagram compete in a much larger market for users’ time and attention. The FTC (2021) describes qualitatively why “personal social networking” may be a distinct service from the user’s perspective, but the time use diversion ratio is the parameter that matters in our formal model of Meta’s incentive to exercise market power through ad load.

The fact that there is a diffuse set of competitors makes our paper’s duopoly model more reasonable, as our model takes other competitors to be a non-strategic competitive fringe. By

contrast, if the data indicated that Facebook and Instagram’s competition was primarily only one or two platforms, it might have been more realistic to endogenize how those competitors might respond to a merger or separation.

One of Meta’s economic experts, John List, subsequently ran similar deactivation experiments, finding strikingly similar results. To our knowledge, the writeup is not publicly available, but [Benedict \(2025\)](#) reports that the diversion ratios were 0.05 from Facebook to Instagram and 0.12 from Instagram to Facebook, again with YouTube and web browsers both being closer substitutes.

We highlight three caveats. First, the substitution effects and diversion ratios are local to people induced to deactivate by the \$150 payment, and the diversion ratios could be different in the full population. For example, people with higher valuations of Facebook or Instagram might have been unwilling to deactivate precisely because they didn’t think the other platform was a good substitute. In this example, the full-population diversion ratios between Facebook and Instagram would be smaller than our estimates, strengthening our finding that the diversion ratios are small.

Second, the FIES experiment incentivized individual-level deactivation. Network effects could change substitution patterns if ad load changes also affect users’ friends’ time use ([Bursztyn et al. 2025](#)). However, since time use is quite inelastic to ad load, it changes little in our counterfactual simulations in Section 5. Thus, this concern does not seem to be important for our research question.

Third, the FIES experiment incentivized deactivation for a total of only six weeks. In theory, substitution patterns could be different over a longer horizon due to switching costs: users must learn about and download other apps, build new social networks, and develop user histories that apps can use to serve more engaging personalized content. However, there are several reasons why long-run diversion ratios may not be much different than our estimates. First, as shown in Table 1 and Figure 1, most Facebook and Instagram users *already* use the other of those two apps and have thus incurred the switching costs. Second, many other substitute apps could have similar switching costs. Thus, even if Facebook or Instagram became more appealing in the long run, so would many other substitutes, limiting any changes in diversion ratios.

3.4 Price Response

While social media users pay zero price, the price response parameter translates the effects of ad load changes into consumer surplus. We identify the price response by estimating the effect of the DA experiment Screen Time Bonus on Facebook and Instagram time use.

Figure 5 presents daily average Facebook and Instagram use for the Bonus and Control groups. The grey shading indicates the 20-day bonus period (from May 25–June 13) when the Bonus group was being paid to reduce social media use but the Control group was not. Panel (a) shows that among Facebook users during the bonus period, Facebook use in the Control and Bonus groups averaged about 64 and 36 minutes per day, respectively. Panel (b) shows that among Instagram users during the bonus period, Instagram use in the Control and Bonus groups averaged about 20 and 13 minutes per day, respectively. Thus, the bonus reduced Facebook and Instagram use by

just over 40 percent. There are statistically zero differences in all weeks before and after the bonus period; see Appendix Figure A5.

To formally estimate the effect of the bonus on Facebook and Instagram use, define B_i as a Bonus group indicator, and define T_{ij0} and T_{ijb} as use of j during the baseline and bonus periods, respectively. We estimate

$$T_{ijb} = \tau_j^B B_i + \beta T_{ij0} + \beta_0 + \epsilon_{ij}. \quad (19)$$

τ_j^B is the effect of the bonus on use of platform j . For the structural estimation in Section 4, we will need $\hat{\tau}_j^B$ and Control group average use for both Facebook and Instagram users, as well as the covariance matrix between those four parameters. Thus, we jointly estimate these parameters using Seemingly Unrelated Regression. See Appendix Table A2 for results.

The estimates are closely consistent with the raw data in Figure 5. Among Facebook users during the bonus period, Facebook use dropped by about 27 minutes per day, or 42 percent relative to the Control group. Among Instagram users, Instagram use dropped by about 8 minutes per day, or 41 percent relative to Control.

These are strikingly large price responses: they mean that users value more than 40 percent of their Facebook and Instagram use at less than \$2.50 per hour. This will have important bearing on our consumer surplus estimates: changes in time on platform or ad load translate to consumer surplus changes that are smaller than they would be if demand were more inelastic.

We highlight two caveats. First, the DA experiment bonus was only for reducing mobile app use, and time use on other devices was not directly tracked. Allcott, Gentzkow, and Song (2022) present self-reports of use on other devices that strengthen the conclusion that app demand is very elastic. Second, the DA experiment bonus incentivized reduced use of multiple apps, not just Facebook or Instagram individually. Since the diversion ratio estimates above show that the other incentivized apps are slight substitutes for Facebook and Instagram, incentivizing reductions in other apps slightly increases Facebook or Instagram use, which biases the price response slightly toward zero relative to a bonus that only incentivized Facebook and/or Instagram reductions. This further strengthens the conclusion that demand is very elastic.

3.5 Diminishing Returns

The Ad Duplication Experiment allows us to estimate diminishing returns, by comparing click-through rates on duplicated versus non-duplicated ad campaigns.

Table 2 reports summary statistics on the 174 follow-up campaigns in the Ad Duplication Experiment primary sample. The average initial campaign identified an audience size of 1,302 users. The average follow-up campaign reached 65.3 percent of that initial audience. The average *duplicated share* is 0.855. This means that for the average duplicated follow-up campaign, 85.5 percent of its impressions were to users that were also impressed by the other duplicated campaign. The average frequency was 4.07 impressions per user per week, and the average click-through

rate was 1.4 percent. Winsorizing the CTR at the 10th percentile leaves the mean and standard deviation unchanged up to the third decimal. The average cost per 1,000 impressions (CPM) was \$12.41. For comparison, the average CPMs reported by Birch (2025), a market research firm, were around \$14 for both Facebook and Instagram during the month we ran the experiment.

Figure 6 presents the data. For each of the product-budget-objective triples in the primary sample, there are two duplicated campaigns and one non-duplicated campaign. Each dot on the figure is a duplicated campaign. The y-axis is the natural log of a duplicated campaign’s CTR over the CTR of its corresponding non-duplicated campaign. The x-axis is the share of users also impressed by the other duplicated campaign.

If there were no diminishing returns and the duplicated campaigns thus had the same average click-through rate as non-duplicated campaigns, then the best-fit line would be flat at a level of $\ln(1) = 0$. On the other extreme, if the second campaign had no returns, then the average CTR across fully duplicated campaigns would be 50 percent of the non-duplicated one. In that case, the best-fit line would have a downward slope, and at the right of the graph with full duplication, the dashed line would be at $\ln(50\%) \approx -0.69$.

The actual data in Figure 6 are in between those two extremes, and closer to the extreme of no additional returns. As the duplicated share of users in the duplicated treatment condition grows, the relative click-through rates on duplicated campaigns falls. At the point where the dashed best-fit line hits a 1.0 duplication share, the average duplicated campaign has $\ln(\text{CTR})$ about 0.32 lower than non-duplicated ones.

To formally estimate the effect of duplication on click-through rates, index ad campaigns by a and product-budget-objective triples by $g(a)$. Define \tilde{D}_a as the duplicated share (for duplicated campaigns) or zero (for non-duplicated campaigns). Further define F_a as the average frequency (in impressions/user-week), R_a as reach (as a share of the initial audience), and $\nu_{g(a)}$ as a product-budget-objective fixed effect. We estimate

$$\ln(\text{CTR}_a) = \lambda \tilde{D}_a + \beta_F F_a + \beta_R R_a + \nu_{g(a)} + \epsilon_a, \quad (20)$$

instrumenting for \tilde{D}_a with D_a , an indicator for whether ad campaign a is duplicated. λ is the difference in click-through rates for fully duplicated versus non-duplicated campaigns.

Table 3 presents results. The first three columns present OLS estimates of equation (20), while the latter three columns present IV estimates, with each set incrementally adding controls for frequency and reach. The OLS λ is identified from the variation illustrated in Figure 6: the association between click-through rates and duplicated share within the set of duplicated campaigns. The IV λ is identified differently: the Wald estimator gets the difference in average $\ln(\text{CTR})$ for duplicated versus non-duplicated campaigns and scales it up by the average duplicated share.

Despite the different identification and controls, the $\hat{\lambda}$ estimates in all six columns are very similar to each other and to the fit of Figure 6, ranging from -0.262 to -0.353. The coefficients on frequency and reach have the expected signs: they are both negatively associated with CTR, due to diminishing marginal returns to impressions and users impressed. We think of column 6 as our

primary estimate, giving $\hat{\lambda} \approx -0.335$. The results are very similar when we do not winsorize CTRs at the 10th percentile or drop the three campaigns where the duplicated campaigns had less than 50 percent overlap; see Appendix Table A4.

This estimate implies that duplication makes impressions materially less valuable: the average CTR in a fully duplicated campaign is $1 - \exp(-0.335) \approx 28\%$ lower than in a non-duplicated campaign. The economic implication of this result is that there could be material economic losses from separating two platforms if they cannot coordinate ad delivery to avoid duplicate ad impressions to the same users.

We emphasize several caveats. First, while we carefully designed our experiment around representative popular products, we do not know what the results would be in a fully random sample of ads and users. Second, the diminishing return parameter we estimate naturally depends on the number of ad impressions in the campaigns. For example, duplicated campaigns with one impression might have higher CTRs than campaigns with ten impressions. Our diminishing return parameter is exactly externally valid if our follow-up campaign frequencies are representative or if the frequency-CTR relationship is has constant semi-elasticity, as in equation (20). To test whether diminishing returns vary by baseline CTR, we estimate equation (20) with an additional interaction between \tilde{D}_a and an indicator for a in a high budget treatment condition. Appendix Table A5 shows that in all specifications, the interaction effect is statistically zero and the main diminishing returns estimate essentially unchanged, even though frequency is about 50 percent higher in high budget treatments. This supports the external validity of our estimates across campaigns with varying frequencies.

4 Structural Estimation

In this section, we use a minimum distance estimator to estimate the model from Section 1 using the experimental results from Section 3 plus additional parameters. We now describe the functional forms, empirical moments, estimation routine, and parameter estimates.

4.1 Functional Forms

To take the model to the data, we need to impose functional forms on utility and diminishing returns to ad impressions.

4.1.1 Utility

Define y_i as income and n_i as numeraire good consumption, both in units of \$/day. Define b as the price per minute of time spent on social media; $b = 0$ normally, but $b = b^B$ in the DA experiment Bonus condition. We assume that users maximize quadratic utility

$$U_i(\mathbf{T}_i, n_i; \boldsymbol{\alpha}) = \underbrace{\sum_j [(\xi_{ij} - \gamma_j \alpha_j) T_{ij} - \sigma_j T_{ij}^2 / 2]}_{\text{quadratic utility from time on platform}} + \underbrace{\rho T_{i1} T_{i2}}_{\text{numeraire}} + n_i, \quad (21)$$

subject to budget constraint $y_i = n_i + b \sum_j T_{ij}$.

We assume that α_j , σ_j , γ_j , and ρ are homogeneous across users, so all time use heterogeneity arises from differences in ξ_{ij} . Under this functional form, the average and marginal disutility from ads are the same, so there is no [Spence \(1975\)](#) quality distortion.

Maximizing utility gives users' choice of time on platform j as a function of time on the other platform $-j$:

$$T_{ij}(\boldsymbol{\alpha}) = \frac{\xi_{ij} - \gamma_j \alpha_j - b + \rho T_{i,-j}}{\sigma_j}. \quad (22)$$

We model three exogenous user types: Facebook single-homers, Instagram single-homers, and multi-homers. Platform j single-homers exogenously have $T_{i,-j} \equiv 0$. Multi-homers have $T_{ij}(\boldsymbol{\alpha}) > 0$ in the baseline merged equilibrium. Let $k \in \{s, m\}$ index single-homer and multi-homer user types, and define μ_j as the share of j 's users that are multi-homers.

Define ξ_{kj} as the mean of ξ_{ij} for platform j 's user type k . The modeled averages of time on platform j for single-homers, multi-homers, and all users are, respectively:

$$T_{sj} = \frac{\xi_{sj} - \gamma_j \alpha_j - b}{\sigma_j} \quad (23)$$

$$T_{mj} = \frac{\xi_{mj} - \gamma_j \alpha_j - b + \rho T_{m,-j}}{\sigma_j} = \frac{(\xi_{mj} - \gamma_j \alpha_j - b) + (\xi_{m,-j} - \gamma_{-j} \alpha_{-j} - b) \cdot \rho / \sigma_{-j}}{\sigma_j - \rho^2 / \sigma_{-j}} \quad (24)$$

$$T_j = (1 - \mu_j) T_{sj} + \mu_j T_{mj}. \quad (25)$$

We model four treatment conditions, indexed by g . First, condition $g = B$ is the DA experiment Bonus group, modeled by setting $b = b^B$ in equations (23) and (24).¹⁰ In all other conditions, $b = 0$. Second, $g = Dj$ is the FIES experiment Deactivation groups if every user fully deactivated, modeled by setting $T_{ij} = 0$. For multi-homers, this gives $T_{m,-j}^D = \frac{\xi_{m,-j} - \gamma_{-j} \alpha_{-j}}{\sigma_{-j}}$. Third, $g = Aj$ is a condition with no ads on platform j , modeled by setting $\alpha_j = 0$. Fourth, $g = C$ is Control.

Define T_j^g as the modeled average time use in treatment condition g , and define T_{kj}^g as that modeled average for user type k . Define \hat{T}_j^g and \hat{T}_{kj}^g as the observed empirical analogues.

To maintain linear aggregate demand, we do not impose a constraint that $T_{ij} \geq 0$. Thus, in some simulations with higher ad load or $b = b^B$, some individual simulated users with low ξ_{ij} may have negative simulated time use.

¹⁰Note that this formulation ignores the fact that the DA experiment bonus was also for reducing time on several apps that are modeled as part of the outside option. As described in Section 3.4, this biases the price response toward zero and strengthens the conclusion that demand is quite elastic.

4.1.2 Diminishing Returns to Ad Impressions

Assumption 3 requires that for all users, the diminishing returns parameter ζ_i is sufficiently large to ensure that the merged platform doesn't serve them any ad campaign twice. To ensure that this holds for all i , we choose a functional form for ζ_i by rearranging the bound from Assumption 3:

$$\zeta_i = 1 - \kappa \cdot \frac{p_i(\boldsymbol{\alpha}^m)}{\eta \cdot (1 + \eta_0)}, \quad (26)$$

for $\kappa \in [0, 1]$. κ captures the return to a duplicated ad campaign. $\kappa = 0$ implies $\zeta_i = 1$, meaning zero clicks on the duplicate campaign. $\kappa = 1$ implies $0 < \zeta_i < 1$, meaning some additional clicks.

In Section 3.5, we used the Ad Duplication Experiment to estimate a parameter λ capturing the difference in log click-through rates between duplicated and non-duplicated campaigns. To construct the modeled value of λ , recall that user i 's click-through rates for the first and second ad campaigns are ω_{ia} and $(1 - \zeta_i) \cdot \omega_{ia}$, respectively. Thus, the average CTR for a representative sample of users exposed to one campaign is $E[\omega_{ia}]$, and the average per-campaign CTR across representative users exposed to two identical campaigns is $\frac{1}{2}E[\omega_{ia} + (1 - \zeta_i) \cdot \omega_{ia}]$. After rearranging and applying $\omega_{ia} \perp \zeta_i$ from Assumption 1, this equals $E[\omega_{ia}] \cdot E[1 - \zeta_i/2]$. The difference in log CTRs between duplicated and non-duplicated campaigns is thus $\lambda = \ln(E[\omega_{ia}] \cdot E[1 - \zeta_i/2]) - \ln(E[\omega_{ia}]) = \ln(E[1 - \zeta_i/2])$. Substituting equation (26) gives

$$\lambda = \ln \left(\frac{1}{2} + \frac{\kappa}{2} \cdot \frac{1}{N} \sum_i \frac{p_i(\boldsymbol{\alpha}^m)}{\eta \cdot (1 + \eta_0)} \right). \quad (27)$$

4.2 Exogenous Parameters and Empirical Moments

Exogenous parameters. Table 4 presents the exogenous parameters, which we assume have zero standard errors. Since much of our empirical data described in Sections 2 and 3 are from 2020, we also use exogenous parameters from that year when possible.

As described in Section 3.1, we use estimates from the NPORS for the share of Facebook and Instagram users that are multi-homers. The DA experiment bonus was $b^B = \$2.50/\text{hour}$.

Facebook and Instagram ad load were computed specially for this project by Similarweb, a large digital data aggregator. Using a panel of over 100,000 mobile device users in the U.S., they compute that Facebook and Instagram ad loads were $\alpha_F^m = 69.9$ and $\alpha_I^m = 57.6$ ads per hour in 2024. (Their data do not extend back to 2020.) The m superscripts represent that these data correspond to our model's merged equilibrium.¹¹

Because we think of marginal cost c_j as partially representing network effect dynamics and Facebook is a mature social media platform, we assume $c_F = 0$ and estimate c_I for our primary analysis. We normalize the total number of Facebook and/or Instagram users to $N = 1$; this rescales c_I but has no other effect. We also normalize $Am = 1000$; this rescales η and η_0 but has

¹¹Hemphill (2025, slides 24-25) reports a similar hourly Facebook ad load and a similar ratio of Facebook to Instagram ad load for 2022.

no other effect.

Empirical moments. Table 5 presents the empirical moments we use for estimation. Control group time use averages \hat{T}_{kj}^C for our primary analysis are from FIES, as reported in Section 3.2. Diversion ratios $\hat{\delta}_{-j}^j$ are also from FIES, as reported in Section 3.3. Percent responses to the DA bonus $\hat{\tau}_j^B / \hat{T}_j^C$ are from the DA data, as reported in Section 3.4. The duplication effect $\hat{\lambda}$ is from the Ad Duplication Experiment, as reported in Section 3.5.

The percent effect of ad removal on time use is $\frac{T_j^{Aj} - T_j^C}{T_j^C}$. We import this empirical moment from Brynjolfsson et al. (2024), who study a long-term Facebook experiment in which a random 0.5 percent of Facebook users have never received ads in their news feeds. For 53,083 users from 13 countries who opted into their survey in March 2022, they estimate that time spent on Facebook in the week before their survey was 9.4 percent higher in the ad holdout group.¹² For our primary estimates, we assume that this parameter is the same for both Facebook and Instagram.

The Brynjolfsson et al. (2024) estimate is from one week of data in a self-selected sample. However, for the Pandora radio app, Goli et al. (2025) estimate that the long-term elasticity of time on platform with respect to ad load is -0.070. The fact that this is very close to the -0.094 arc elasticity implied by Brynjolfsson et al. (2024) gives additional credibility to the estimates.

Birch, a large firm that helps advertisers optimize social media campaigns, reports weekly Facebook and Instagram ad prices for US audiences (Birch 2025). The average across the two platforms over the 52 weeks in 2020 was $\hat{p}^m = \$10.18$ per 1000 impressions.

4.3 Estimation

We estimate the structural parameters using a minimum distance estimator that minimizes the sum of squared errors between model-predicted moments and their empirical analogues. Define $\Theta := \{\{\xi_{kj}\}, \rho, \{\sigma_j\}, \{\gamma_j\}, \kappa, \eta, \eta_0, c_I\}$ as the vector of 13 structural parameters to be estimated, and define $\mathbf{h}(\Theta) := \left\{ \left\{ h_{kj}^C \right\}, h^D, \left\{ h_j^B \right\}, \left\{ h_j^A \right\}, h^L, h_j^P, \left\{ h_j^F \right\} \right\}$ as the vector of 13 distance functions to be described below. Our estimate of Θ minimizes the sum of squared distance functions:

$$\hat{\Theta} = \arg \min_{\Theta} \mathbf{h}(\Theta)' \mathbf{h}(\Theta). \quad (28)$$

The model is just-identified, so parameter estimates are invariant to choice of weighting matrix. We construct standard errors using the Delta method. See Appendix D.2 for details.

We now detail the distance functions. Following Andrews, Gentzkow, and Shapiro (2017), we also describe which parameters are most elastic to each empirical moment, using the estimated sensitivity matrix presented in Appendix D.3.

Control group use. There are four control group use distance functions, matching average Facebook and Instagram use for single-homers and multi-homers:

¹²They do not report a standard error, but we approximate a standard error of 0.019 percent by visually inspecting the confidence intervals for \hat{T}_j^{Aj} and \hat{T}_j^C reported in Figure 2 of their working paper.

$$h_{kj}^C(\Theta) = T_{kj}^C - \hat{T}_{kj}^C. \quad (29)$$

While the utility function parameters are identified jointly, the average demand shifters ξ_{kj} are particularly sensitive to these empirical moments.

Diversion ratio. There is one diversion ratio distance function, matching the average diversion ratio from Facebook and Instagram deactivation:

$$h^D(\Theta) = \frac{1}{2} \sum_j \left[\frac{T_{-j}^{Dj} - T_{-j}^C}{T_j^C} - \hat{\delta}_{-j}^j \right]. \quad (30)$$

The substitution parameter ρ is most sensitive to this empirical moment.

Price response. There are two price response distance functions, matching the percent reductions in Facebook and Instagram use from the DA experiment bonus:

$$h_j^B(\Theta) = \frac{T_j^B - T_j^C}{T_j^C} - \frac{\hat{\tau}_j^B}{\hat{T}_j^C}. \quad (31)$$

The utility function curvature parameters σ_j are most sensitive to these empirical moments.

Ad response. There are two ad response distance functions, matching the percent increases in Facebook and Instagram use from ad removal:

$$h_j^A(\Theta) = \frac{T_j^{Aj} - T_j^C}{T_j^C} - \frac{\widehat{T_j^{Aj} - T_j^C}}{T_j^C}. \quad (32)$$

The ad load disutility parameters γ_j are particularly sensitive to these empirical moments.

The distance functions described so far fully identify the utility function parameters $\{\xi_{kj}\}$, ρ , $\{\sigma_j\}$, and $\{\gamma_j\}$. In other words, those parameters have zero sensitivity to the remaining moments described below.

Diminishing return. The diminishing return distance function matches the difference in log CTRs between duplicated and non-duplicated campaigns:

$$h^L(\Theta) = \lambda - \hat{\lambda}. \quad (33)$$

The return to duplication κ is the only parameter sensitive to this empirical moment.

Ad price. There is one ad price distance function, matching the Facebook and Instagram average ad price:

$$h_j^P(\Theta) = \frac{\sum_{i \in \mathcal{U}} \alpha \cdot T_i(\alpha^m) \cdot p_i}{\sum_{i \in \mathcal{U}} \alpha \cdot T_i(\alpha^m)} - \hat{p}^m. \quad (34)$$

The modeled moment is the time use-weighted average of user-level ad prices p_i , which is equivalent to the average ad price across impressions.

The merged equilibrium price p_i is a function of α , \mathbf{T}_i , and other variables, per equation (4). After substituting that equation into equation (34), this distance function can be rewritten as a function of the means, variances, and cross-platform covariance of merged equilibrium time use across users, instead of as a sum over i . To speed up estimation, we use that rewritten distance function with time use moments from the observed distribution described in Section 3.2; see Appendix D.1 for details.

Platform first-order condition. Our final two distance functions are the first-order conditions for profit-maximizing ad load on the two merged platforms:

$$h_j^F(\Theta) = \sum_i \left[\frac{\partial p_i}{\partial \alpha_j} \cdot \alpha \cdot \mathbf{T}_i(\alpha) + p_i \cdot \left(T_{ij}(\alpha) + \alpha^m \cdot \frac{\partial \mathbf{T}_i(\alpha)}{\partial \alpha_j} \right) \right] - c_j. \quad (35)$$

From the functional forms in Section 4.1, we have $\frac{\partial \mathbf{T}_i(\alpha)}{\partial \alpha_j} = \frac{-\gamma_j}{\sigma_j - \rho^2 / \sigma_{-j}}$. As with the ad price distance functions, we substitute p_i and $\frac{\partial p_i}{\partial \alpha_j}$ from equation (4) and estimate a rewritten distance function with observed time use moments; again see Appendix D.1 for details.

These distance functions are inspired by the approach of Berry, Levinsohn, and Pakes (1995) and other papers that estimate demand and then use the first-order conditions to infer marginal costs. We reverse that approach: we instead assume zero marginal cost on Facebook and then use the Facebook FOC to infer the demand elasticity. Then the Instagram marginal cost adjusts so that the Instagram FOC also holds. The advertiser demand slope and intercept η and η_0 are jointly sensitive to both the Facebook FOC and the ad price moment. Instagram ad cost c_I is the only parameter sensitive to the Instagram FOC.

4.4 Parameter Estimates

Table 6 presents the structural parameter estimates. Within each platform, the estimated single-homer and multi-homer demand intercepts $\hat{\xi}_{kj}$ are similar, driven by the similar observed average time use for single-homers versus multi-homers. The estimated platform substitution parameter $\hat{\rho}$ is negative, driven by the result that the platforms are mild substitutes. The estimated curvature $\hat{\sigma}_j$ is about three times larger for Instagram for Facebook, driven by the result that the Facebook and Instagram price responses are similar as a percent of Control group use, but Instagram Control group use is about three times smaller. Instagram's larger $\hat{\sigma}_j$ implies that Instagram use will respond less than Facebook use (in absolute minutes) to counterfactual changes in ad load. The estimated ad load disutilities $\hat{\gamma}_j$ are similar between the two platforms, driven by the same assumed ad load response moment.

The estimated return to duplication parameter is $\hat{\kappa} \approx 0.557$, driven by the relatively large decrease in click-through rates on duplicated campaigns in the Ad Duplication Experiment. Recalling the functional form for ζ_i in equation (26), this estimate means that across all users, the CTR on

the second ad campaign is never more than about 56 percent of the CTR on the first. We calculate that in the merged equilibrium, the time use-weighted average diminishing return parameters for Facebook and Instagram are $\zeta_F \approx 0.66$ and $\zeta_I \approx 0.64$. This means that on average, a second campaign on the respective platforms would have CTRs about 66 and 64 percent lower than the first.

The estimated Instagram ad load cost, driven by the Instagram FOC, is $c_I \approx \$0.0007$ per ad/hour. Given the ad load of 57.6 ads/hour, this implies a cost of \$0.043 per user-day. Given ad load, prices, and time use, this is about 39 percent of revenues.

As defined in Section 1, the parameter η is the negative of advertisers' inverse demand slope for impressions to each user. The estimate is $\hat{\eta} \approx 0.080$ (\$/impression)/(share of A), meaning that if ad prices decrease by \$0.001 per impression (about 10 percent of baseline \hat{p}^m), about $\$0.001/(0.080) \approx 1.26\%$ of all advertisers in the market would additionally buy impressions for each user. To translate into an elasticity, we must compute baseline ad quantity. Using formulas in Appendix D.4, we calculate that at Meta's profit-maximizing ad load, the aggregate elasticities of advertiser demand are -1.10 on Facebook and -2.0 on Instagram. This corresponds to intuition from the inverse elasticity markup rule. Since user time is relatively inelastic to ad load and we set $c_F = 0$, Facebook ads have low marginal opportunity cost, and Facebook ad load is optimally set close to the point where advertiser demand is unit elastic. Since the implied c_I is a moderate share of revenues, Instagram ad load is set where advertiser demand is moderately more elastic.

For counterfactuals, we also need estimates of the distribution of user demand shifters ξ_{ij} . We invert equation (22) to back out ξ_{ij} , giving $\hat{\xi}_{ij} = T_{ij}\hat{\sigma}_j + \hat{\gamma}_j\alpha_j^m - \hat{\rho}T_{i,-j}$. We then construct the distribution of $\hat{\xi}_i$ given the estimated parameters and the time use distribution from Figure 1.

5 Counterfactual Simulations

In this section, we use the estimated model to compare the social optimum and merged and separated equilibria. To solve for socially optimal ad load, we numerically maximize total surplus from equation (10). To solve for separated equilibrium ad load, we iterate over the reaction functions until reaching a fixed point. We use a grid of starting points to rule out multiple equilibria. We first present our primary results, followed by alternative specifications and parameter sensitivity analysis. Appendix E presents implementation details.

5.1 Primary Simulation Results

Table 7 presents counterfactual simulation results. Panel (a) presents market outcomes, while Panel (b) presents surplus effects normalized by N , the total number of people that use Facebook and/or Instagram. Column (1) presents the merged equilibrium baseline, while the remaining columns present changes relative to that baseline.

Consider first the merged equilibrium baseline in column (1). The market outcomes in Panel (a) are the same as used for estimation in Section 4. Although all multi-homing users have the same

ad price p_i^m when served on either platform, the average ad prices differ across platforms because the user populations have different time use distributions.

Panel (b) presents baseline levels of consumer and advertiser surplus under our globally linear functional forms. The rough magnitudes are broadly consistent with external estimates. In our model, total annual consumer surplus from Facebook and Instagram is \$1,839 per person who uses Facebook and/or Instagram. For comparison, [Brynjolfsson, Collis, and Eggers \(2019\)](#) estimate that the median Facebook user in 2016 and 2017 would need to be paid \$38–\$48 to give up Facebook for one month, while [Allcott et al. \(2020\)](#) estimate that the median person that used Facebook more than 15 minutes per day in 2018 would need to be paid \$100 to give up Facebook for 28 days. In our model, Facebook and Instagram, respectively, earn \$163 and \$19 in annual ad revenue per adult that uses one or both of the platforms. The Facebook number is much larger because Facebook has more users and higher average time per user. For comparison, [Meta \(2021b\)](#) reported \$164 in total revenue (including Facebook and Instagram) per Facebook monthly active user for the U.S. and Canada in 2020.

Because globally linear demand is a strong assumption, we do not place much emphasis on the exact values of baseline consumer and advertiser surplus. However, it is economically important that consumer surplus is an order of magnitude larger than advertiser surplus or platform profits. Because the estimated ad load response from [Brynjolfsson et al. \(2024\)](#) is highly inelastic, time use changes only slightly as we consider alternative scenarios in columns (2)–(6). For the same reason, consumer surplus changes little in percent terms. However, even these small percent changes in consumer surplus weigh heavily in total surplus because consumer surplus is so large.

Columns (2) and (3) compare the social optimum to the baseline. To understand how ad load changes in the social optimum, recall from Section 1.3 that the planner restricts ad load to avoid consumer harm, while the platform restricts ad load to increase ad prices. Specifically, equation (14) showed that while the planner considers user ad disutility γ_j , the platform considers the level and variance of time use, which govern how ad price changes affect revenue. Since Figure 1 shows that Facebook users have much higher time use variance than Instagram, merged equilibrium ad load is more suppressed on Facebook than Instagram, relative to the social optimum. We calculate that this is the primary reason why our model predicts that in the social optimum, ad load increases on Facebook while decreasing on Instagram.

Aggregating across the two platforms, we calculate that merged equilibrium ad load is too low: ad impressions per person increase from 53.3 impressions/user in the merged equilibrium to 54.3 impressions/user-day in the social optimum. This qualitative finding holds if we re-estimate parameters and re-simulate counterfactuals after equalizing time use variance across platforms. Thus, our conclusion that merged equilibrium ad load is too low depends on our estimates of γ_j and the effect of ad load on revenue, not asymmetric time use variance.

Panel (b) shows that these socially optimal ad load changes would shift surplus from Meta and its users to advertisers, but total surplus is only slightly higher than the merged equilibrium level.

Columns (4) and (5) present the separated equilibrium with coordinated ad delivery. Recall from

Section 1 that in this scenario, Facebook and Instagram independently set ad load to maximize their own profits, but then the available ad slots are allocated optimally across platforms, with one ad price p_i per user. In theory, separating the platforms could either increase or decrease ad load, depending on the relative magnitude of the advertiser-side Cournot effect versus the user-side substitution effect. Since the estimated user diversion ratio and ad load response are both small, the user-side substitution effect is small, and thus the advertiser-side Cournot effect dominates: separation increases ad load as it induces the platforms to compete harder for advertisers. This effect is stronger for Instagram because it has more multi-homers: ad load increases by 1.8 and 38.2 percent on Facebook and Instagram, respectively. As a result, ad prices decrease by 3.4 percent and 9.2 percent on Facebook and Instagram, respectively.

As described above, the ad load increases cause only small percent changes in time use and consumer surplus, but consumer surplus is still a key part of the total surplus change. Overall, consumer surplus decreases by about \$10.18 per user-year, advertiser surplus increases by \$9.10 per user-year, Facebook profits decrease as the Instagram ad load increase cannibalizes Facebook profits, and Instagram profits increase. Total surplus decreases by \$2.62 per user-year, or about 0.1 percent. Thus, separating the platforms generates a net transfer from the platforms and their users to advertisers and a small overall social loss.

Columns (6) and (7) present the separated equilibrium with uncoordinated ad delivery. Recall from Section 1 that in this equilibrium, Facebook and Instagram allocate ad slots optimally within each platform, but the two platforms may serve duplicate ad impressions to the same multi-homing user. When the platforms are separated, inefficient duplication affects profit-maximizing ad load beyond the advertiser-side Cournot effect by reducing ad prices and generating the “business stealing” incentive to reduce marginal overlap. The overall effect is to increase ad loads by 9.4 and 46.4 percent on Facebook and Instagram, respectively, relative to the merged equilibrium baseline. Since duplication reduces the value of ads, ad prices are lower than in the coordinated ad delivery scenario—especially for Instagram, which has higher marginal duplication than Facebook because it has more multi-homing users and lower average time use.

Duplication loss also substantially affects surplus. At the separated equilibrium ad load, we compute $\zeta_F \approx 0.66$ and $\zeta_I \approx 0.64$, meaning that the second ad campaign on the two platforms has 66 and 64 percent lower click-through rate. Advertiser surplus increases by 15.0 percent relative to the merged equilibrium. However, if there were no duplication loss (i.e., if $\zeta_i = 0, \forall i$) but the same ad loads and prices, advertiser surplus would increase by 56.5 percent relative to the merged equilibrium.

If Facebook and Instagram were separated in reality, duplication loss would likely be somewhere in between the two scenarios we model. Fully coordinated ad delivery seems unlikely due to technical and privacy constraints. However, the large duplication loss in the uncoordinated ad delivery case also seems unlikely, for several reasons. First, the separated platforms could eventually predict different ω_{ia} given different data and algorithms, as we model in Appendix A.3. Second, platforms could adjust ad frequency in a way that our model does not contemplate. Third, some social

media advertising is via “custom lists” of specific users provided by advertisers, and multi-homing advertisers could submit disjoint custom lists on separate platforms to avoid duplication. Fourth, even without explicit data on which users multi-home, separated platforms’ ad delivery systems could infer lower ω_{ia} for multi-homing users as they start to click less because of seeing duplicate impressions on another platform. Thus, we think of these scenarios as possible bounds on the effects of separation through ad load and duplication.

5.2 Alternative Specifications

As described in Section 3.2, the FIES data imply that average daily Facebook use is considerably higher than average Instagram use, while eMarketer (2025) reports more similar values. Appendix E.5 presents alternative parameter estimates and counterfactual simulations under the eMarketer (2025) time use assumptions. The magnitudes of various predictions change, but the qualitative implications are similar.

We think of the Instagram marginal cost c_I as a reduced form for network effects and other reasons why the ad load first order condition doesn’t exactly match the data. Appendix E.5.2 presents results under an alternative model where we set $c_I = c_F = 0$, drop the Instagram ad response distance function h_I^A from the estimation, and use the Instagram FOC to identify the Instagram ad disutility γ_I . In that appendix, we also present a model with explicit network effects and interpret the estimates through the lens of that model. The estimated elasticity of Instagram time use with respect to ad load is much larger than the individual-level direct effect from Brynjolfsson et al. (2024). As a result, the modeled social optimum involves zero ads on Instagram, and separation decreases Instagram ad load as Instagram competes harder on the user side. We do not currently think of this as our primary specification because we think that the implied ad load elasticity may be too large and because it takes a more specific stand on the reason why the FOCs don’t exactly match the data.

5.3 Parameter Sensitivity Analysis

We now explore the sensitivity of the counterfactual simulation results to different values of key parameters. We perturb one structural parameter at a time, leaving the rest unchanged, and find equilibrium ad load and total surplus. In each of Figures 7–10, Panel (a) presents ad load on each platform in the merged equilibrium and separated equilibrium with uncoordinated ad delivery, relative to ad load in the merged equilibrium at baseline parameter value. The merged equilibria are in solid lines, while the separated equilibria are in dashed lines; Facebook and Instagram are blue and orange, respectively. Panel (b) presents the effect of separation with uncoordinated ad delivery on total surplus, as a share of total surplus in the merged equilibrium at the baseline parameter value.

Figure 7 presents the effects of varying the platform substitution parameter ρ . The baseline value is $\hat{\rho} \approx -1.18$ \$/hour², from diversion ratios of 0.054 and 0.096. Moving to the right on Panel (a) shows that as the platforms become weaker substitutes and eventually stronger complements,

separation causes larger ad load increases, as the separated platforms have less incentive to restrain ad load to compete for users. The platforms would have to be much stronger substitutes than the FIES diversion ratios suggest for separation to reduce ad load in this model. These effects are stronger for Instagram, because more of its users are multi-homers. Panel (b) shows that the total surplus effect of separation is less negative as the platforms become stronger substitutes.

Panel (b) shows the importance of credibly estimating the user diversion ratio: if the platforms were stronger substitutes, then platform separation could increase total surplus as the decreased ad load would increase user surplus by enough to overwhelm the loss of advertiser surplus and increased duplication of impressions.

Figure 8 presents the effects of varying the ad disutility parameter γ . The baseline values for Facebook and Instagram are $\gamma_F \approx \$0.0078$ and $\gamma_I \approx \$0.0087$ of disutility per ad. All lines in Panel (a) are downward sloping, confirming that platforms serve fewer ads when users dislike ads more. At low γ_j , separating the platforms causes them to compete harder for advertisers by increasing ad load relative to the merged equilibrium, so the dashed lines are above the solid lines. At high γ_j , separation causes the platforms to instead compete harder for users by decreasing ad load relative to the merged equilibrium, so the dashed lines are eventually below the solid lines.

This generates the non-monotonic relationship in Panel (b). At low γ_j , the high ad load increases advertiser surplus but does not harm user surplus because users don't care about ads. At intermediate γ_j , separation still increases ad load as platforms compete primarily for advertisers, but the user surplus loss overwhelms the advertiser surplus gain. At high γ_j , separation decreases ad load, and the user surplus gain eventually outweighs the lost advertiser surplus.

Figure 9 presents the effects of varying user overlap. To increase overlap (moving to the right of the graph from the baseline), we combine pairs of Facebook and Instagram single-homers into multi-homers. To decrease overlap, (moving to the left from the baseline), we split multi-homers into separate Facebook and Instagram single-homers. As we combine or split users, we adjust utility functions so that time use and consumer surplus are both unchanged at merged equilibrium ad load; see Appendix E.4 for details. There is a kink in the predictions at the baseline because single-homers and multi-homers have different time use distributions, but we don't think of this as economically substantive. We stop increasing overlap once all Instagram users are multi-homers, and stop decreasing overlap once all users are single-homers.

Panel (a) shows that in the merged equilibrium, ad load is mostly decreasing in overlap. When more users are single-homers, higher ad load on platform j decreases inframarginal revenue on platform $-j$ (and hence total revenue) by less, encouraging higher ad load. The effect is greater on Instagram, since a greater share of Instagram multi-homer time use is on Facebook than vice versa. Separation has no effect on ad load when all users are single-homers, as even separated platforms are monopolists over their single-homers. When more users are multi-homers, separation increases ad load by more, due to the advertiser-side Cournot and business stealing effects.

Panel (b) shows that more overlap implies less benefit and eventually larger total surplus loss from separation. This is for two reasons. First, the larger ad load increase at higher overlap harms

users. Second, more overlap causes more inefficient duplication. The y-axis scale indicates that the effect of separation on total surplus is relatively sensitive to overlap, underscoring the importance of reliable user data. With 40 percent multi-homers instead of 50 percent, separation increases instead of decreases total surplus.

Finally, Figure 10 presents the effects of varying diminishing returns. To do this, we vary κ on its entire admissible range from its maximum at $\kappa = 1$, implying low ζ_j and thus low diminishing returns, to its minimum at $\kappa = 0$, implying $\zeta_j = 1$ and thus fully diminishing returns. For this figure only, we set $c_I = 0$ and present changes relative to the re-computed merged equilibrium. (This eliminates an effect where c_I becomes very important as ad prices drop, which we do not think is economically substantive.)

Panel (a) shows that higher ζ_j causes a greater ad load increase from platform separation. This is because higher ζ_j amplifies the business stealing incentive for platforms to increase ad load to avoid duplication. The effect is greater on Instagram than on Facebook because Instagram has more multi-homers.

Panel (b) shows that more strongly diminishing returns implies more total surplus loss from separation. This is both because users dislike the higher ad load and because duplicated ad impressions generate less value.

6 Conclusion

This paper lays out a new model of competition between digital media platforms with targeted advertising. The model unifies earlier models of two-sided platforms with other models of advertising markets with multi-homing users and inefficient duplication. The setup is tailored to the institutional details of digital advertising, which has become increasingly important in recent years. Our model characterizes the distortions when media platforms are merged versus separated, highlighting the key empirical parameters for antitrust policy evaluation. We apply the model to the proposed separation of Facebook and Instagram, presenting evidence that Instagram has more multi-homing users, the user-side diversion ratio and ad load elasticity are both low, and returns to duplicate ads could be limited.

We present a variety of counterfactual scenarios with coordinated versus uncoordinated ad delivery and alternative assumptions for time use, user substitution, ad aversion, overlap, and diminishing returns. Across these scenarios, the magnitudes of various predictions change. However, the core qualitative predictions are driven by credible empirical moments and are fairly robust across alternative specifications and parameter values. Separating Facebook and Instagram would primarily increase competition for advertisers, not for users, likely increasing ad load and reducing ad prices, especially on Instagram. This would harm users, benefit advertisers, and generate only a small percent change in the total surplus that Facebook and Instagram provide.

While we disseminated the working paper and have publicly presented results as the *FTC v. Meta* case was in process, the final paper may not be published before the case is decided. We think

of our contributions as being durable far beyond the life of this case, by offering an empirically tractable model of media platform competition and demonstrating one policy relevant application with an extraordinary collection of data.

References

- Allcott, Hunt, Luca Braghieri, Sarah Eichmeyer, and Matthew Gentzkow. 2020. “The Welfare Effects of Social Media.” *American Economic Review* 110 (3):629–676.
- Allcott, Hunt, Matthew Gentzkow, Winter Mason, Arjun Wilkins, Annie Franco, Chad Kiewiet de Jonge, Natalie Jomini Stroud, Joshua Tucker et al. 2024. “The Effects of Facebook and Instagram on the 2020 Election: A Deactivation Experiment.” *Proceedings of the National Academy of Sciences* 121 (21).
- Allcott, Hunt, Matthew Gentzkow, and Lena Song. 2022. “Digital Addiction.” *American Economic Review* 112 (7):2424–2463.
- Allcott, Hunt, Matthew Gentzkow, Benjamin Wittenbrink, Chad Kiewiet de Jonge, Winter Mason, Natalie Jomini Stroud, Joshua Tucker et al. 2025. “The Effect of Deactivating Facebook and Instagram on Users’ Emotional State.” *American Economic Journal: Economic Policy* forthcoming.
- Allcott, Hunt, Levi Kiefer, and Poum Tangkitvanich. 2025. “The Effects of Facebook and Instagram on Political Outcomes for the Average User.” SSRN Working Paper 5341362, URL: https://papers.ssrn.com/sol3/papers.cfm?abstract_id=5341362.
- Ambrus, Attila, Emilio Calvano, and Markus Reisinger. 2016. “Either or Both Competition: A “Two-Sided” Theory of Advertising With Overlapping Viewerships.” *American Economic Journal: Microeconomics* 8 (3):189–222.
- Anderson, Simon and Stephen Coate. 2005. “Market Provision of Broadcasting: A Welfare Analysis.” *Review of Economic Studies* 72 (4):947–972.
- Anderson, Simon and André De Palma. 2012. “Competition for Attention in the Information (Overload) Age.” *RAND Journal of Economics* 43 (1):1–25.
- Anderson, Simon, Øystein Foros, and Hans Jarle Kind. 2018. “Competition for Advertisers and for Viewers in Media Markets.” *Economic Journal* 128 (608):34–54.
- Anderson, Simon, Øystein Foros, Hans Jarle Kind, and Martin Peitz. 2012. “Media Market Concentration, Advertising Levels, and Ad Prices.” *International Journal of Industrial Organization* 30 (3):321–325.
- Anderson, Simon and Martin Peitz. 2023. “Ad Clutter, Time Use, and Media Diversity.” *American Economic Journal: Microeconomics* 15 (2):227–270.

- Andrews, Isaiah, Matthew Gentzkow, and Jesse Shapiro. 2017. “Measuring the Sensitivity of Parameter Estimates to Estimation Moments.” *Quarterly Journal of Economics* 132 (4):1553–1592.
- Aridor, Guy. 2025. “Measuring Substitution Patterns in the Attention Economy: An Experimental Approach.” *RAND Journal of Economics* forthcoming.
- Armstrong, Mark. 2006. “Competition in Two-Sided Markets.” *RAND Journal of Economics* 37 (3):668–691.
- Athey, Susan, Emilio Calvano, and Joshua Gans. 2018. “The Impact of Consumer Multi-Homing on Advertising Markets and Media Competition.” *Management Science* 64 (4):1574–1590.
- Benedict, Brendan. 2025. “Lies, Damned Lies, and Statistics: Meta’s Case-in-Chief Draws Sharp Words.” URL: <https://www.bigtechontrial.com/p/lies-damned-lies-and-statistics-metas>.
- Benzell, Seth and Avinash Collis. 2022. “Regulating Digital Platform Monopolies: The Case of Facebook.” SSRN Working Paper 3619535, URL: https://papers.ssrn.com/sol3/papers.cfm?abstract_id=3619535.
- Bergemann, Dirk and Alessandro Bonatti. 2011. “Targeting in Advertising Markets: Implications for Offline Versus Online Media.” *RAND Journal of Economics* 42 (3):417–443.
- Berry, Steven, James Levinsohn, and Ariel Pakes. 1995. “Automobile Prices in Market Equilibrium.” *Econometrica* 63 (4):841–890.
- Berry, Steven and Joel Waldfogel. 2001. “Do Mergers Increase Product Variety? Evidence From Radio Broadcasting.” *Quarterly Journal of Economics* 116 (3):1009–1025.
- Birch. 2025. “Facebook Advertising Costs by CPM.” URL: <https://app.bir.ch/facebook-advertising-costs>. Accessed May 30, 2023.
- Brynjolfsson, Erik, Avinash Collis, and Felix Eggers. 2019. “Using Massive Online Choice Experiments to Measure Changes in Well-being.” *Proceedings of the National Academy of Sciences* 116 (15):7250–7255.
- Brynjolfsson, Erik, Avinash Collis, Asad Liaqat, Daley Kutzman, Haritz Garro, Daniel Deisenroth, and Nils Wernerfelt. 2024. “The Consumer Welfare Effects of Online Ads: Evidence From a 9-Year Experiment.” NBER Working Paper 32846, URL: www.nber.org/papers/w32846.
- Bursztyn, Leonardo, Matthew Gentzkow, Rafael Jiménez-Durán, Aaron Leonard, Milojević Filip, and Christopher Roth. 2025. “Measuring Markets for Network Goods.” NBER Working Paper 33901, URL: <https://www.nber.org/system/files/working-papers/w33901/w33901.pdf>.

- Chandra, Ambarish and Allan Collard-Wexler. 2009. “Mergers in Two-Sided Markets: an Application to the Canadian Newspaper Industry.” *Journal of Economics and Management Strategy* 18 (4):1045–1070.
- Chen, Daniel. 2024. “The Market for Attention.” Unpublished, URL: danieltchen.com.
- CMA. 2020. “Online Platforms and Digital Advertising: Market Study Final Report.” URL: https://assets.publishing.service.gov.uk/media/5efc57ed3a6f4023d242ed56/Final_report_1_July_2020_.pdf.
- Comscore. 2014. “US Digital Future in Focus 2014.” URL: <https://www.comscore.com/Insights/Presentations-and-Whitepapers/2014/2014-US-Digital-Future-in-Focus>.
- Conlon, Christopher and Julie Mortimer. 2013. “Demand Estimation Under Incomplete Product Availability.” *American Economic Journal: Microeconomics* 5 (4):1–30.
- Conlon, Christopher, Julie Mortimer, and Paul Sarkis. 2021. “Estimating Preferences and Substitution Patterns From Second Choice Data Alone.” Working Paper at IIOC, URL: www.editorialexpress.com/conference/IIOC2023/program/IIOC2023.html.
- Conlon, Christopher and Julie Holland Mortimer. 2021. “Empirical Properties of Diversion Ratios.” *RAND Journal of Economics* 52 (4):693–726.
- Dentsu. 2024. “Global Ad Spent Forecasts: December 2024.” URL: <https://insight.dentsu.com/ad-spend-dec-2024/>.
- eMarketer. 2025. “Forecasts.” URL: <https://www.emarketer.com/forecasts/>.
- Fan, Ying. 2013. “Ownership Consolidation and Product Characteristics: A Study of the US Daily Newspaper Market.” *American Economic Review* 103 (5):1598–1628.
- Federal Trade Commission. 2021. “Amended Complaint, Case No. 1:20-cv-03590-JEB.” URL: https://www.ftc.gov/system/files/documents/cases/ecf_75-1_ftc_v_facebook_public_redacted_fac.pdf.
- Gentzkow, Matthew, Jesse Shapiro, and Michael Sinkinson. 2014. “Competition and Ideological Diversity: Historical Evidence From US Newspapers.” *American Economic Review* 104 (10):3073–3114.
- Gentzkow, Matthew, Jesse Shapiro, Frank Yang, and Ali Yurukoglu. 2024. “Pricing Power in Advertising Markets: Theory and Evidence.” *American Economic Review* 114 (2):500–533.
- Goldfarb, Avi. 2006. “The Medium-Term Effects of Unavailability.” *Quantitative Marketing and Economics* 4:143–171.

- Goli, Ali, Jason Huang, David Reiley, and Nickolai Riabov. 2025. “Measuring Consumer Sensitivity to Audio Advertising: a Long-run Field Experiment on Pandora Internet Radio.” *Quantitative Marketing and Economics*.
- Hemphill, C Scott. 2025. “FTC v. Meta, Case No. 1:20-cv-03590-JEB, Illustrative Aid PDX0149.” URL: <https://ftcvmeta.app.box.com/s/b8m39toze8ucgmj93jjssjtp0k0w97qz/file/1877125814096>.
- Jeziorski, Przemysław. 2014. “Effects of Mergers in Two-Sided Markets: the US Radio Industry.” *American Economic Journal: Microeconomics* 6 (4):35–73.
- Johnson, Garret, Randall Lewis, and David Reiley. 2016. “Location, Location, Location: Repetition and Proximity Increase Advertising Effectiveness.” SSRN Working Paper 2268215, URL: papers.ssrn.com/sol3/papers.cfm?abstract_id=2268215.
- Kemp, Simon. 2020. “Digital 2020: The United States of America.” URL: <https://datareportal.com/reports/digital-2020-united-states-of-america>.
- . 2025. “Digital 2025: Global Overview Report.” URL: <https://datareportal.com/reports/digital-2025-global-overview-report>.
- Lewis, Randall. 2010. *Where’s the “Wear-Out?” Online Display Ads and the Impact of Frequency*. Ph.D. thesis, MIT.
- Meta. 2016. “Effective Frequency: Reaching Full Campaign Potential.” URL: <https://www.facebook.com/business/news/insights/effective-frequency-reaching-full-campaign-potential>.
- . 2021a. “Facebook Files Second Motion to Dismiss the Lawsuit Brought by the FTC.” URL: <https://about.fb.com/news/2021/10/facebook-files-second-motion-to-dismiss-the-lawsuit-brought-by-the-ftc/>.
- . 2021b. “Facebook, Inc. Form 10-K.” URL: <https://d18rn0p25nwr6d.cloudfront.net/CIK-0001326801/4dd7fa7f-1a51-4ed9-b9df-7f42cc3321eb.pdf>.
- Pew Research Center. 2020. “2020 National Public Opinion Reference Survey (NPORS).” URL: <https://www.pewresearch.org/methods/dataset/2020-national-public-opinion-reference-survey-npors/>.
- Prat, Andrea and Tommaso Valletti. 2022. “Attention Oligopoly.” *American Economic Journal: Microeconomics* 14 (3):530–557.
- Rochet, Jean-Charles and Jean Tirole. 2003. “Platform Competition in Two-Sided Markets.” *Journal of the European Economic Association* 1 (4):990–1029.

- . 2006. “Two-Sided Markets: a Progress Report.” *RAND Journal of Economics* 37 (3):645–667.
- Rysman, Marc. 2009. “The Economics of Two-Sided Markets.” *Journal of Economic Perspectives* 23 (3):125–143.
- Scott Morton, Fiona and David Dinielli. 2020. “Roadmap for an Antitrust Case Against Facebook.” *Omidyar Network* URL: <https://omidyar.com/news/roadmap-for-an-antitrust-case-against-facebook/>.
- SensorTower. 2024. “Digital Market Index: Q1 2024.” URL: <https://sensortower.com/q1-2024-digital-market-index>.
- Spence, A Michael. 1975. “Monopoly, Quality, and Regulation.” *Bell Journal of Economics* 6 (2):417–429.
- Stigler Center. 2019. “Stigler Committee on Digital Platforms Final Report.” URL: <https://www.chicagobooth.edu/-/media/research/stigler/pdfs/digital-platforms---committee-report---stigler-center.pdf>.
- Weyl, E Glen. 2010. “A Price Theory of Multi-Sided Platforms.” *American Economic Review* 100 (4):1642–1672.
- Wollmann, Thomas. 2018. “Trucks Without Bailouts: Equilibrium Product Characteristics for Commercial Vehicles.” *American Economic Review* 108 (6):1364–1406.
- Zubarov, Andrey. 2021. “The TV Advertising Industry: Demographic Segmentation and the Impact of Viewership Decline.” SSRN Working Paper 3853300, URL: https://papers.ssrn.com/sol3/papers.cfm?abstract_id=3853300.

Table 1: **Facebook and Instagram Use and Overlap**

	(1)	(2)
	Facebook	Instagram
Share of FB+IG users that use app	0.933	0.586
Share of app users that use other app	0.556	0.885

Notes: This table presents Facebook and Instagram use statistics from the 2020 National Public Opinion Reference Survey ([Pew Research Center 2020](#)).

Table 2: **Ad Duplication Experiment Summary Statistics**

	(1)	(2)
	Mean	Std. Dev.
Initial audience size	1,302	452
Reach (share of initial audience)	0.653	0.544
Frequency (impressions/week)	4.07	1.35
Duplicated share	0.855	0.120
Click-through rate	0.014	0.016
Click-through rate (winsorized at 10th percentile)	0.014	0.016
Cost per click	3.09	4.04
Cost per 1,000 impressions	12.41	4.87

Notes: This table presents summary statistics for the Ad Duplication Experiment. The sample size is 174 observations.

Table 3: **Effects of Duplication on Ad Campaign Click-Through Rates**

	OLS			IV		
	(1)	(2)	(3)	(4)	(5)	(6)
Duplicated share	-0.270 (0.044)	-0.326 (0.053)	-0.353 (0.051)	-0.262 (0.045)	-0.316 (0.054)	-0.335 (0.052)
Frequency (impressions/week)		-0.073 (0.041)	-0.160 (0.045)		-0.068 (0.040)	-0.150 (0.044)
Reach (share of initial audience)			-0.451 (0.107)			-0.443 (0.104)
Product-stratum fixed-effects	Yes	Yes	Yes	Yes	Yes	Yes
Observations	174	174	174	174	174	174
Within Adjusted R ²	0.184	0.193	0.229	0.184	0.192	0.228
F-test (1st stage), Duplicated share				5,037	3,206	3,348

Notes: This table presents estimates of equation (20), measuring the change in click-through rates from fully duplicated relative to non-duplicated ad campaigns. Columns (1)–(3) are OLS estimates, while columns (4)–(6) are IV estimates instrumenting for *duplicated share* with the duplicated treatment group indicator. Standard errors are robust and clustered by product-objective-budget-treatment group, i.e., with three observations per cluster.

Table 4: **Exogenous Parameters**

Parameter	Description	Value	Source
μ_F	Share of FB users that are multi-homers	0.556	NPORS
μ_I	Share of IG users that are multi-homers	0.885	NPORS
b^B	DA experiment bonus (\$/hour)	2.50	DA
α_F^m	FB ad load (ads/hour)	69.9	Similarweb
α_I^m	IG ad load (ads/hour)	57.6	Similarweb
c_F	FB marginal cost of ad load (\$/(ad/hour))	0	Assumption
N	Number of Facebook and/or Instagram users	1	Normalization
Am	Advertisers \times impressions/campaign	1,000	Normalization

Notes: This table presents the exogenous parameters used to construct the distance functions described in Section 4. “NPORS” refers to the National Public Opinion Reference Survey. “DA” refers to the Digital Addiction experiment.

Table 5: **Empirical Moments**

Parameter	Description	Value	SE	Source
\hat{T}_{sF}^C	Single-homer average FB use (hours/day)	0.720	0.04	FIES
\hat{T}_{mF}^C	Multi-homer average FB use (hours/day)	0.685	0.02	FIES
\hat{T}_{sI}^C	Single-homer average IG use (hours/day)	0.263	0.04	FIES
\hat{T}_{mI}^C	Multi-homer average IG use (hours/day)	0.220	0.0093	FIES
$\frac{\hat{\delta}_I^F + \hat{\delta}_F^I}{2}$	Average diversion ratio	0.075	0.05	FIES
$\frac{\hat{\tau}_F^B}{\hat{T}_F^C}$	FB bonus response	-0.416	0.05	DA
$\frac{\hat{\tau}_I^B}{\hat{T}_I^C}$	IG bonus response	-0.411	0.08	DA
$\frac{\widehat{T_j^{Aj} - T_j^C}}{T_j^C}$	Effect of ad removal	0.094	0.019	Brynjolfsson et al. (2024)
$\hat{\lambda}$	Duplication effect on $\ln(\text{CTR})$	-0.335	0.053	Ad Duplication Experiment
\hat{p}^m	Average ad price (\$/1000 impressions)	10.18	0.351	Birch (2025)

Notes: This table presents the empirical moments used to construct the distance functions described in Section 4. “FIES” refers to the Facebook and Instagram Election Study. “DA” refers to the Digital Addiction experiment.

Table 6: **Parameter Estimates**

Parameter	Description	Units	Estimate	SE
ξ_{sF}	FB single-homer demand intercept	\$/hour	6.6	0.74
ξ_{mF}	FB multi-homer demand intercept	\$/hour	6.5	0.72
ξ_{sI}	IG single-homer demand intercept	\$/hour	6.8	1.52
ξ_{mI}	IG multi-homer demand intercept	\$/hour	6.6	0.99
ρ	Platform substitution	\$/hour ²	-1.18	0.77
σ_F	FB curvature	\$/hour ²	8.4	0.93
σ_I	IG curvature	\$/hour ²	23.8	4.53
γ_F	FB ad load disutility	\$/ad	0.0078	0.0018
γ_I	IG ad load disutility	\$/ad	0.0087	0.0024
κ	Return to duplication		0.557	0.10
η	Advertiser demand slope	$\frac{\$/impression}{\text{share of } A}$	0.080	0.01
η_0	Advertiser demand intercept	share of A	-0.765	0.03
c_I	IG ad load cost	\$/ (ad/hour)	0.0007	0.0001

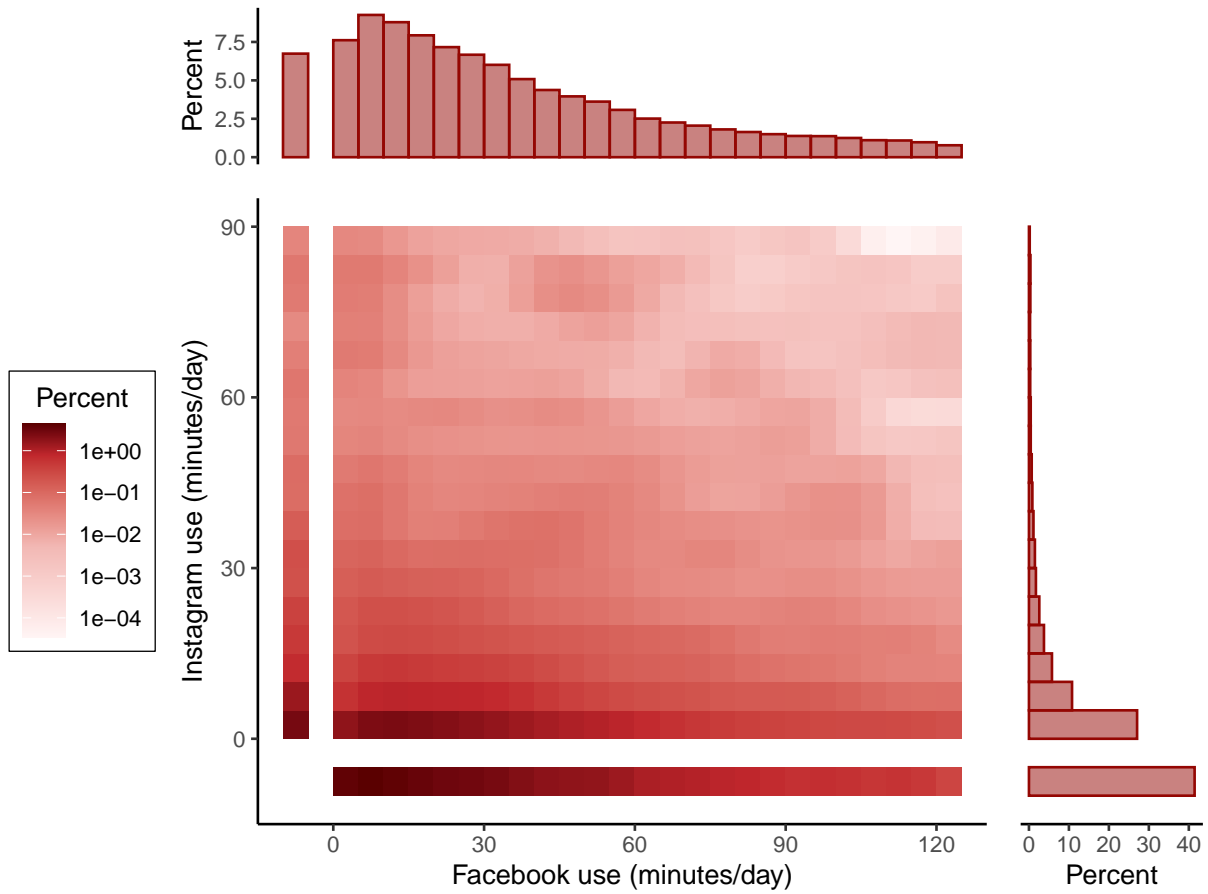
Notes: This table presents the parameter estimates from the estimation procedure described in Section 4.

Table 7: Counterfactual Simulations

	Baseline	Social optimum		FB-IG separation coordinated ads		FB-IG separation uncoordinated ads	
	(1)	(2)	(3)	(4)	(5)	(6)	(7)
		Δ from baseline	% Δ from baseline	Δ from baseline	% Δ from baseline	Δ from baseline	% Δ from baseline
Panel (a): Market Outcomes							
FB ad load (ads/hour)	69.9	7.4	10.6%	1.3	1.8%	6.6	9.4%
IG ad load (ads/hour)	57.6	-26.4	-45.7%	22.0	38.2%	26.7	46.4%
Average time on FB (hours/day)	0.70	-0.01	-1.1%	-0.00	-0.1%	-0.01	-0.8%
Average time on IG (hours/day)	0.23	0.01	4.4%	-0.01	-3.6%	-0.01	-4.2%
Average FB ad price (\$/1000 impressions)	9.8	-0.65	-6.6%	-0.34	-3.4%	-0.99	-10.1%
Average IG ad price (\$/1000 impressions)	12.5	0.97	7.7%	-1.2	-9.2%	-4.4	-35.1%
Panel (b): Surplus							
Consumer surplus (\$/user-year)	1,839	-3.7	-0.2%	-10.2	-0.6%	-21.5	-1.2%
Advertiser surplus (\$/user-year)	82.7	8.5	10.2%	9.1	11.0%	12.4	15.0%
if no duplication loss (\$/user-year)	82.7	8.5	10.2%	9.1	11.0%	46.7	56.5%
duplication loss (\$/user-year)	0.00	0.00	0.0%	0.00	0.0%	34.3	41.5%
Advertiser + consumer surplus (\$/user-year)	1,922	4.8	0.2%	-1.1	-0.1%	-9.1	-0.5%
Platform surplus: FB (\$/user-year)	163	3.5	2.1%	-2.9	-1.8%	-4.9	-3.0%
Platform surplus: IG (\$/user-year)	19.2	-6.4	-33.5%	1.4	7.1%	-10.5	-54.9%
Total surplus (\$/user-year)	2,104	1.8	0.1%	-2.6	-0.1%	-24.6	-1.2%

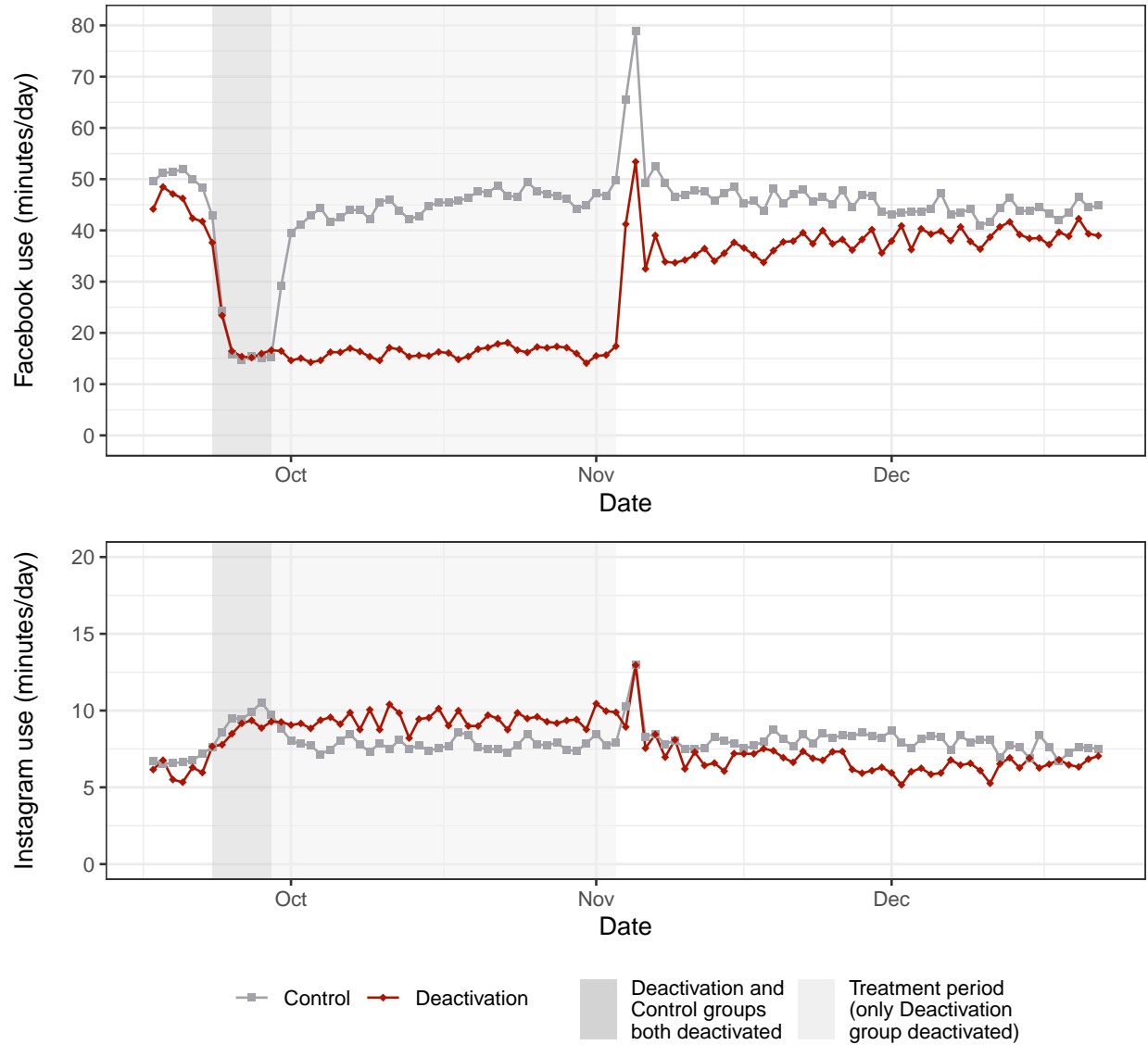
Notes: This table presents the counterfactual simulation results. Column (1) presents the merged equilibrium, which we label as the “baseline.” Columns (2) and (3) present the social optimum, columns (4) and (5) present the separated equilibrium with uncoordinated ad delivery, and columns (6) and (7) present the separated equilibrium with coordinated ad delivery.

Figure 1: **Distribution of Facebook and Instagram Time Use**



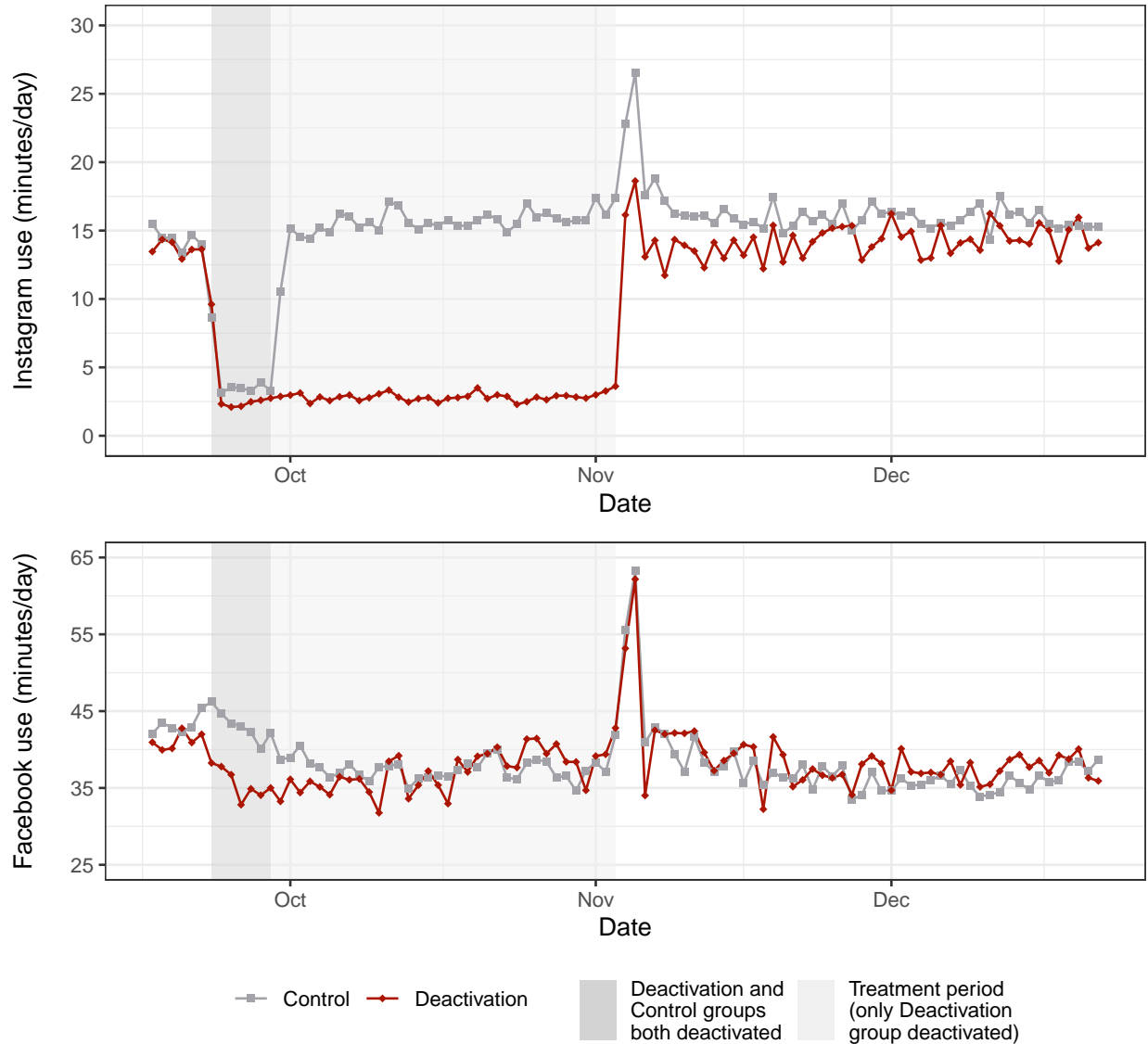
Notes: This figure describes the distribution of Facebook and Instagram time use in the Facebook and Instagram Election Study passive tracking sample Control groups in the last four weeks of the treatment period (October 7–November 3). The histograms at the top and right, respectively, present the marginal distributions of Facebook and Instagram use. Single-homers (consumers with exactly zero time use on a platform) are plotted separately as values less than zero.

Figure 2: **Daily Facebook and Instagram Use in Facebook Deactivation Experiment**



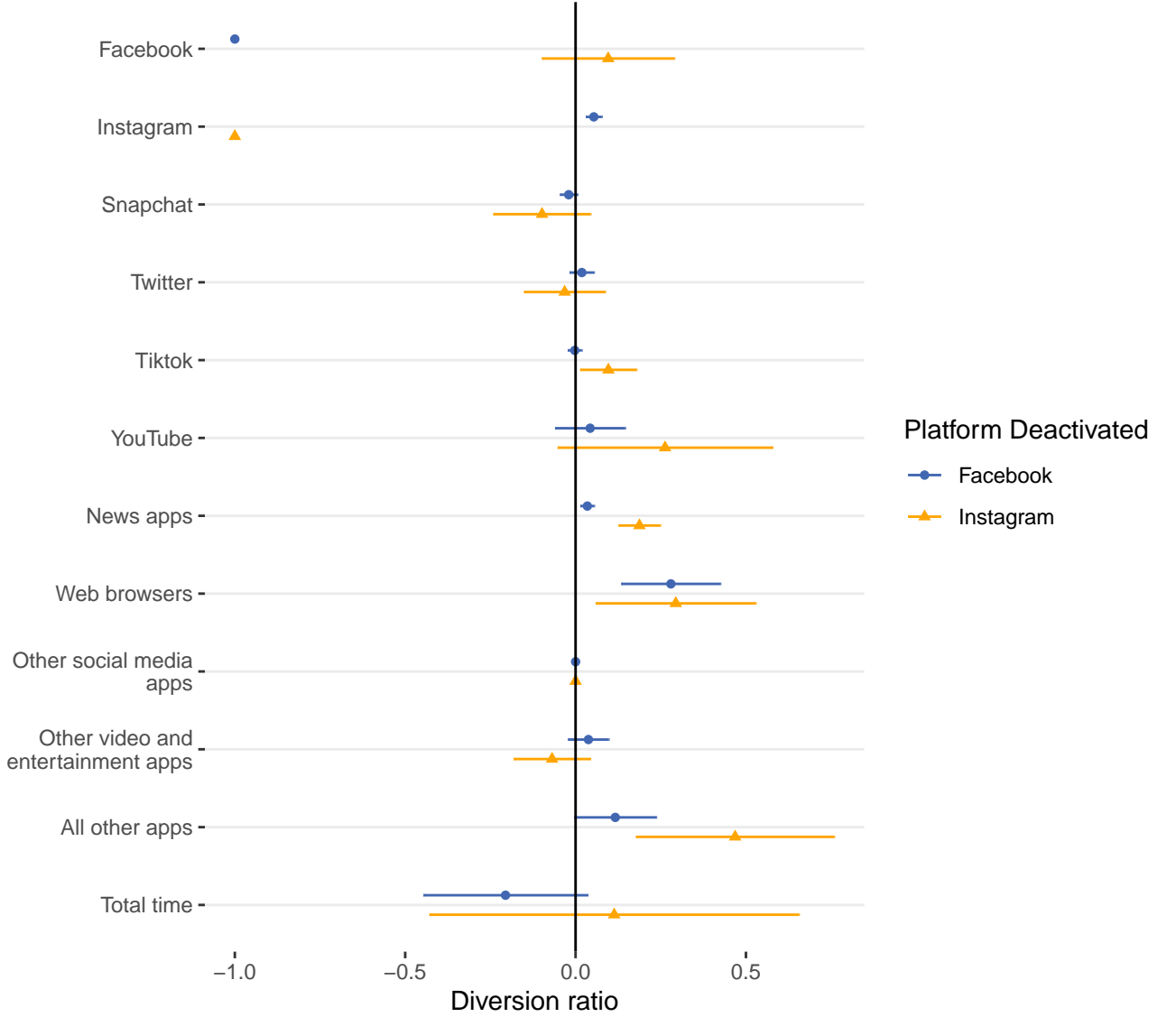
Notes: This figure presents daily average Facebook and Instagram use in the Deactivation and Control groups in the Facebook deactivation experiment passive tracking sample from the Facebook and Instagram Election Study. The dark grey shaded area indicates the Control group's 7-day deactivation period, while the light grey shaded area indicates the Deactivation group's 35-day additional deactivation period.

Figure 3: **Daily Facebook and Instagram Use in Instagram Deactivation Experiment**



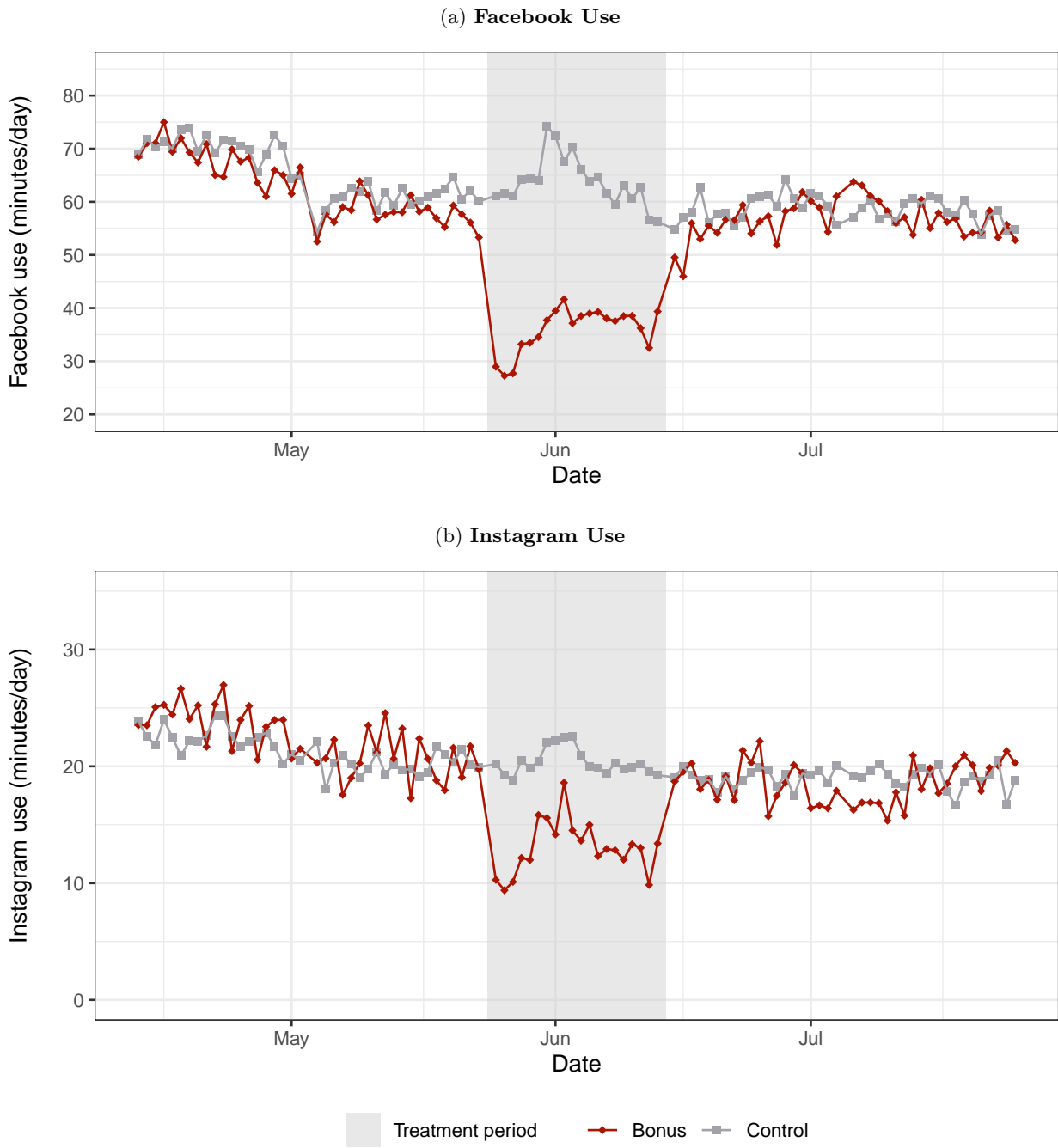
Notes: This figure presents daily average Facebook and Instagram use in the Deactivation and Control groups in the Instagram deactivation experiment passive tracking sample from the Facebook and Instagram Election Study. The dark grey shaded area indicates the Control group's 7-day deactivation period, while the light grey shaded area indicates the Deactivation group's 35-day additional deactivation period.

Figure 4: **Diversion Ratios from Facebook and Instagram Deactivation Experiments**



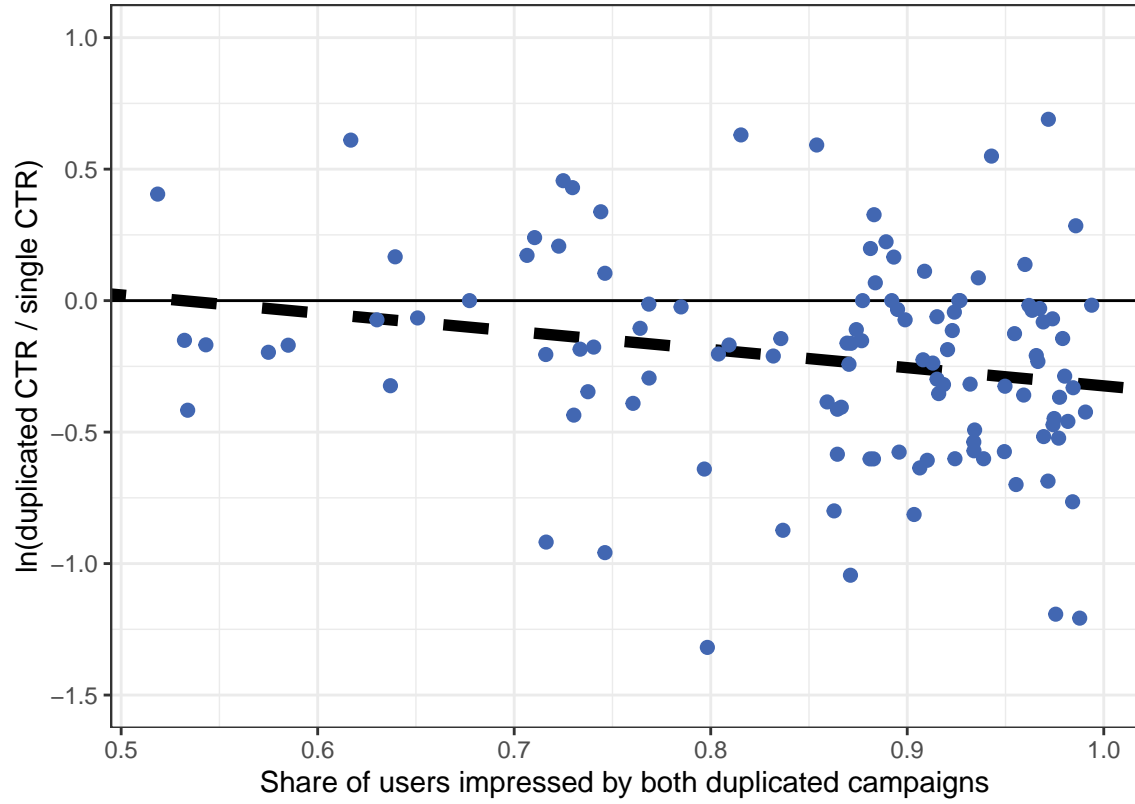
Notes: This figure presents estimated diversion ratios and 95 percent confidence intervals estimated from the Facebook and Instagram deactivation experiments in the Facebook and Instagram Election Study. If τ_j^{Dj} and τ_{-j}^{Dj} , respectively, are the local average treatment effects of fully deactivating platform j on use of j and $-j$ presented in Appendix Figure A2, these diversion ratios are $\delta_{-j}^j = -\tau_{-j}^{Dj} / \tau_j^{Dj}$. We calculate confidence intervals via the Delta method, assuming zero covariance between the parameter estimates.

Figure 5: **Digital Addiction Facebook and Instagram Use**



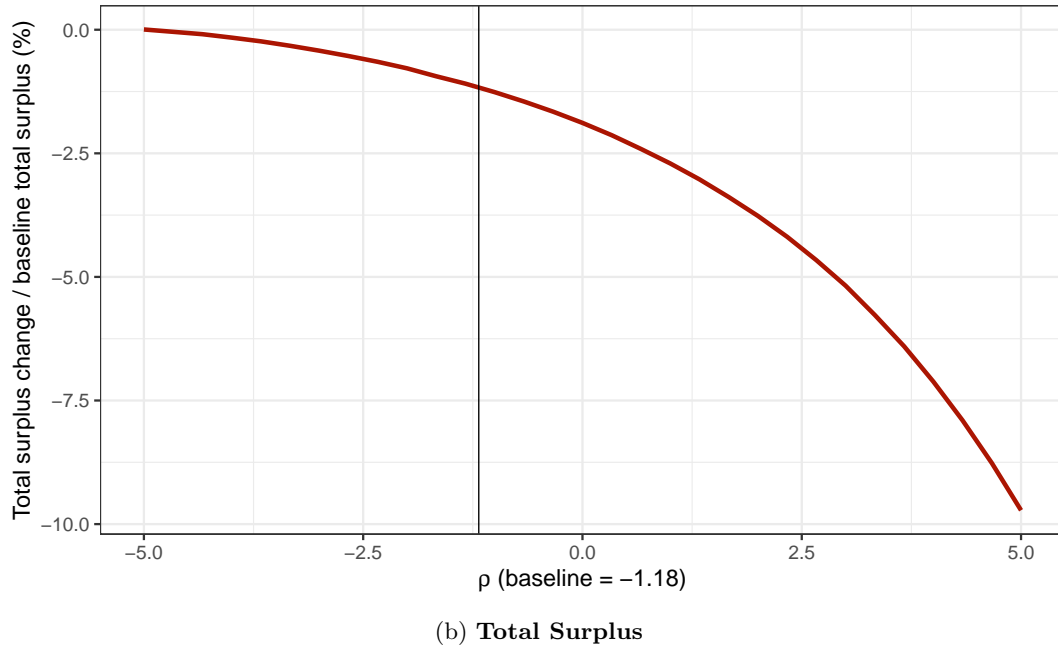
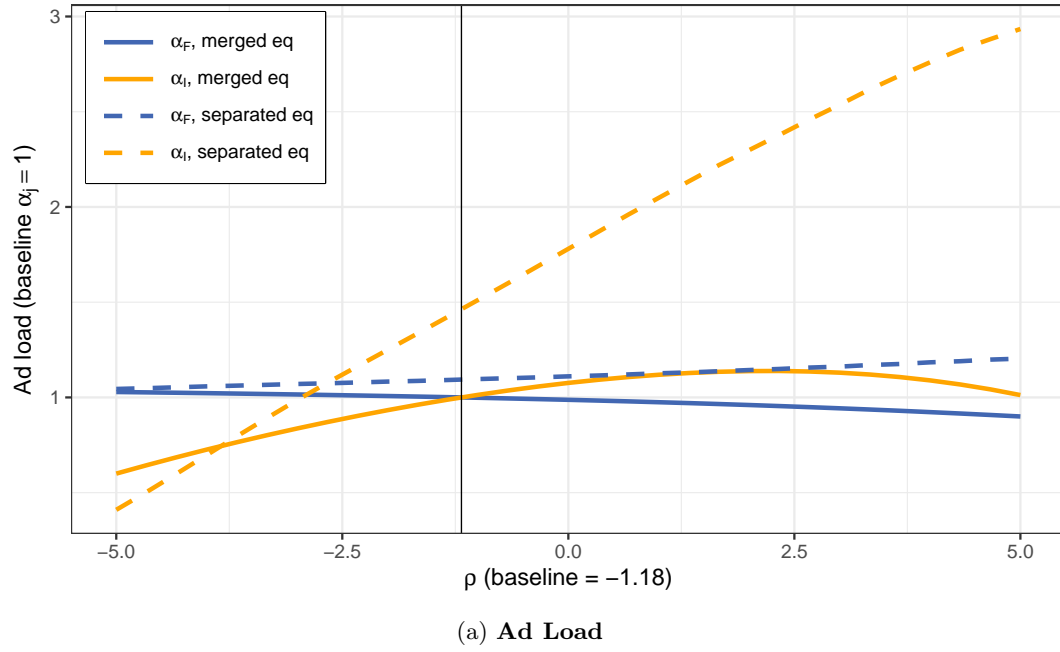
Notes: Panels (a) and (b) present average Facebook and Instagram use in the Digital Addiction experiment Bonus and Bonus Control groups, limiting the sample to the Limit Control group.

Figure 6: **Effects of Duplication on Click-through Rates**



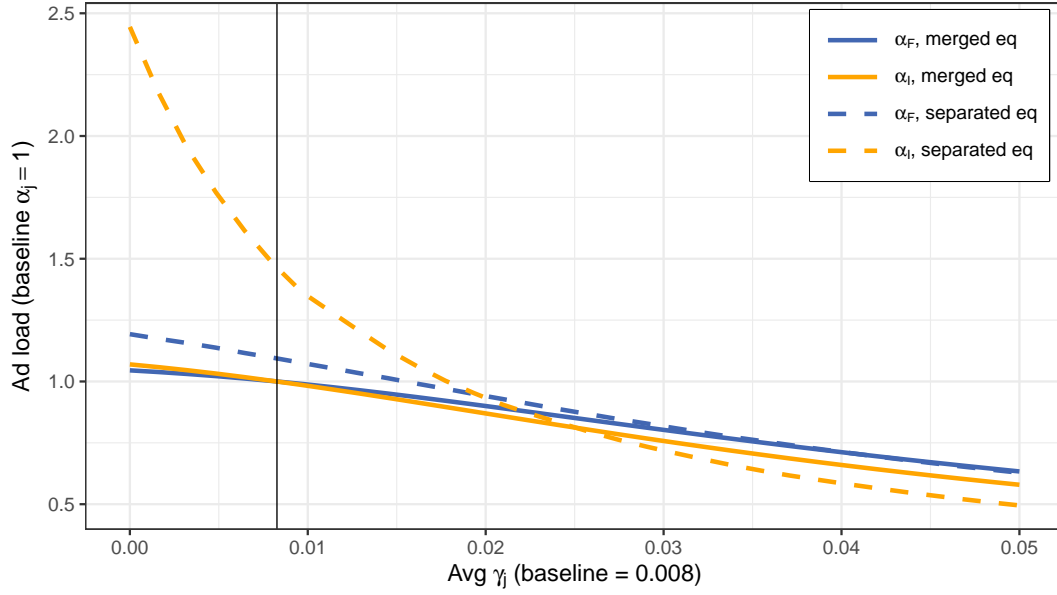
Notes: This figure shows results from the advertiser duplication loss experiment. Each observation conditions on a specific ad creative, ad budget, and ad campaign objective, and shows the log difference in average click-through rates between duplicated and non-duplicated follow-up campaigns. Click-through rates for duplicated campaigns are impression-weighted averages.

Figure 7: Sensitivity to Platform Substitution Parameter

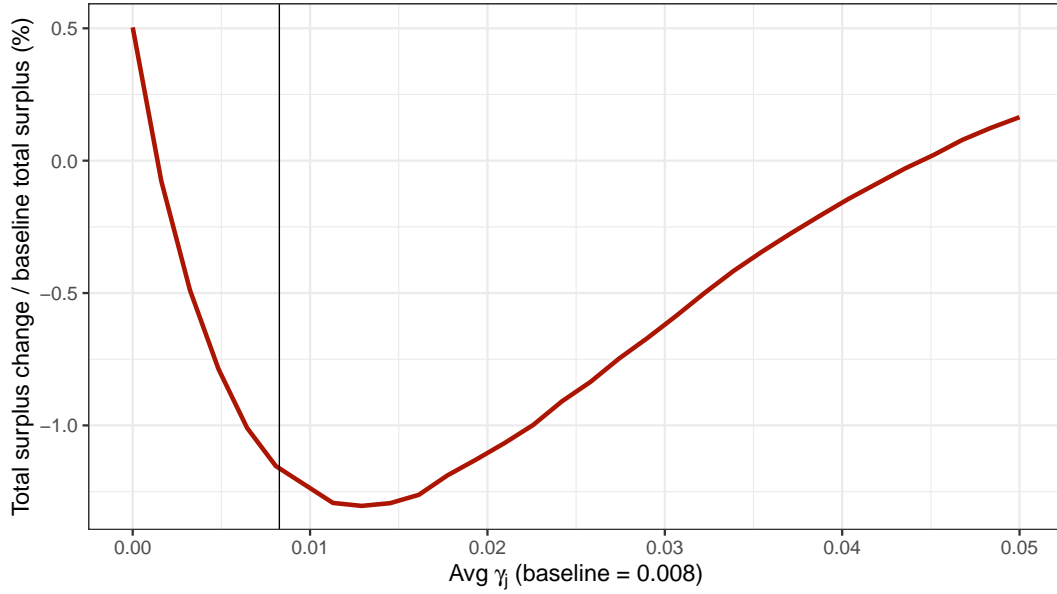


Notes: This figure presents the equilibrium effects of alternative values of the platform substitution parameter ρ , holding the other structural parameters constant. Panel (a) presents ad load on each platform in the merged equilibrium and separated equilibrium with uncoordinated ad delivery, relative to ad load in the merged equilibrium at baseline parameter values. Panel (b) presents the effect of separation with uncoordinated ad delivery on total surplus as a share of total surplus in the merged equilibrium at baseline parameter values.

Figure 8: Sensitivity to Ad Load Disutility Parameter



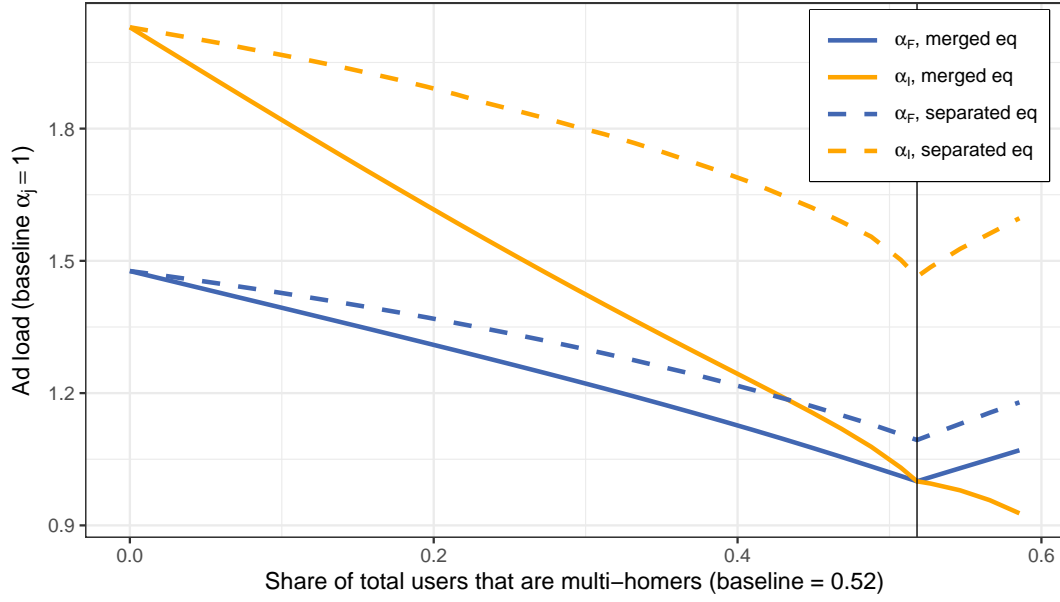
(a) Ad Load



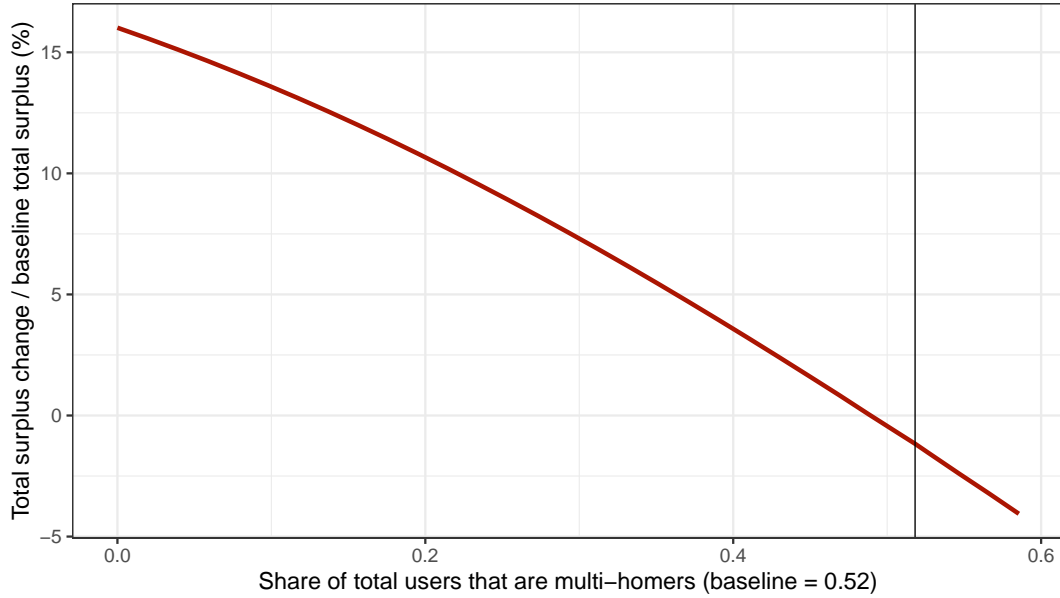
(b) Total Surplus

Notes: This figure presents the equilibrium effects of alternative values of the average ad load disutility parameters γ_j , holding the other structural parameters constant. To change the average γ_j , we change γ_F and γ_I proportionally. Panel (a) presents ad load on each platform in the merged equilibrium and separated equilibrium with uncoordinated ad delivery, relative to ad load in the merged equilibrium at baseline parameter values. Panel (b) presents the effect of separation with uncoordinated ad delivery on total surplus as a share of total surplus in the merged equilibrium at baseline parameter values.

Figure 9: Sensitivity to Overlap Parameter



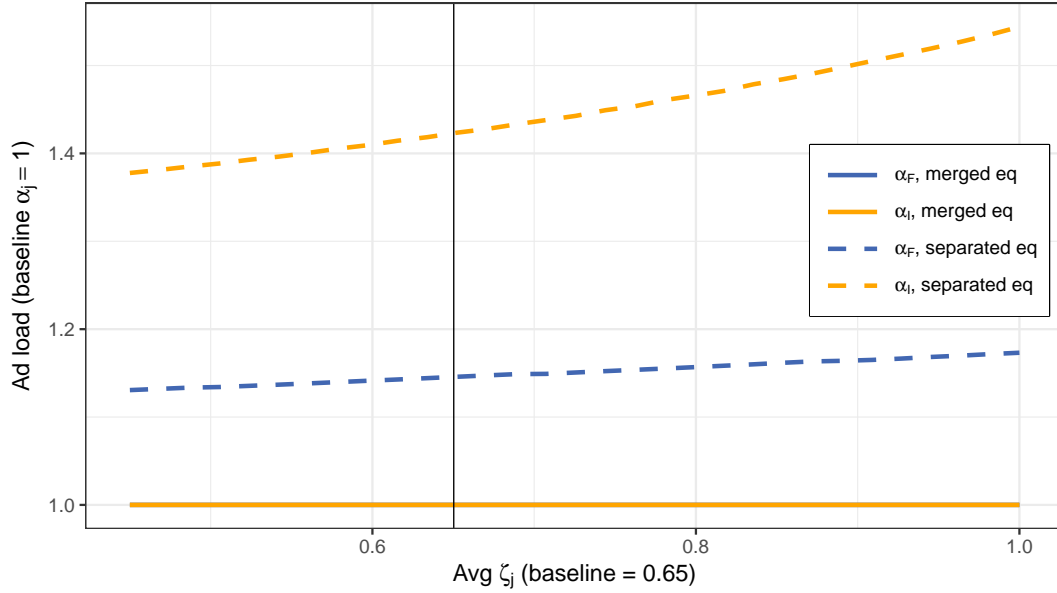
(a) Ad Load



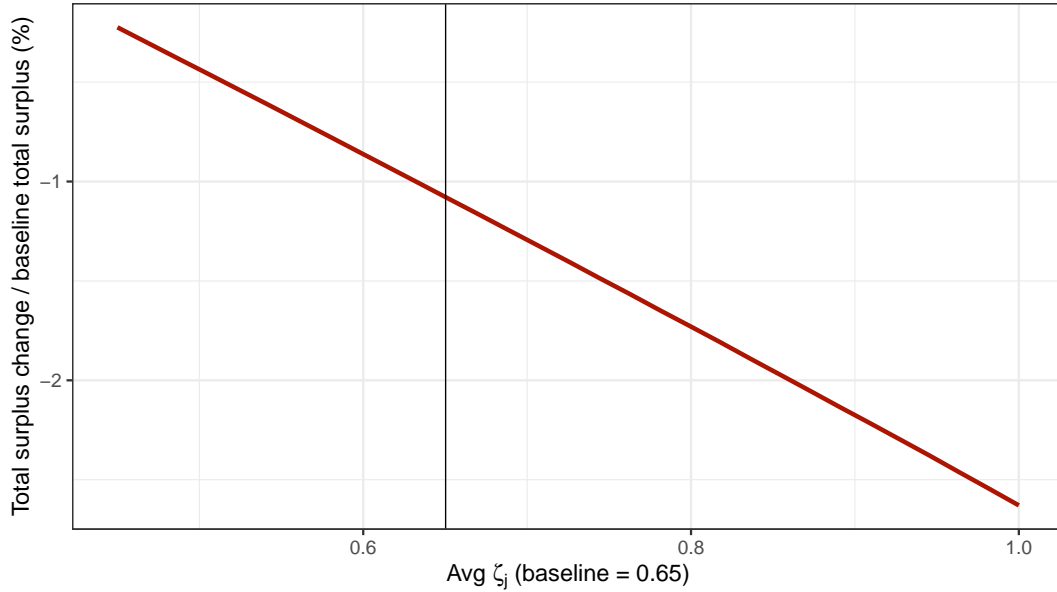
(b) Total Surplus

Notes: This figure presents the equilibrium effects of alternative values of overlap, holding the other structural parameters constant. To change overlap, we vary the number of multi-homers as a share of total users, and allocate the single-homers to hold constant the ratio of single-homers on Facebook versus Instagram. Panel (a) presents ad load on each platform in the merged equilibrium and separated equilibrium with uncoordinated ad delivery, relative to ad load in the merged equilibrium at baseline parameter values. Panel (b) presents the effect of separation with uncoordinated ad delivery on total surplus as a share of total surplus in the merged equilibrium at baseline parameter values.

Figure 10: Sensitivity to Diminishing Return Parameter



(a) Ad Load



(b) Total Surplus

Notes: This figure presents the equilibrium effects of alternative values of average diminishing returns ζ_j , holding the other structural parameters constant. To change the average ζ_j , we vary κ on its full range $\kappa \in [0, 1]$. Panel (a) presents ad load on each platform in the merged equilibrium and separated equilibrium with uncoordinated ad delivery, relative to ad load in the merged equilibrium at baseline parameter values. Panel (b) presents the effect of separation with uncoordinated ad delivery on total surplus as a share of total surplus in the merged equilibrium at baseline parameter values.

Online Appendix

Digital Media Mergers: Theory and Application to Facebook-Instagram

Justin Katz and Hunt Allcott

Table of Contents

A Model Appendix	3
A.1 Alternative to Constant Impressions Per Campaign	3
A.2 Derivation of Marginal Duplication Function	3
A.3 Duplication Loss with Imperfectly Correlated CTR Predictions	4
A.4 Reaction Functions	6
A.5 Derivations for Section A.4	10
A.6 Derivations for Section 1.3	14
B Ad Duplication Experiment Appendix	17
B.1 Ad Selection and Ad Design	17
B.2 Experimental Design Details	17
C Model-Free Empirical Evidence Appendix	21
C.1 Facebook and Instagram Election Study	21
C.2 Digital Addiction Experiment	24
C.3 Ad Duplication Experiment	25
D Structural Estimation Appendix	28
D.1 Average Time Use and FOCs as a Function of Time Use Moments	28
D.2 Standard Errors	29
D.3 Sensitivity Matrix	31

D.4	Aggregate Elasticity of Ad Demand in Merged Equilibrium	34
E	Counterfactual Simulation Appendix	36
E.1	Setup	36
E.2	Welfare Formulas	37
E.3	Miscellaneous Formulas	41
E.4	Overlap Sensitivity Analysis Implementation Details	42
E.5	Structural Estimates and Counterfactuals with Alternative Parameter Values . . .	45

A Model Appendix

A.1 Alternative to Constant Impressions Per Campaign

This subsection provides an alternative assumption that delivers equivalent equilibrium prices as the assumption in the text that users have the same optimal impressions per campaign m .

Assumption 4. *The optimal number of impressions per campaign for user i and advertiser a is given by*

$$m_{ia}(\omega_{ia}\pi_a, p_i) = \frac{f \cdot \omega_{ia}\pi_a}{p_i + \eta \cdot (1 + \eta_0)},$$

where f is a constant.

Assumption 4 has sensible comparative statics – the optimal number of impressions is increasing in profits per impression, and decreasing in price per impression. The specific functional form ensures that market clearing prices are unchanged relative to their implied value if $f = 2m$. Under Assumption 4, the market clearing condition in the merged equilibrium becomes

$$\begin{aligned} \boldsymbol{\alpha} \cdot \mathbf{T}_i(\boldsymbol{\alpha}) &= \sum_a m_i \cdot \mathbf{1}[p_i \leq \omega_{ia}\pi_a] \\ &= E[m_i | \omega_{ia}\pi_a \geq p_i] \cdot A \cdot (1 - H_i(p_i)) \\ &= \frac{f}{2} \cdot \frac{1}{p_i + \eta \cdot (1 + \eta_0)} \cdot (p_i + \eta \cdot (1 + \eta_0)) A \cdot (1 - H_i(p_i)) \\ &= m \cdot A \cdot (1 - H_i(p_i)), \end{aligned} \tag{36}$$

where equation (36) is the same as equation (3) under the assumption in the main text.

A.2 Derivation of Marginal Duplication Function

This subsection derives the marginal duplication function in Section 1.2.2.

Proof. By definition,

$$\begin{aligned} O'_{aj}(\mathbf{q}) &= \Pr(i \text{ (infra)marginal on } -j \text{ given } q_{-j} \text{ given } i \text{ marginal on } j \text{ given } q_j) \\ &= \Pr\left(\frac{p_{ij'}}{\omega_{ia}} \leq \pi_a \cdot (1 - \zeta_{j'} O'_{aj'}(\mathbf{q})) \mid \frac{p_{ij}}{\omega_{ia}} = \pi_a \cdot (1 - \zeta_j O'_{aj}(\mathbf{q}))\right) \\ &= \Pr\left(\frac{p_{ij'}}{p_{ij}} \leq \frac{\pi_a (1 - \zeta_{j'} O'_{aj'}(\mathbf{q}))}{\pi_a (1 - \zeta_j O'_{aj}(\mathbf{q}))}\right). \end{aligned} \tag{37}$$

Next, use market clearing to get $\frac{p_{ij'}}{p_{ij}}$:

$$\begin{aligned}\alpha_j T_{ij}(\boldsymbol{\alpha}) &= \sum_a \mathbf{1} [\pi_a (1 - \zeta_j O'_{aj}(\mathbf{q})) \omega_{ia} \geq p_{ij}] \\ &= A \left[1 - H_i \left(\frac{p_{ij}}{1 - \zeta_j O'_{aj}(\mathbf{q})} \right) \right].\end{aligned}\tag{38}$$

Going from the first line to the second implicitly applies Assumption 1 because it says that the distribution of $\pi_a \omega_{ia}$ does not depend on (for instance) different time usage on different platforms and can be described by a single person-specific distribution. This follows from independent click-through rates. Solving for p_{ij} gives

$$p_{ij} = (1 - \zeta_j O'_{aj}(\mathbf{q})) H_i^{-1} \left(1 - \frac{\tilde{\alpha}_j T_{ij}(\boldsymbol{\alpha})}{Am} \right).$$

Therefore,

$$\frac{p_{i,-j}}{p_{ij}} = \frac{\left(1 - \zeta_{-j} O'_{aj'}(\mathbf{q}) \right) H_i^{-1} \left(1 - \frac{\alpha_{j'} T_{ij'}(\boldsymbol{\alpha})}{Am} \right)}{\left(1 - \zeta_j O'_{aj}(\mathbf{q}) \right) H_i^{-1} \left(1 - \frac{\alpha_j T_{ij}(\boldsymbol{\alpha})}{Am} \right)}.\tag{39}$$

Substituting (39) into (37), the ratios $\frac{(1 - \zeta_{j'} O'_{aj'}(\mathbf{q}))}{(1 - \zeta_j O'_{aj}(\mathbf{q}))}$ cancel, and we have

$$\begin{aligned}O'_{aj}(\mathbf{q}^*) &= O'_{aj} = \Pr \left(\frac{H_i^{-1} \left(1 - \frac{\alpha_{j'} T_{ij'}(\boldsymbol{\alpha})}{Am} \right)}{H_i^{-1} \left(1 - \frac{\alpha_j T_{ij}(\boldsymbol{\alpha})}{Am} \right)} \leq 1 \right) \\ &= \Pr[\alpha_j T_{ij}(\boldsymbol{\alpha}) \leq \alpha_{j'} T_{ij'}(\boldsymbol{\alpha})] \\ &= \frac{\sum_{i \in \mathcal{U}_j} \mathbf{1}[\alpha_j T_{ij}(\boldsymbol{\alpha}) \leq \alpha_{j'} T_{ij'}(\boldsymbol{\alpha})]}{N_j}.\end{aligned}\tag{40}$$

Going from the first to the second line to the second uses the fact that H_i^{-1} is monotone increasing. The third line follows by definition and gives the expression in the text. \square

A.3 Duplication Loss with Imperfectly Correlated CTR Predictions

This appendix section re-derives O'_{aj} after relaxing the main text assumption that separated platforms predict the same click-through rates for each user. For expositional clarity, we will use \tilde{O}'_{aj} to refer to marginal duplication derived under the assumption that platform's CTR predictions are imperfectly correlated.

Let ω_{iaj} be platform j 's estimation of ω_{ia} . Decompose $\omega_{iaj} = \omega_{ia} u_{ij}$, where $u_{ij} \geq 0$ and $E[u_{ij}] = 1$, so that (i) platforms are right on average; and (ii) platform under- or over-estimation of CTRs applies equally to all advertisers. Further assume that u_{ij} is distributed iid with $u_{ij} \perp \omega_{ia}, T_{ij}, \zeta_i$.

Following the same steps as in Section A.2,

$$\tilde{O}'_{aj}(\mathbf{q}) = \Pr \left(\frac{p_{ij'}}{\omega_{ia} u_{ij'}} \leq \pi_a \cdot (1 - \zeta_{j'} \tilde{O}'_{aj'}(\mathbf{q})) \middle| \frac{p_{ij}}{\omega_{ia} u_{ij}} = \pi_a \cdot (1 - \zeta_j \tilde{O}'_{aj}(\mathbf{q})) \right) \quad (41)$$

$$= \Pr \left(\frac{p_{ij'}}{p_{ij}} \leq \frac{u_{ij'}}{u_{ij}} \frac{\pi_a (1 - \zeta_{j'} \tilde{O}'_{aj'}(\mathbf{q}))}{\pi_a (1 - \zeta_j \tilde{O}'_{aj}(\mathbf{q}))} \right). \quad (42)$$

Market clearing now implies that

$$\alpha_j T_{ij}(\boldsymbol{\alpha}) = \sum_a \mathbf{1} \left[\pi_a (1 - \zeta_j \tilde{O}'_{aj}(\mathbf{q})) \omega_{iaj} \geq p_{ij} \right] \quad (43)$$

$$= \sum_a \mathbf{1} \left[\pi_a (1 - \zeta_j \tilde{O}'_{aj}(\mathbf{q})) \omega_{ia} \geq p_{ij} / u_{ij} \right] \quad (44)$$

$$= Am \cdot \left[1 - H_i \left(\frac{p_{ij} / u_{ij}}{1 - \zeta_j \tilde{O}'_{aj}(\mathbf{q})} \right) \right]. \quad (45)$$

Thus,

$$p_{ij} / u_{ij} = (1 - \zeta_j \tilde{O}'_{aj}(\mathbf{q})) H_i^{-1} \left(1 - \frac{\alpha_j T_{ij}(\boldsymbol{\alpha})}{Am} \right), \quad (46)$$

and hence

$$\frac{p_{ij'}}{p_{ij}} = \frac{u_{ij}}{u_{ij'}} \frac{\left(1 - \zeta_{j'} \tilde{O}'_{aj'}(\mathbf{q}) \right) H_i^{-1} \left(1 - \frac{\alpha_{j'} T_{ij'}(\boldsymbol{\alpha})}{Am} \right)}{\left(1 - \zeta_j \tilde{O}'_{aj}(\mathbf{q}) \right) H_i^{-1} \left(1 - \frac{\alpha_j T_{ij}(\boldsymbol{\alpha})}{Am} \right)}. \quad (47)$$

Putting everything together,

$$\tilde{O}'_{aj}(\mathbf{q}^*) = \Pr \left(\frac{H_i^{-1} \left(1 - \frac{\alpha_{j'} T_{ij'}(\boldsymbol{\alpha})}{Am} \right)}{H_i^{-1} \left(1 - \frac{\alpha_j T_{ij}(\boldsymbol{\alpha})}{Am} \right)} \leq \frac{u_{ij'}^2}{u_{ij}^2} \right) \quad (48)$$

$$= \Pr \left(\frac{1 + \eta_0 - \frac{\alpha_{j'} T_{ij'}(\boldsymbol{\alpha})}{Am}}{1 + \eta_0 - \frac{\alpha_j T_{ij}(\boldsymbol{\alpha})}{Am}} \leq \frac{u_{ij'}^2}{u_{ij}^2} \right) \quad (49)$$

$$= \Pr \left(\alpha_j T_{ij}(\boldsymbol{\alpha}) \leq Am \cdot \left(1 - \frac{u_j^2}{u_{j'}^2} \right) (1 + \eta_0) + \frac{u_j^2}{u_{j'}^2} \alpha_{j'} T_{ij'}(\boldsymbol{\alpha}) \right). \quad (50)$$

With $\frac{u_j^2}{u_{j'}^2} \sim U_j$,¹³ we can rewrite \tilde{O}'_{aj} as

$$\tilde{O}'_{aj} = \int_z \Pr (\alpha_j T_{ij}(\boldsymbol{\alpha}) \leq Am \cdot (1 + \eta_0)(1 - z) + z \cdot \alpha_{j'} T_{ij'}(\boldsymbol{\alpha})) dU_j(z) \quad (51)$$

$$= \sum_{i \in \mathcal{U}_j} \int_z \frac{\mathbf{1} [z^{-1} \alpha_j T_{ij}(\boldsymbol{\alpha}) \leq Am \cdot (1 + \eta_0)(z - 1) + \alpha_{j'} T_{ij'}(\boldsymbol{\alpha})]}{N_j} dU_j(z). \quad (52)$$

¹³For example, if u_j^2 are distributed $\Gamma(a, 1)$, then their ratio is a Beta prime distribution with scale and location a .

To compare \tilde{O}'_{aj} and O'_{aj} , fix i and z and consider three cases.

First, when $z = 1$, the argument in the integral in equation (52) coincides exactly with O'_{aj} for all i .

Second, when $z < 1$, the argument in the integral is higher than O'_{aj} for all i . The intuition is that $z < 1$ implies platform j assesses i 's click-through rate as lower than platform j' does. The advertiser allocated to the marginal ad slot on j is more likely to have been given a slot on j' conditional on $\alpha_{j'}T_{ij'}$, increasing overlap.

Finally, when $z > 1$, the argument in the integral is lower than O'_{aj} for all i . The intuition is the opposite of the previous paragraph. That $z > 1$ implies platform j assesses i 's click-through rate as higher than platform j' does. The advertiser allocated to the marginal ad slot on j is less likely to have been given a slot on j' conditional on $\alpha_{j'}T_{ij'}$, decreasing overlap.

The net effect of these two forces is uncertain, and depends both on the joint distribution of $(T_{ij}, T_{ij'})$ and U_j .

Discussion. The above analysis highlights two key insights. First, marginal duplication does not monotonically diminish or increase with lower correlation. Thus, the baseline assumption of perfect correlation doesn't systematically distort overlap in one direction or another. Imperfect correlation does affect the "business stealing" incentive, as shown by the fact that α_j is multiplied by z^{-1} . This may make the incentive stronger or weaker depending on the distribution of U_j and the joint distribution of $(T_{ij}, T_{ij'})$.

Second, the result that imperfect correlation has ambiguous effects on marginal overlap does not directly map to welfare effects. The welfare effects of imperfect correlation, however, are also uncertain. If platforms are separated, can't share data, and hence have more coarse targeting predictions, there are two offsetting effects. On the one hand, total inefficient duplication may be lower, which is good for welfare. On the other hand, ads are less well targeted on average, which is bad for welfare. The net effect is ambiguous. So even if the assumption of perfect correlation overstates the welfare effect of duplication loss, it doesn't necessarily overstate the advertiser-side welfare loss from separation.

A.4 Reaction Functions

This appendix presents additional intuition on strategic incentives as the two platforms compete. We do this primarily with reaction functions computed numerically at example parameter values. To simplify the analysis, we restrict the model from the main text in two ways. First, we assume time on platform T_i is exogenous but not necessarily homogeneous. Second, we assume $\zeta_j = 1$, so that duplicated impressions are fully wasted, and that $\mathbf{c} = \mathbf{0}$. We first present the first-order conditions before illustrating them using numerical examples. Derivations are in Appendix A.5.

A.4.1 First-Order Conditions

Re-arranging equation (13), the merged platform chooses ad load to satisfy

$$\alpha_j^{e,m} = \frac{\sum_i \alpha_{-j} \cdot T_{i,-j} \cdot \frac{\partial p_i}{\partial \alpha_j} + T_{ij} \cdot p_i}{-\sum_i T_{ij} \cdot \frac{\partial p_i}{\partial \alpha_j}} \quad (53)$$

where $\frac{\partial p_i}{\partial \alpha_j} = -\frac{\eta}{Am} \cdot T_{ij}$.

Rearranging equation (16), the separated platforms choose ad load to satisfy

$$\alpha_j^{e,s} = \frac{\sum_{i \in \mathcal{U}_j} T_{ij} \cdot p_{ij}}{-\sum_{i \in \mathcal{U}_j} T_{ij} \cdot \frac{\partial p_{ij}}{\partial \alpha_j}}. \quad (54)$$

A.4.2 Numerical Examples

We explore how the above forces impact ad load in the separated relative to combined equilibrium through several numerical examples. We parameterize the distribution of time use with a measure M of multi-homers with $\mathbf{T}_{mi} \sim \mathcal{N}(\frac{1}{2}, \Sigma_T)$, and a measure N_j of single-homers $T_{si} = 1$. Unless otherwise specified, we set $\zeta_j = m = 1$ and the remaining model parameters to their estimated value from Section 4.

Example 1: Partial user overlap (with coordinated ad delivery). We first focus on how partial user overlap impacts the magnitude of the advertiser-side Cournot externality when separated platforms can coordinate to avoid duplication. We set $\Sigma_T = 0$, so that multi-homers split one unit of time equally across platforms.

The merged equilibrium solution is standard linear Cournot: $\alpha_j^{e,m} = \frac{1}{2}Am \cdot (1 + \eta_0)$. In separated equilibrium, reaction functions are:

$$\alpha_j^{e,s,i}(\alpha_{-j}) = \frac{2 - \mu_j}{(4 - 3\mu_j)} Am \cdot (1 + \eta_0) - \frac{1}{2} \frac{\mu_j}{(4 - 3\mu_j)} \alpha_{-j}. \quad (55)$$

When there is no overlap ($\mu_j = 0$), each separated platform behaves as a monopolist. As overlap increases, separated platforms respond more to their rival's actions, as they have a greater impact on revenue, and internalize less the price impact of increased ad load. Appendix Section A.5.1 derives a closed-form expression for separated equilibrium ad load, and shows that the percent change relative to the merged equilibrium *only* depends on overlap statistics and is independent of ad demand parameters.

Figure A1, panel (a) plots reaction functions and equilibria in to show these forces concretely. Facebook reaction functions to Instagram ad load are plotted horizontally, and Instagram reaction functions to Facebook ad load are plotted vertically. Equilibria are plotted with black dots where the reaction functions intersect. Black lines plot vertical reaction functions when $\mu_j = 0$, because platforms ignore their rival's actions. The blue and orange solid lines plot reaction functions when $\mu_j = 1$ for both platforms, indicating a 40% increase in ad load relative to the monopolist

equilibrium. The dashed lines plot reaction functions given empirically-observed μ_j , with $\mu_{IG} > \mu_{FB}$. Since Instagram has more overlap than Facebook, it will internalize less of the impact of increased ad load on equilibrium prices, and hence increase ad load by much more than Facebook.

Example 2: Uncoordinated ad delivery (with full user overlap). We next consider a separated equilibrium where platforms cannot coordinate to avoid duplication. To focus on the role of duplication, we assume all users are multi-homers with heterogeneous time use parameterized by $\Sigma_T = \text{diag}(\sigma^2, \sigma^2)$. Heterogeneous time use ensures that the marginal duplication function is continuous and differentiable.

Reaction functions no longer have a closed form, but are given by

$$\alpha_j^{e,s,i}(\alpha_{-j}) = \arg \max_{\alpha_j} (1 - O'_{aj}) \cdot \eta \left(\sum_i \alpha_j T_{ij} \cdot \left(1 + \eta_0 - \frac{\alpha_j T_{ij}}{Am} \right) \right), \quad (56)$$

This expression comes from substituting $c_j = 0$, $T_{ij}(\alpha) = T_{ij}$, and the formula for separated equilibrium prices in equation (8) into problem (15), where O'_{aj} is given by equation (9). Rival ad load α_{-j} only enters the expression through marginal duplication O'_{aj} . This makes clear how duplication affects revenue from ad prices directly and strategically through the business stealing effect. Moreover, the variance of time use, controlled by σ^2 , will alter separated platform incentives. When σ^2 is very low, platforms can precisely affect marginal duplication and user prices through changes in ad load, amplifying strategic differences relative to the merged equilibrium. When σ^2 is very high, changes in ad load have little impact on marginal duplication, dampening differences relative to the merged equilibrium.

Figure A1, panel (b) illustrates these points. The solid blue and orange lines plot Facebook and Instagram reaction functions when σ^2 is relatively low. Ad load increases significantly. Because platforms have fine control over marginal duplication, the business stealing effect is strong, making choice of ad load a strategic complement. The dashed lines plot reaction functions when σ^2 is high. Ad load still shifts out due to the direct effect. However, platforms have much less control over marginal duplication through choice of ad load, severely dampening the business stealing effect.

Example 3: Uncoordinated ad delivery and partial user overlap together. Finally, we consider the impact of uncoordinated ad delivery and partial user overlap jointly. Reaction functions are the same as in equation (56). However, the value of O'_{aj} changes because O'_{aj} is lower when a lower fraction of users are multi-homers. To see this, note that:

$$O'_{aj} = \frac{\sum_{i \in \mathcal{U}_m} \mathbf{1}[\alpha_j T_{ij} \leq \alpha_{-j} T_{i,-j}]}{N_j} \quad (57)$$

$$= \mu_j \cdot \Pr(\alpha_j T_{ij} \leq \alpha_{-j} T_{i,-j} | i \in \mathcal{U}_m). \quad (58)$$

The first line follows because $T_{i,-j} = 0$ implies the numerator is zero for $i \notin \mathcal{U}_m$. The second line means that a lower fraction of multi-homers, and hence lower μ_j , implies lower marginal overlap,

holding fixed α and the time use distribution.

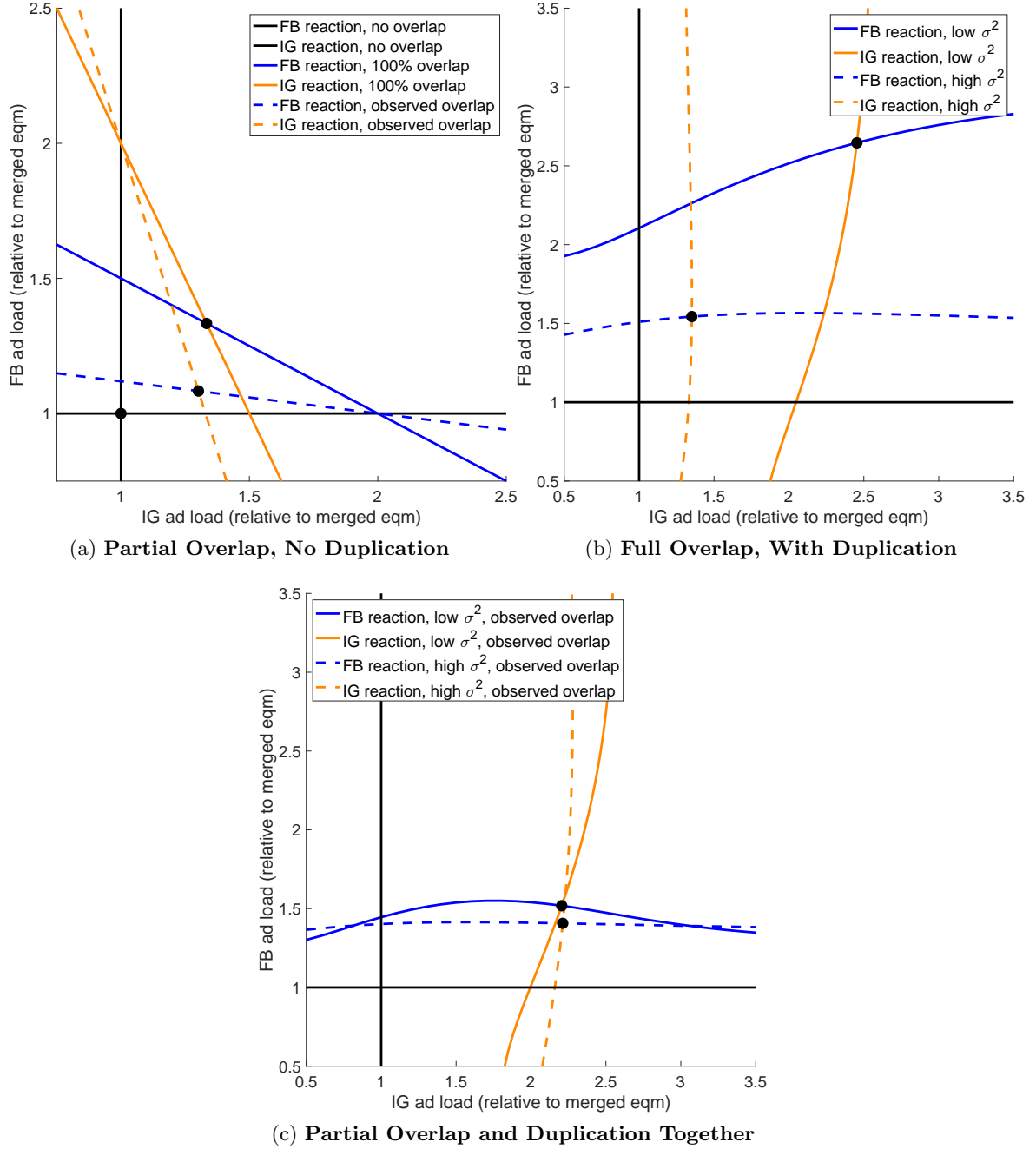
Figure A1, panel (c) plots the resulting reaction functions, where all reaction functions use the empirical overlap μ_j on Facebook and Instagram. First, partial overlap ($\mu_j < 1$) dampens the impact of duplication, since each platform has a user population for whom strategic incentives do not change relative to the merged equilibrium. Second, the business stealing motive appears stronger for Instagram than Facebook. This is because Instagram has greater overlap, magnifying the returns to business stealing. Finally, higher time use variance again dampens the business stealing effect, although to a lesser degree as it is already dampened by overlap.

Summary of numerical examples. With exogenous but heterogeneous time use, separating platforms leads to a greater increase in ad load when user overlap across platforms is greater. First, higher overlap leads merged platforms to constrain ad load by more relative to separated platforms, which do not consider the impact of lower ad prices on their rival’s revenue. Second, if platforms can’t coordinate to avoid inefficient duplication, ad load increases by even more in the separated equilibrium due to the “business stealing” incentive to increase ad load and reduce marginal duplication.

A.4.3 Possibility of Strategic Complementarity

Section A.4.2 gives examples where business stealing changes ad load from strategic substitutes into strategic complements: reaction functions are globally downwards-sloping in Figure A1, panel (a) with coordinated ad delivery, but can be upwards sloping in panel (c) with uncoordinated ad delivery. The following proposition shows formally that optimal ad loads are always strategic substitutes when ad delivery is coordinated but may be strategic complements when ad delivery is uncoordinated.

Proposition 1 (Advertiser-side strategic complementarity). *Suppose that time use T_i is exogenous with $\frac{\partial T_i}{\partial \alpha_j} = \mathbf{0}$ and a well-defined distribution for $\frac{T_{ij}}{T_{i,-j}}$, O'_{aj} is twice differentiable, Assumptions 1 and 2 hold, $\mathbf{c} = \mathbf{0}$, and $\zeta_j = 1$. Then in the separated equilibrium in Problem (15), ad load choices are strategic substitutes if ad delivery is coordinated, and either strategic complements or substitutes if ad delivery is uncoordinated.*

Figure A1: **Key Advertiser-Side Forces: Numerical Examples**

Notes: This figure presents numerical examples described in Section A.4.2. Panel (a) plots reaction functions in an example with partial overlap but no duplication in separated equilibrium. Panel (b) plots reaction functions in an example with full overlap and duplication. Panel (c) plots reaction functions in an example with partial overlap and duplication.

A.5 Derivations for Section A.4

This subsection derives expressions in Section A.4.

Derivation of equation (53). The monopolist problem is

$$\alpha^{e,m} = \arg \max_{\alpha} \sum_i p_i \cdot \alpha \cdot T_i, \quad (59)$$

where the only difference relative to equation (12) is that time use does not depend on α as it is exogenous and $\mathbf{c} = \mathbf{0}$. The first-order conditions are

$$\begin{aligned} 0 &= \frac{\partial}{\partial \alpha_j} \left[\sum_i p_i \cdot \alpha \cdot T_i \right] \\ &= \sum_i \alpha \cdot T_i \cdot \frac{\partial p_i}{\partial \alpha_j} + p_i \cdot T_{ij}. \end{aligned} \quad (60)$$

Rearranging:

$$\alpha_j = - \frac{\sum_i \alpha_{-j} \cdot T_{i,-j} \cdot \frac{\partial p_i}{\partial \alpha_j} + T_{ij} \cdot p_i}{\sum_i T_{ij} \cdot \frac{\partial p_i}{\partial \alpha_j}} \quad \text{where} \quad \frac{\partial p_i}{\partial \alpha_j} = - \frac{\eta}{Am} \cdot T_{ij}, \quad (61)$$

and where the value of $\frac{\partial p_i}{\partial \alpha_j}$ comes from differentiating equation (4) with respect to α_j and applying the inverse function rule. \square

Derivation of equation (54). The separated platform problem is

$$\alpha_j^{e,s,i} = \arg \max_{\alpha_j} \sum_{i \in \mathcal{U}_j} \alpha_j \cdot T_{ij} \cdot p_{ij} \quad (62)$$

The first-order condition is

$$0 = \sum_{i \in \mathcal{U}_j} \alpha_j \cdot T_{ij} \cdot \frac{\partial p_{ij}}{\partial \alpha_j} + T_{ij} \cdot p_{ij}. \quad (63)$$

Rearranging gives the expression:

$$\alpha_j = - \frac{\sum_{i \in \mathcal{U}_j} T_{ij} \cdot p_{ij}}{\sum_{i \in \mathcal{U}_j} T_{ij} \cdot \frac{\partial p_{ij}}{\partial \alpha_j}}, \quad (64)$$

where

$$\frac{\partial p_{ij}}{\partial \alpha_j} = - (1 - O'_{aj}) \cdot \frac{\eta}{Am} \cdot T_{ij} - \frac{p_{ij}}{(1 - O'_{aj})} \frac{\partial O'_{aj}}{\partial \alpha_j}, \quad (65)$$

which gives the expressions in the text. \square

Proof of Proposition 1. To show ad load choices are strategic substitutes in Problem (16) with coordinated ad delivery, first note that given Assumptions 1 and 2,

$$\frac{\partial p_i}{\partial \alpha_j} = - \frac{\eta}{Am} \cdot T_{ij} \implies \frac{\partial^2 p_i}{\partial \alpha_{-j} \partial \alpha_j} = 0. \quad (66)$$

Differentiate equation (54) with respect to α_{-j} and substitute $p_{ij} = p_i$ to reflect coordinated ad

delivery:

$$\begin{aligned}\frac{\partial \alpha_j^{e,s,i}}{\partial \alpha_{-j}} &= -\frac{\sum_{i \in \mathcal{U}_j} T_{ij} \cdot \frac{\partial p_i}{\partial \alpha_{-j}}}{\sum_{i \in \mathcal{U}_j} T_{ij} \cdot \frac{\partial p_i}{\partial \alpha_j}} \\ &= -\frac{\sum_{i \in \mathcal{U}_j} T_{ij} T_{i,-j}}{\sum_{i \in \mathcal{U}_j} T_{ij}^2}.\end{aligned}\quad (67)$$

This proves that $\frac{\partial \alpha_j^{e,s,i}}{\partial \alpha_{-j}} \leq 0$, meaning choices of ad load are strategic substitutes.

To show that ad load choices can be strategic complements in Problem (15) with uncoordinated ad delivery, define the distribution of $T_{ij}/T_{i,-j}$ as \mathcal{T}_{-j} and note that

$$O'_{aj} = \Pr(\alpha_j T_{ij} \leq \alpha_{-j} T_{i,-j}) = \mathcal{T}_{-j}(\alpha_{-j}/\alpha_j). \quad (68)$$

Therefore,

$$\frac{\partial O'_{aj}}{\partial \alpha_{-j}} = \mathcal{T}'_{-j}\left(\frac{\alpha_{-j}}{\alpha_j}\right) \cdot \alpha_j^{-1} \geq 0, \quad \frac{\partial O'_{aj}}{\partial \alpha_j} = -\mathcal{T}'_{-j}\left(\frac{\alpha_{-j}}{\alpha_j}\right) \cdot \frac{\alpha_{-j}}{\alpha_j^2} \leq 0. \quad (69)$$

Moreover,

$$\frac{\partial O'_{aj}}{\partial \alpha_{-j} \partial \alpha_j} = -\mathcal{T}'_{-j}\left(\frac{\alpha_{-j}}{\alpha_j}\right) \cdot \frac{1}{\alpha_j^2} - \frac{\alpha_{-j}}{\alpha_j^3} \cdot \mathcal{T}''_{-j}\left(\frac{\alpha_{-j}}{\alpha_j}\right), \quad (70)$$

which has ambiguous sign. Differentiate equation (54) with respect to α_{-j} in the case with uncoordinated ad delivery (with p_{ij} separate on each platform and given by equation (8)):

$$\frac{\partial \alpha_j^{e,s,i}}{\partial \alpha_{-j}} = -\frac{\sum_{i \in \mathcal{U}_j} T_{ij} \cdot p_{ij}}{\left(\sum_{i \in \mathcal{U}_j} T_{ij} \cdot \frac{\partial p_{ij}}{\partial \alpha_j}\right)^2} \cdot \sum_{i \in \mathcal{U}_j} T_{ij} \cdot \frac{\partial^2 p_{ij}}{\partial \alpha_{-j} \partial \alpha_j}. \quad (71)$$

Strategic complementarity occurs when $\frac{\partial^2 p_{ij}}{\partial \alpha_{-j} \partial \alpha_j} < 0$, and strategic substitutes when $\frac{\partial^2 p_{ij}}{\partial \alpha_{-j} \partial \alpha_j} > 0$. Moreover,

$$\begin{aligned}\frac{\partial^2 p_{ij}}{\partial \alpha_{-j} \partial \alpha_j} &= \frac{\partial O'_{aj}}{\partial \alpha_{-j}} \cdot \frac{\eta}{Am} T_{ij} + \frac{p_{ij}}{(1 - O'_{aj})^2} \frac{\partial O'_{aj}}{\partial \alpha_{-j}} \frac{\partial O'_{aj}}{\partial \alpha_j} \\ &\quad - \frac{p_{ij}}{(1 - O'_{aj}(\alpha^{e,s,d}))} \frac{\partial^2 O'_{aj}}{\partial \alpha_{-j} \partial \alpha_j}.\end{aligned}\quad (72)$$

The first term is positive because $\frac{\partial O'_{aj}}{\partial \alpha_{-j}}$ is. The second term is negative because $\frac{\partial O'_{aj}}{\partial \alpha_j}$ is. The third term has a sign depending on the sign of $\frac{\partial^2 O'_{aj}}{\partial \alpha_{-j} \partial \alpha_j}$, which is ambiguous and depends on the shape of the pdf of $T_{ij}/T_{i,-j}$. Overall, it is thus possible that $\frac{\partial^2 p_{ij}}{\partial \alpha_{-j} \partial \alpha_j} < 0$, implying that $\frac{\partial \alpha_j^{e,s,i}}{\partial \alpha_{-j}} < 0$ (making ad load choices strategic complements). \square

Remark. Proposition 1 also holds with arbitrary \mathbf{c} and ζ_i that satisfy Assumption 3, where the

proof focuses on the restricted case for notational clarity.

A.5.1 Derivations for Section A.4.2

This subsection derives expressions in Section A.4.2. Throughout, we use the notation M and N_j to refer to the number of multi-homers and users on platform j , respectively, satisfying $\mu_j = M/N_j$ and $M + \sum_j (N_j - M) = N$.

Derivation of monopoly ad load. Monopoly revenue is

$$R^m(\alpha) = \eta \cdot \left(\frac{M}{2} (\alpha_1 + \alpha_2) \cdot \left(1 + \eta_0 - \frac{\alpha_1 + \alpha_2}{2Am} \right) + \sum_j (N_j - M) \alpha_j \left(1 + \eta_0 - \frac{\alpha_j}{Am} \right) \right). \quad (73)$$

The first-order condition with respect to α_j is

$$\begin{aligned} 0 &= \frac{M}{2} \left(\left(1 + \eta_0 - \frac{\alpha_j + \alpha_{-j}}{Am} \right) + (N_j - M) \left(1 + \eta_0 - 2 \frac{\alpha_j}{Am} \right) \right) \\ &= \frac{\alpha_j}{Am} (3M - 4N_j) + (1 + \eta_0) (2N_j - M) - \frac{O}{A} \alpha_{-j}. \end{aligned} \quad (74)$$

Therefore,

$$\alpha_j = \frac{2N_j - M}{4N_j - 3M} Am(1 + \eta_0) - \frac{M}{4N_j - 3M} \alpha_{-j}. \quad (75)$$

Substituting in for α_{-j} and simplifying gives

$$\alpha_j = \left(\frac{(2N_j - M)(4N_{-j} - 3M) - M(2N_{-j} - M)}{(4N_j - 3M) \cdot (4N_{-j} - 3M) - M^2} \right) Am(1 + \eta_0). \quad (76)$$

The numerator simplifies to $8N_j N_{-j} - 6M(N_j + N_{-j}) + 4M^2$ and the denominator simplifies to $2 \cdot (8N_j N_{-j} - 6M(N_j + N_{-j}) + 4M^2)$. Therefore, the expression becomes:

$$\alpha_j^{e,m} = \frac{1}{2} Am(1 + \eta_0), \quad (77)$$

as reported in the text. \square

Derivation of Equation (55). Separated platform revenue is

$$R_j^s(\alpha) = \eta \cdot \left(\frac{M}{2} \alpha_j \cdot \left(1 + \eta_0 - \frac{\alpha_1 + \alpha_2}{2Am} \right) + (N_j - M) \alpha_j \left(1 + \eta_0 - \frac{\alpha_j}{Am} \right) \right). \quad (78)$$

The first-order condition is

$$\begin{aligned} 0 &= \frac{M}{2} \left(1 + \eta_0 - \frac{\alpha_j + \alpha_{-j}}{2Am} - \frac{\alpha_j}{2Am} \right) + (N_j - M) \left(1 + \eta_0 - 2 \frac{\alpha_j}{Am} \right) \\ &= \frac{\alpha_j}{Am} (3M - 4N_j) + (1 + \eta_0) (2N_j - M) - \frac{M}{Am} \alpha_{-j}. \end{aligned} \quad (79)$$

Therefore,

$$\begin{aligned}\alpha_j^{e,s,i}(\alpha_{-j}) &= \frac{2N_j - M}{4N_j - 3M} Am(1 + \eta_0) - \frac{M}{(4N_j - 3M)} \alpha_{-j} \\ &= \frac{2 - \mu_j}{4 - 3\mu_j} Am(1 + \eta_0) - \frac{\mu_j}{4 - 3\mu_j} \alpha_{-j},\end{aligned}\tag{80}$$

where we factor out N_j from the numerator and denominator to express in terms of μ_j . Substituting for α_{-j} and simplifying yields:

$$\alpha_j^{e,s,i} = \left(\frac{(2N_j - M)(4N_{-j} - 3M) - O(2N_{-j} - M)}{(4N_j - 3M) \cdot (4N_{-j} - 3M) - M^2} \right) Am(1 + \eta_0).\tag{81}$$

□

Percent change in ad load only depends on overlap statistics. Using equations (77) and (81), the percent increase in ad load in the separated equilibrium is

$$\begin{aligned}\frac{\alpha_j^{e,s,i}}{\alpha_j^{e,m}} - 1 &= 2 \cdot \left(\frac{(2N_j - M)(4N_{-j} - 3M) - M(2N_{-j} - M)}{(4N_j - 3M) \cdot (4N_{-j} - 3M) - M^2} \right) - 1 \\ &= 2 \cdot \left(\frac{(2 - \mu_j)(4 - 3\mu_{-j}) - \mu_j(2 - \mu_{-j})}{(4 - 3\mu_j) \cdot (4 - 3\mu_{-j}) - \mu_j\mu_{-j}} \right) - 1.\end{aligned}\tag{82}$$

This only depends on overlap statistics, proving the claim in the text. □

A.6 Derivations for Section 1.3

This section analyzes the full model under various ownership structures. Throughout, we will apply assumptions 1 and 2.

A.6.1 Social Planner Benchmark

The analysis follows each point in Section 1.3.1. The planner chooses

$$\alpha^o = \arg \max_{\alpha} \sum_i U_i^*(\mathbf{T}(\alpha), n; \alpha) + \sum_i Am \cdot \int_{x=p_i(\alpha)}^{(\pi\omega)^{\max}} x dH(x) - \mathbf{c} \cdot \alpha.\tag{83}$$

The first-order condition is

$$0 = \sum_i \frac{\partial U_i^*(\cdot; \alpha)}{\partial \alpha_j} - \sum_i \frac{Am}{\eta} \cdot p_i(\alpha) \cdot \frac{\partial p_i(\alpha)}{\partial \alpha_j} - c_j.\tag{84}$$

Since

$$\frac{\partial p_i(\alpha)}{\partial \alpha_j} = -\frac{\eta}{Am} \cdot \left[T_{ij} + \alpha_j \frac{\partial T_{ij}}{\partial \alpha_j} + \alpha_{-j} \frac{\partial T_{i,-j}}{\partial \alpha_j} \right],\tag{85}$$

the FOC becomes

$$0 = \sum_i \frac{\partial U_i^*(\cdot; \alpha)}{\partial \alpha_j} - \sum_i p_i(\alpha) \cdot \left[T_{ij} + \alpha_j \frac{\partial T_{ij}}{\partial \alpha_j} + \alpha_{-j} \frac{\partial T_{i,-j}}{\partial \alpha_j} \right] - c_j. \quad (86)$$

Solving for α_j gives

$$\alpha_j^o = \frac{\sum_i \frac{\partial U_i^*(\cdot; \alpha)}{\partial \alpha_j} + \sum_i p_i(\alpha) \cdot \left(T_{ij} + \alpha_{-j} \frac{\partial T_{i,-j}}{\partial \alpha_j} \right) - c_j}{-\sum_i p_i(\alpha) \cdot \frac{\partial T_{ij}}{\partial \alpha_j}}. \quad (87)$$

A.6.2 Merged Platform Solution

The problem is:

$$\max_{\alpha} \sum_i p_i(\alpha) \cdot \alpha \cdot T_i(\alpha) - c \cdot \alpha. \quad (88)$$

The first-order conditions are

$$0 = \sum_i \left[\frac{\partial p_i}{\partial \alpha_j} \cdot \alpha \cdot T_i(\alpha) + p_i(\alpha) \cdot T_{ij}(\alpha) + p_i(\alpha) \cdot \alpha \cdot \frac{\partial T_i(\alpha)}{\partial \alpha_j} \right] - c_j. \quad (89)$$

Solving for α_j gives

$$\alpha_j^m = \frac{\sum_i \frac{\partial p_i}{\partial \alpha_j} \cdot \alpha \cdot T_i(\alpha) + \sum_i p_i(\alpha) \cdot \left(T_{ij}(\alpha) + \alpha_{-j} \cdot \frac{\partial T_{i,-j}}{\partial \alpha_j}(\alpha) \right) - c_j}{-\sum_i p_i(\alpha) \cdot \frac{\partial T_{ij}}{\partial \alpha_j}(\alpha)}. \quad (90)$$

A.6.3 Separated Platform Solution with Coordinated Ad Delivery

The problem is

$$\max_{\alpha_j} \sum_{i \in \mathcal{U}_j} p_i(\alpha) \cdot \alpha_j \cdot T_{ij}(\alpha) - c_j \alpha_j. \quad (91)$$

The first-order conditions are

$$0 = \sum_i \frac{\partial p_i}{\partial \alpha_j} \cdot \alpha_j \cdot T_{ij}(\alpha) + p_i(\alpha) \cdot T_{ij} + p_i(\alpha) \cdot \alpha_j \cdot \frac{\partial T_{ij}}{\partial \alpha_j}(\alpha) - c_j. \quad (92)$$

Solving for α_j gives

$$\alpha_j^{s,c} = \frac{\sum_{i \in \mathcal{U}_j} \frac{\partial p_i}{\partial \alpha_j} \cdot \alpha_j \cdot T_{ij}(\alpha) + \sum_{i \in \mathcal{U}_j} p_i(\alpha) \cdot T_{ij} - c_j}{-\sum_{i \in \mathcal{U}_j} p_i(\alpha) \cdot \frac{\partial T_{ij}}{\partial \alpha_j}(\alpha)}. \quad (93)$$

This differs from equation (16) in the main text because rather than depending on platform-specific prices p_{ij} , it depends on an integrated price p_i . This means duplication loss does not impact ad load. The difference in incentives in the separated versus merged equilibrium still depends on user overlap, however. When all users are single-homers, the separated equilibrium is identical to

the merged equilibrium. As the share of multi-homers increases, two differences emerge. First, as in Section A.4, the advertiser-side Cournot externality increases, which increases ad load in the separated equilibrium. Second, if platforms are substitutes, user diversion reduces the incentive to withhold ad load in the merged equilibrium relative to the separated equilibrium, which increases ad load in the merged equilibrium relative to the separated equilibrium. In general, ad load can be higher or lower than in the merged equilibrium, depending on overlap, user diversion, and price elasticity.

A.6.4 Separated Platform Solution with Uncoordinated Ad Delivery

The problem is

$$\max_{\alpha_j} \sum_{i \in \mathcal{U}_j} p_{ij}(\boldsymbol{\alpha}) \cdot \alpha_j \cdot T_{ij}(\boldsymbol{\alpha}) - c_j \alpha_j. \quad (94)$$

Taking the first-order condition and solving for α_j gives

$$\alpha_j = \frac{\sum_{i \in \mathcal{U}_j} \frac{\partial p_{ij}}{\partial \alpha_j} \cdot \alpha_j \cdot T_{ij}(\boldsymbol{\alpha}) + \sum_{i \in \mathcal{U}_j} p_{ij}(\boldsymbol{\alpha}) \cdot T_{ij} - c_j}{-\sum_{i \in \mathcal{U}_j} p_{ij}(\boldsymbol{\alpha}) \cdot \frac{\partial T_{ij}}{\partial \alpha_j}(\boldsymbol{\alpha})}, \quad (95)$$

where, assuming that $\frac{\partial \zeta_j}{\partial \alpha_j} \approx 0$,

$$\frac{\partial p_{ij}}{\partial \alpha_j} \approx -(1 - O'_{aj}) \cdot \frac{\eta \cdot \left(T_{ij} + \alpha_j \frac{\partial T_{ij}(\boldsymbol{\alpha})}{\partial \alpha_j} \right)}{Am} - \frac{p_{ij} \zeta_j}{(1 - \zeta_j O'_{aj})} \frac{\partial O'_{aj}}{\partial \alpha_j}. \quad (96)$$

The numerator in equation (95) captures both the advertiser-side Cournot effect and the business stealing effect, both of which increase ad load relative to the merged equilibrium. The absence of $\frac{\partial T_{i,-j}}{\partial \alpha_j}$ in the numerator reflects the same user-diversion force expressed in the previous sub-section. This implies that ad load may be higher or lower than the combined equilibrium social optimum.

However, since the separated equilibrium now has inefficiently duplicated ad impressions, comparing ad load versus the social planner benchmark is not sufficient to make welfare judgements. For example, even if ad load were identical in the separated platform equilibrium with duplication as in Equation (87), social welfare would be lower in the separated equilibrium because some ads would be inefficiently duplicated, lowering advertiser surplus. See Section 5 for details.

B Ad Duplication Experiment Appendix

B.1 Ad Selection and Ad Design

We developed 15 creatives for distinct products spanning five product categories. We selected products and categories to be representative of typical ads on Facebook and Instagram. To do so, we first picked five top product categories and the top three advertisers within each category by ad spending from the 2024 SensorTower Digital Market Index ([SensorTower 2024](#)). We identified each resulting advertiser’s best-selling product and created ads that linked to pages promoting or allowing users to purchase that product.¹⁴ To promote our ads, we created a “product picks” Facebook page for each product category. Such third-party product recommendations are allowed by Meta’s terms of use.

Our five product categories were shopping, consumer packaged goods, media and entertainment, health and wellness, and food and dining. The Facebook pages used to promote products in each category were called, respectively, “The Shopping Spot,” “Everyday Care Essentials,” “Media Roundup,” “Health and Wellness Essentials,” and “Culinary Crave.” These pages are public and viewable on Facebook.¹⁵ Ad creatives used public-source advertising materials to approximate campaigns consumers would likely see. Where relevant, ads link to a site to purchase the advertised product, and otherwise link to a site describing the product in more detail.

Table [A1](#) summarizes the companies, products, and creatives used within each category.

B.2 Experimental Design Details

For each ad creative, we first recruited 8 audiences to target in campaigns. To recruit audiences, we ran campaigns targeting US adults aged 18–65. To delineate audiences for retargeting, we used Meta’s “Custom Audiences” feature. This feature allows advertisers to identify a set of users based on behaviors or characteristics, such as whether they have previously interacted with another ad or visited an advertisers’ website. We used a feature that builds an audience based on users who view at least 25% of a video ad. We made video ads using the 3-second GIFs of the creatives displayed in Table [A1](#), such that users for whom the ad is displayed for 0.75 seconds became part of an audience. For each audience, we excluded users from being targeted once they became part of any of the other audiences to ensure that the eight audiences recruited for each ad were non-overlapping. The campaigns used to recruit custom audiences were run over four days in January 2025, with a daily budget of \$2.

¹⁴In August 2024, we used online sources to identify the top selling product for each company over the past month. When we could not identify clear top selling products, we identified a product recently the subject of a major ad campaign. We used some discretion to ensure the advertised product was associated with the target company – for example, although the top selling product on Amazon in July 2024 was the Stanley Cup water bottle, we selected the Amazon Fire TV stick (second most popular).

¹⁵The Facebook page IDs are: 61565619873336 (Shopping Spot), 61565078579057 (Everyday Care Essentials), 61564728493259 (Media Roundup), 61565433650990 (Health and Wellness Essentials), and 61565407492274 (Culinary Crave).



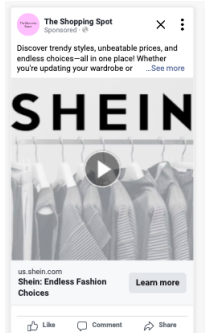
We then targeted these audiences with follow-up campaigns that ran for one week and started after the initial recruitment campaign began. Across audiences, we experimentally varied ad intensity, ad frequency, and campaign duplication. We designated 4 audiences to target with non-duplicated campaigns, and the remaining 4 to target with duplicated campaigns. Audiences assigned to the non-duplicated condition were targeted by one follow-up campaign. Audiences assigned to the duplicated condition were targeted by two identical follow-up campaigns to induce diminishing returns.

The four audiences within the non-duplicated and duplicated conditions were assigned to one of four treatments consisting of a daily campaign budget and campaign objective. These conditions were: (i) “low spend, clicks objective”, (iii) “low spend, reach objective”, (iv) “high spend, clicks objective”, and (v) “high spend, reach objective.” Low and high spend campaigns received a daily budget of \$2 and \$12 per day, respectively. Campaigns with a clicks objective were given the Meta performance goal of maximizing the number of link clicks, whereas campaigns with a reach objective were given the Meta performance goal of maximizing daily unique reach.

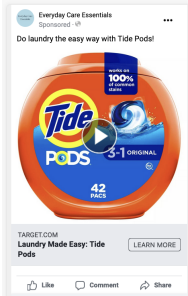
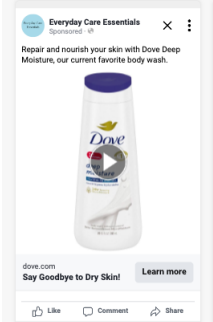
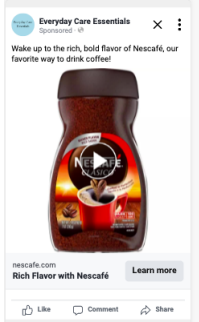
For each campaign, we measured the click-through rate, number of impressions, and campaign reach. We also gathered Meta’s estimates of the combined unique reach of campaigns assigned to the duplicated condition, which, along with data on unique reach of each individual campaign, allows us to back out the fraction of a campaign audience that is impressed by both duplicated campaigns. We estimate campaign frequency as the ratio of number of impressions and reach, and follow-up campaign reach as the fraction of the initial audience impressed by the follow-up campaign.

Table A1: Duplication Loss Experiment Creatives

(a) Shopping Ads

Company	Amazon	Temu	Shein
Product	Fire Stick	Shopping	Shopping
Ad creative			

(b) Consumer Packaged Goods Ads

Company	Proctor & Gamble	Unilever	Nestle
Product	Tide Pods	Dove	Nescafe
Ad creative			

(c) Media and Entertainment Ads

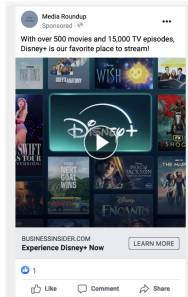
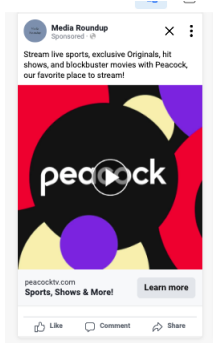

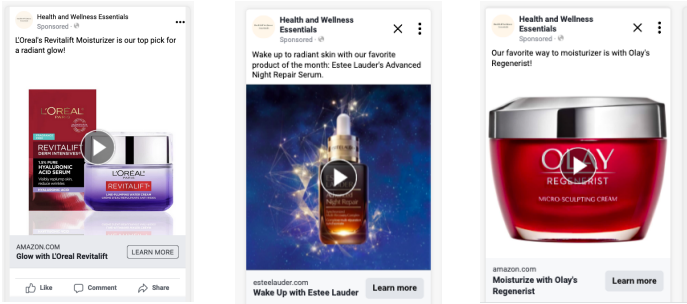
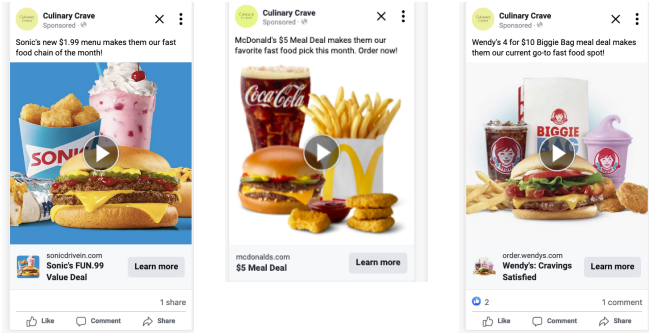
Company	Disney	NBC Universal	Amazon
Product	Disney+	Peacock	Amazon Prime
Ad creative			

Table A1: **Duplication Loss Experiment Creatives, Continued****(d) Health and Wellness Ads**

Company	L'Oreal	Estee Lauder	Olay
Product	Revitalift moisturizer	Night repair serum	Regenerist moisturizer
Ad creative			

(e) Food and Dining Services Ads

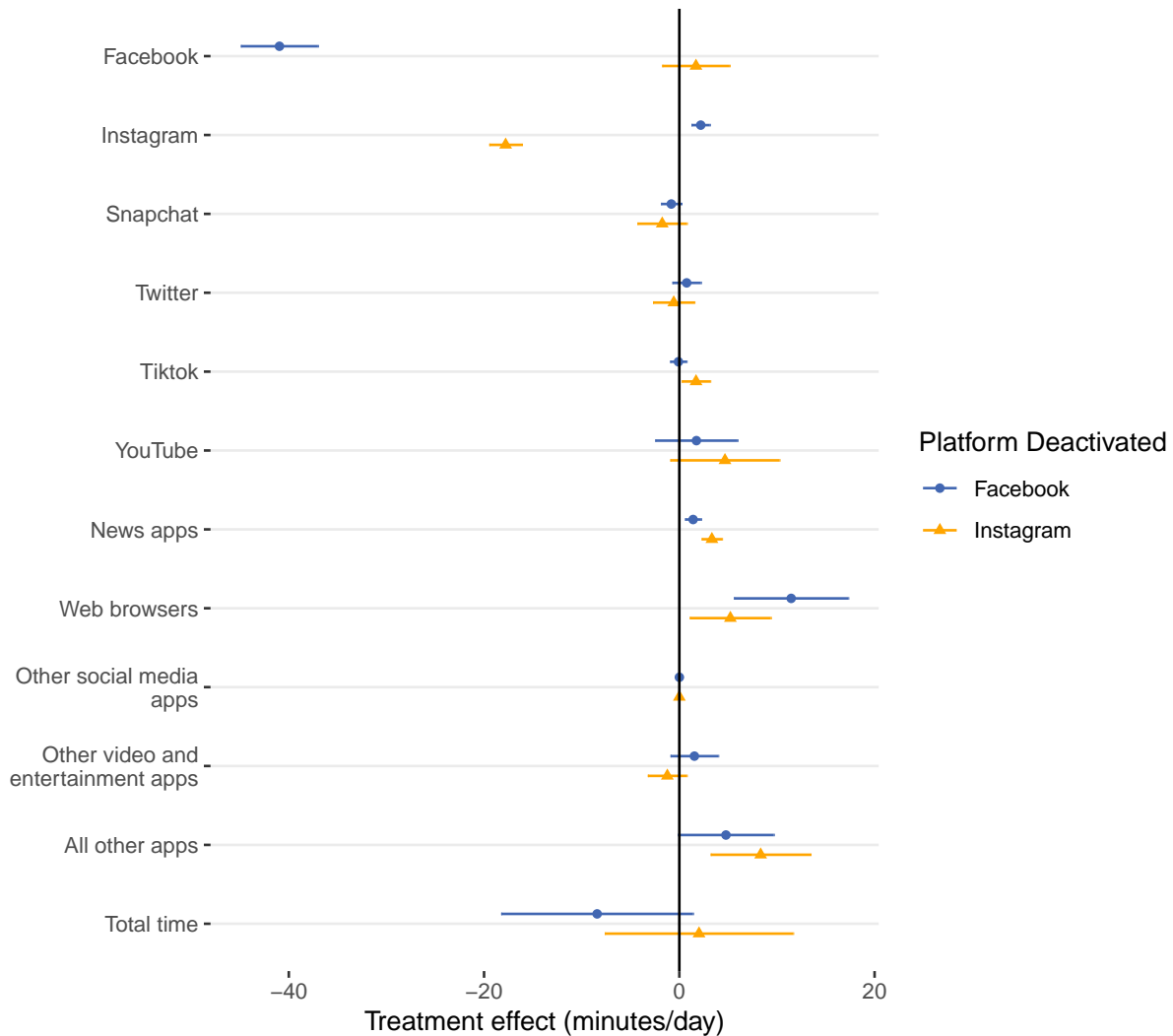
Company	Sonic	McDonald's	Wendy's
Product	Sonic's \$1.99 menu	\$5 meal deal	Biggie Bag
Ad creative			

Notes: This figure describes top companies and products used to develop ad creatives for the duplication experiment. Screen captures of ad creatives are for the video ads used to initially recruit custom audiences, as described in Section B.2, but are identical to the static ads used for follow-up campaigns.

C Model-Free Empirical Evidence Appendix

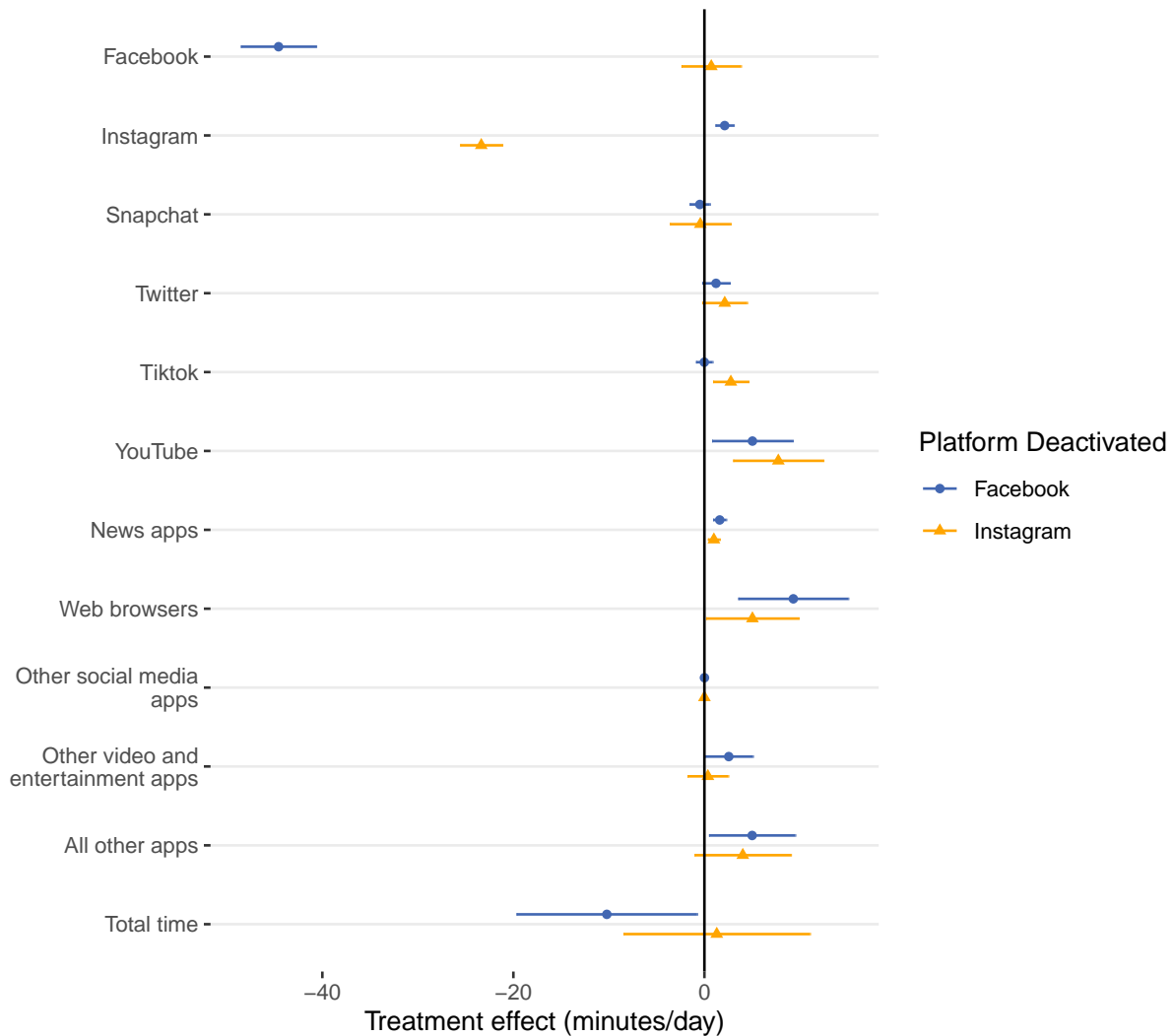
C.1 Facebook and Instagram Election Study

Figure A2: Effects of Facebook or Instagram Deactivation on App Use



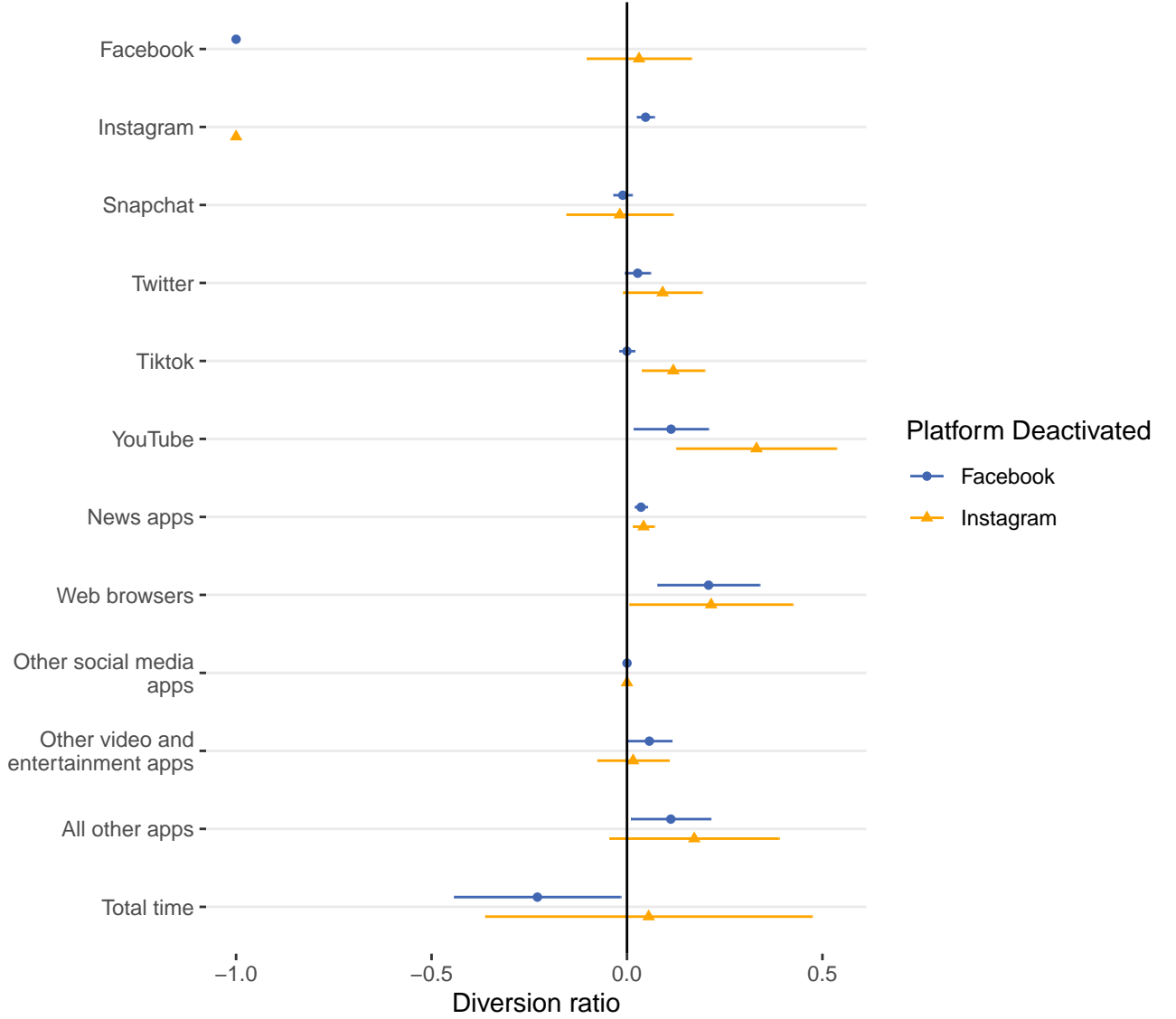
Notes: This figure presents the local average treatment effects of deactivating Facebook or Instagram on app time use in the Facebook and Instagram Election Study passive tracking samples, as estimated by [Allcott, Kiefer, and Tangkitvanich \(2025\)](#) using equation (18).

Figure A3: **Effects of Facebook or Instagram Deactivation on App Use (Primary Samples)**



Notes: This figure presents the local average treatment effects of deactivating Facebook or Instagram on app time use in the Facebook and Instagram Election Study passive tracking samples, as estimated by [Allcott, Kiefer, and Tangkitvanich \(2025\)](#) using equation (18). This figure parallels figure A2, except that it is based on estimates from the “primary sample,” which includes only people who used the focal platform for more than 15 minutes per day during the baseline period.

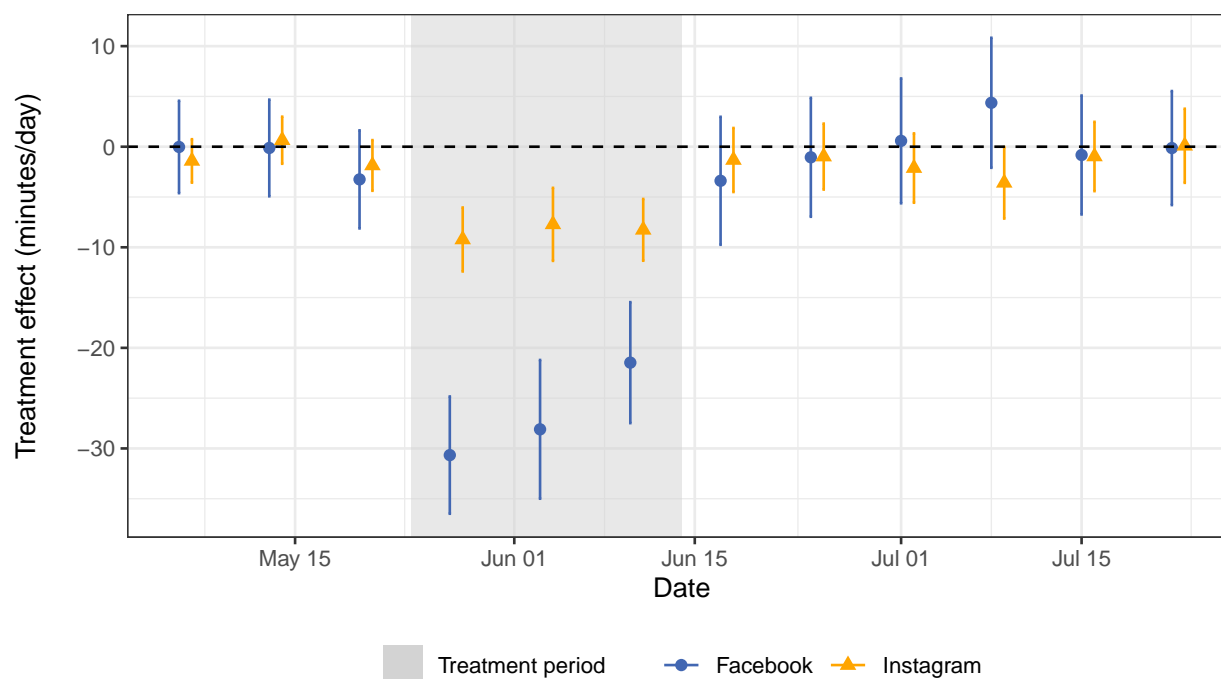
Figure A4: **Diversion Ratios from Facebook and Instagram Deactivation Experiments (Primary Samples)**



Notes: This figure presents estimated diversion ratios and 95 percent confidence intervals estimated from the Facebook and Instagram deactivation experiments in the Facebook and Instagram Election Study. This figure parallels figure 4, except that it is based on estimates from the “primary sample,” which includes only people who used the focal platform for more than 15 minutes per day during the baseline period. If τ_j^{Dj} and τ_{-j}^{Dj} , respectively, are the local average treatment effects of fully deactivating platform j on use of j and $-j$ presented in Appendix Figure A3, these diversion ratios are $\delta_{-j}^j = -\tau_{-j}^{Dj} / \tau_j^{Dj}$. We calculate confidence intervals via the Delta method, assuming zero covariance between the parameter estimates.

C.2 Digital Addiction Experiment

Figure A5: Effects of Screen Time Bonus on Facebook and Instagram Use by Week



Notes: This figure presents the effects of the Digital Addiction experiment Screen Time Bonus on Facebook and Instagram use. The grey shaded region indicates the 20-day period when the Bonus group was being paid \$2.50 per hour to reduce use of Facebook, Instagram, Twitter, Snapchat, web browsers, and YouTube.

Table A2: **Control Group Use and Effect of Screen Time Bonus in Digital Addiction Experiment**

	Facebook use (minutes/day)		Instagram use (minutes/day)	
	(1)	(2)	(3)	(4)
Constant	63.81 (2.66)	10.82 (2.01)	20.36 (1.46)	4.61 (0.91)
1(Bonus group)		-26.57 (2.95)		-8.36 (1.48)
Baseline Facebook use (minutes/day)		0.76 (0.03)		
Baseline Instagram use (minutes/day)				0.70 (0.04)
Observations	500	669	407	540
R ²		0.70		0.73

Notes: This table uses data from the Digital Addiction experiment. Columns 1 and 2 include only people with positive Facebook use before the bonus period; columns 3 and 4 include only people with positive Instagram use before the bonus period. Columns 1 and 3 limit the samples to the Control groups, presenting estimates of average Control group use during the bonus period. Columns 2 and 4 present estimates of equation (19), a regression of bonus period average Facebook or Instagram use on the Bonus group indicator, baseline focal app use, and a constant. Standard errors clustered at the user level are in parentheses. We jointly estimate these four regressions using Seemingly Unrelated Regression to recover the covariance matrix for the parameter estimates.

C.3 Ad Duplication Experiment

Table A3: **Ad Duplication Experiment Summary Statistics by Treatment Group**

	(1)	(2)	(3)	(4)
	High spend clicks	High spend reach	Low spend clicks	Low spend reach
Frequency (impressions/week)	5.27	4.61	3.08	3.30
Reach (share of initial audience)	1.04	0.840	0.376	0.548
Cost per 1,000 impressions	14.28	16.19	11.52	7.74

Notes: This table presents average frequency, reach, and CPM for follow-up campaigns in the Ad Duplication Experiment, depending on campaign objective (clicks versus reach) and budget (high versus low spend).

Table A4: **Alternative Estimates of Effects of Duplication on Ad Campaign Click-Through Rates**

	OLS			IV		
	(1)	(2)	(3)	(4)	(5)	(6)
Duplicated share	-0.265 (0.063)	-0.352 (0.080)	-0.348 (0.082)	-0.237 (0.065)	-0.321 (0.080)	-0.317 (0.082)
Frequency (impressions/week)		-0.108 (0.054)	-0.102 (0.059)		-0.096 (0.052)	-0.085 (0.059)
Reach (share of initial audience)			0.019 (0.146)			0.036 (0.147)
Product-stratum fixed-effects	Yes	Yes	Yes	Yes	Yes	Yes
Observations	176	176	176	176	176	176
Within Adjusted R ²	0.100	0.118	0.110	0.099	0.117	0.109
F-test (1st stage), Duplicated share				3,519	2,497	3,261

Notes: This table presents estimates of equation (20), measuring the change in click-through rates from fully duplicated relative to non-duplicated ad campaigns. Columns (1)–(3) are OLS estimates, while columns (4)–(6) are IV estimates instrumenting for *Duplicated share* with the duplicated treatment group indicator. Standard errors are robust and clustered by product-objective-budget-treatment group, i.e., with three observations per cluster. This table is the same as Table 3, except that here we do not winsorize CTRs at the 10th percentile or drop the three campaigns where the duplicated campaigns had less than 50 percent overlap. One campaign had zero CTR and thus undefined $\ln(CTR)$, so when we do not winsorize, we drop that observation, leaving 176 observations.

Table A5: **Effects of Duplication on Ad Campaign Click-Through Rates: Heterogeneity**

	IV		
	(1)	(2)	(3)
Duplicated share	-0.238 (0.070)	-0.279 (0.072)	-0.310 (0.068)
Duplicated share x High spend treatment	-0.045 (0.091)	-0.090 (0.091)	-0.060 (0.088)
Frequency (impressions/week)		-0.080 (0.041)	-0.158 (0.045)
Reach (share of initial audience)			-0.438 (0.103)
Product-stratum fixed-effects	Yes	Yes	Yes
Observations	174	174	174
Within Adjusted R ²	0.177	0.189	0.224
F-test (1st stage), Duplicated share	3,181	2,091	2,355
F-test (1st stage), Duplicated share x High spend treatment	3,773	2,712	3,915

Notes: This table presents estimates of equation (20), measuring the change in click-through rates from fully duplicated relative to non-duplicated ad campaigns. Columns (1)–(3) are IV estimates instrumenting for *Duplicated share* and *Duplicated share x High spend treatment* with the duplicated treatment group indicator and its interaction with an indicator for a campaign assigned to a high daily budget treatment. Standard errors are robust and clustered by product-objective-budget-treatment group, i.e., with three observations per cluster. This table is the same as Table 3, but for interaction terms.

D Structural Estimation Appendix

Throughout this appendix section, we use the notation M and N_j to refer to the number of multi-homers and users on platform j , respectively, satisfying $\mu_j = M/N_j$ and $M + \sum_j (N_j - M) = N$.

D.1 Average Time Use and FOCs as a Function of Time Use Moments

This appendix describes how to re-write equations (34) and (35) as functions of time use moments.

Define $e_{ij} := T_{ij} - T_{kj}$ as residual time use for group k , and \mathcal{E}_{sj}^2 , \mathcal{E}_{mj}^2 , and \mathcal{E}_{m12} as the variance of e_{ij} for single-homers on j , the variance of e_{ij} for multi-homers on j , and \mathcal{E}_{m12} as the covariance of e_{i1} and e_{m2} for multi-homers.

The modeled time-use weighted average of user-level ad prices p_i is given by:

$$\frac{\sum_{i \in \mathcal{U}} \boldsymbol{\alpha} \cdot \mathbf{T}_i(\boldsymbol{\alpha}^m) \cdot p_i}{\sum_{i \in \mathcal{U}} \boldsymbol{\alpha} \cdot \mathbf{T}_i(\boldsymbol{\alpha}^m)} = \frac{\sum_j \sum_{i \in \mathcal{U}_j} \alpha_j \cdot T_{ij}(\boldsymbol{\alpha}^m) \cdot p_i}{N \cdot (\alpha_1 T_1 + \alpha_2 T_2)} \quad (97)$$

where the denominator follows because residual time use averages to zero. Since in the numerator T_{ij} is multiplied by p_i , which itself depends on \mathbf{T}_i , the numerator depends on residual time use variances and covariances. Specifically:

$$\sum_{i \in \mathcal{U}_j} \alpha_j T_{ij} p_i = \sum_{i \in \mathcal{U}_j} \eta \cdot \left(1 + \eta_0 - \frac{\boldsymbol{\alpha} \cdot \mathbf{T}_i}{Am} \right) \alpha_j T_{ij} \quad (98)$$

$$\begin{aligned} &= O \cdot \eta \cdot \left[(1 + \eta_0) \alpha_j T_{mj} - \frac{\alpha_j^2 (T_{mj}^2 + \mathcal{E}_{mj}^2) + \alpha_j \alpha_{-j} (T_{mj} T_{m,-j} + \mathcal{E}_{12})}{Am} \right] + \\ &\quad (N_j - O) \cdot \eta \cdot \left[(1 + \eta_0) \alpha_j T_{sj} - \frac{\alpha_j^2 (T_{sj}^2 + \mathcal{E}_{sj}^2)}{Am} \right] \end{aligned} \quad (99)$$

The FOC on platform j is:

$$\sum_i \left[\frac{\partial p_i}{\partial \alpha_j} \cdot \boldsymbol{\alpha} \cdot \mathbf{T}_i(\boldsymbol{\alpha}) + p_i \cdot \left(T_{ij}(\boldsymbol{\alpha}) + \boldsymbol{\alpha}^m \cdot \frac{\partial \mathbf{T}_i(\boldsymbol{\alpha})}{\partial \alpha_j} \right) \right] - c_j = 0 \quad (100)$$

Rearranging slightly:

$$0 = \sum_i \frac{\partial \boldsymbol{\alpha} \cdot \mathbf{T}_i(\boldsymbol{\alpha})}{\partial \alpha_j} \cdot \left(p_i(\boldsymbol{\alpha} \cdot \mathbf{T}_i(\boldsymbol{\alpha}) + \boldsymbol{\alpha} \cdot \mathbf{T}_i(\boldsymbol{\alpha})) \cdot \frac{dp_i}{d\boldsymbol{\alpha} \cdot \mathbf{T}_i(\boldsymbol{\alpha})} \right) - c_j \quad (101)$$

$$= \sum_i \left[T_{ij}(\boldsymbol{\alpha}) + \alpha_j \frac{\partial T_{ij}(\boldsymbol{\alpha})}{\partial \alpha_j} + \alpha_{-j} \frac{\partial T_{i,-j}(\boldsymbol{\alpha})}{\partial \alpha_j} \right] \cdot \left[p_i(\boldsymbol{\alpha} \cdot \mathbf{T}_i(\boldsymbol{\alpha}) + \boldsymbol{\alpha} \cdot \mathbf{T}_i(\boldsymbol{\alpha})) \cdot \frac{dp_i}{d\boldsymbol{\alpha} \cdot \mathbf{T}_i(\boldsymbol{\alpha})} \right] - c_j \quad (102)$$

If i is a multi-homer:

$$\frac{\partial T_{ij}(\alpha)}{\partial \alpha_j} = -\frac{\gamma_j \sigma_{-j}}{\sigma_j \sigma_{-j} - \rho^2}, \quad \frac{\partial T_{i,-j}(\alpha)}{\partial \alpha_j} = -\frac{\gamma_j \rho}{\sigma_j \sigma_{-j} - \rho^2} \quad (103)$$

If i is a single-homer:

$$\frac{\partial T_{ij}}{\partial \alpha_j} = \frac{-\gamma_j}{\sigma_j}, \quad \frac{\partial T_{i,-j}}{\partial \alpha} = 0 \quad (104)$$

Moreover:

$$p_i(\alpha \cdot \mathbf{T}_i(\alpha)) + \alpha \cdot \mathbf{T}_i(\alpha) \cdot \frac{dp_i}{d\alpha \cdot \mathbf{T}_i(\alpha)} = \eta \left(1 + \eta_0 - \frac{\alpha \cdot \mathbf{T}_i(\alpha)}{Am} \right) + \quad (105)$$

$$\alpha \cdot \mathbf{T}_i(\alpha) \cdot \frac{\partial}{\partial \alpha \cdot \mathbf{T}_i(\alpha)} \left[\eta \left(1 + \eta_0 - \frac{\alpha \cdot \mathbf{T}_i(\alpha)}{Am} \right) \right] \\ = \eta \left(1 + \eta_0 - \frac{\alpha \cdot \mathbf{T}_i(\alpha)}{Am} \right) + \alpha \cdot \mathbf{T}_i(\alpha) \cdot \frac{-\eta}{Am} \quad (106)$$

$$= \eta \left(1 + \eta_0 - 2 \frac{\alpha \cdot \mathbf{T}_i(\alpha)}{Am} \right) \quad (107)$$

Substituting into equation (102) and summing across multi-homers and single-homers, we have:

$$0 = FOC_m + \sum_j FOC_{sj} - c_j$$

where:

$$FOC_m = M\eta \cdot (1 + \eta_0) \left[T_{mj} - \alpha_j \cdot \frac{\gamma_j \sigma_{-j}}{\sigma_j \sigma_{-j} - \rho^2} - \alpha_{-j} \cdot \frac{\gamma_j \rho}{\sigma_j \sigma_{-j} - \rho^2} \right] \\ - \frac{2}{Am} M\eta \left[\alpha_j \cdot (T_{mj}^2 + \mathcal{E}_{mj}^2) + \alpha_{-j} \cdot (T_{mj} T_{m,-j} + \mathcal{E}_{m12}^2) \right] \\ + \frac{2}{Am} \cdot M\eta \left[(\alpha_j^2 T_{mj} + \alpha_j \alpha_{-j} T_{m,-j}) \cdot \frac{\gamma_j \sigma_{-j}}{\sigma_j \sigma_{-j} - \rho^2} + (\alpha_{-j}^2 T_{m,-j} + \alpha_j \alpha_{-j} T_{mj}) \cdot \frac{\gamma_j \rho}{\sigma_j \sigma_{-j} - \rho^2} \right] \quad (108)$$

and

$$FOC_{sj} = (N_j - M) \cdot \eta \cdot (1 + \eta_0) \cdot \left[T_{sj} - \alpha_j \cdot \frac{\gamma_j}{\sigma_j} \right] \\ - \frac{2\eta}{Am} \cdot (N_j - M) \cdot \left[\alpha_j \cdot (T_{sj}^2 + \mathcal{E}_{sj}^2) - \alpha_j^2 T_{sj} \frac{\gamma_j}{\sigma_j} \right] \quad (109)$$

D.2 Standard Errors

The covariance matrix of Θ is

$$\Sigma = \mathbf{H}^{-1} \cdot \Omega_h \cdot \mathbf{H}^{-1}, \quad (110)$$

where H is

$$\mathbf{H} = \mathbf{R}'_{\Theta} W \mathbf{R}_{\Theta}. \quad (111)$$

Because $\sqrt{n}(\hat{\boldsymbol{\delta}} - \boldsymbol{\delta}) \rightarrow_d N(0, \boldsymbol{\Omega}_{\delta})$, according to delta method, $\boldsymbol{\Omega}_h$ is

$$\sqrt{n}h(\boldsymbol{\Theta}_D, \pi) \rightarrow_d N(0, \boldsymbol{\Omega}_h) = N(0, \mathbf{R}'_{\Theta} W \mathbf{R}_{\delta} \boldsymbol{\Omega}_{\delta} \mathbf{R}'_{\delta} W \mathbf{R}_{\Theta}) \quad (112)$$

The matrices \mathbf{R}_{Θ} and \mathbf{R}_{δ} represent the Jacobian matrices with respect to the parameters $\boldsymbol{\Theta}$ to be estimated and the empirical moments $\boldsymbol{\delta}$:

$$\mathbf{R}_{\Theta} = \frac{\partial}{\partial \boldsymbol{\Theta}_D} h(\boldsymbol{\Theta}, \boldsymbol{\delta}) \quad (113)$$

$$\mathbf{R}_{\delta} = \frac{\partial}{\partial \boldsymbol{\delta}} h(\boldsymbol{\Theta}, \boldsymbol{\delta}). \quad (114)$$

A consistent estimator of Σ is

$$\hat{\boldsymbol{\Sigma}} = \hat{\mathbf{H}}^{-1} \cdot \hat{\boldsymbol{\Omega}}_h \cdot \hat{\mathbf{H}}^{-1}, \quad (115)$$

where $\hat{\boldsymbol{\Omega}}_h$ is

$$\hat{\boldsymbol{\Omega}}_h = \hat{\mathbf{R}}'_{\Theta} \hat{W} \hat{\mathbf{R}}_{\delta} \hat{\boldsymbol{\Omega}}_{\delta} \hat{\mathbf{R}}'_{\delta} \hat{W} \hat{\mathbf{R}}_{\Theta}, \quad (116)$$

\hat{H} is

$$\hat{\mathbf{H}} = \hat{\mathbf{R}}'_{\Theta} \hat{W} \hat{\mathbf{R}}_{\Theta}, \quad (117)$$

and $\hat{\boldsymbol{\Omega}}_{\delta}$ is

$$\hat{\boldsymbol{\Omega}}_{\delta} = \begin{pmatrix} \hat{\boldsymbol{\Omega}}_F & & & & & & \\ & \hat{\boldsymbol{\Omega}}_E & & & & & \\ & & \hat{\boldsymbol{\Omega}}_D & & & & \\ & & & \hat{\boldsymbol{\Omega}}_B & & & \\ & & & & \hat{\boldsymbol{\Omega}}_G & & \\ & & & & & \hat{\boldsymbol{\Omega}}_P & \\ & & & & & & \hat{\boldsymbol{\Omega}}_L \end{pmatrix}. \quad (118)$$

In the $\hat{\boldsymbol{\Omega}}_{\delta}$ matrix just above, $\hat{\boldsymbol{\Omega}}_F$ is the sample covariance matrix for $\left(\left\{\hat{T}_{kj}^C\right\}_{kj}\right)$ from FIES; $\hat{\boldsymbol{\Omega}}_E$ is the sample covariance matrix for $\left(\left\{\hat{\mathcal{E}}_{kj}^2\right\}_{j,k}, \hat{\mathcal{E}}_{mFI}\right)$ estimated from FIES; $\hat{\boldsymbol{\Omega}}_D$ is the sample covariance matrix for $\left(\left\{\delta_{-j}^j\right\}_j\right)$ from FIES; $\hat{\boldsymbol{\Omega}}_B$ is the sample covariance matrix for $\left(\left\{\hat{T}_j^B\right\}_j, \left\{\hat{\tau}_j^C\right\}_j\right)$, estimated using Seemingly Unrelated Regressions in the DA data; $\hat{\boldsymbol{\Omega}}_G$ is the sample covariance ma-

trix of $\left(\left\{ \frac{\widehat{T_j^{Aj} - T_j^C}}{T_j^C} \right\}_j \right)$ from Brynjolfsson et al. (2024), $\hat{\Omega}_P$ is the variance of \hat{p}^m , and $\hat{\Omega}_L$ gives the variance of $\hat{\lambda}$ from the duplication loss experiment. We calculate $\hat{\Omega}_P$ without assuming time-series draws of Birch (2025) prices follow the same distribution.¹⁶

We assume no covariance across different data sources—for example, between DA, the two different FIES experiments, Brynjolfsson et al. (2024), and our duplication loss experiment. Lacking micro-data for FIES diversion ratio estimates from Allcott, Kiefer, and Tangkitvanich (2025) and Brynjolfsson et al. (2024), we also assume $Cov(\hat{\delta}_F^I, \hat{\delta}_I^F) = Cov(\frac{\widehat{\Delta_{\alpha} T_F}}{T_F^C}, \frac{\widehat{\Delta_{\alpha} T_I}}{T_I^C}) = 0$ and that there is no correlation between estimated diversion ratios, Control group time use, and residual time use variance. We expect the effect on standard errors to be small, since (i) we control for baseline time use in diversion ratio estimation, limiting potential correlation with average time use; and (ii) time use appears approximately jointly lognormal, in which case means and standard deviations are close to independent.

Since the estimator is just-identified, we use $\hat{W} = I$. We compute the Jacobians of $\mathbf{h}(\cdot)$ using MATLAB symbolic differentiation.

D.3 Sensitivity Matrix

Table A6 presents the Λ sensitivity matrix defined in Andrews, Gentzkow, and Shapiro (2017) for our estimator described in Section 4. In the notation of Appendix D.2, this is $-(\mathbf{R}'_{\Theta} \mathbf{I} \mathbf{R}_{\Theta})^{-1} \mathbf{R}'_{\Theta} \mathbf{I}$. As described in Andrews, Gentzkow, and Shapiro (2017), each entry is the local sensitivity of parameter listed in the row to a small perturbation of the moment listed in the column. We divide each row by the parameter estimate and multiply each column by the empirical moment, so that each cell can be interpreted as the local elasticity of the parameter with respect to the moment. The Facebook and Instagram FOCs are not empirical moments, so we do not multiply those two columns by anything. Each cell in those two columns can be interpreted as the local percent change in the parameter in the row with respect to the moment in the column.

Table A7 presents a version of the matrix without multiplying by the empirical moment, so that each cell can be interpreted as the local percent change in the parameter in the row with respect to the moment in the column.

¹⁶Specifically, we assume that rather than observing $2T$ observations of p_t^m , we instead observe T draws of p_{tj}^m on each platform j , where p_{tj}^m have the same expectation but do not necessarily follow the same distribution. Then $\hat{\Omega}_p = \hat{\text{Var}}(\hat{p}^m) = \hat{\text{Var}}\left(\frac{\hat{p}_F^m + \hat{p}_I^m}{2}\right) = \frac{1}{4} \left(\hat{\text{Var}}(\hat{p}_F^m) + \hat{\text{Var}}(\hat{p}_I^m) \right) + \frac{1}{2} \hat{\text{Cov}}(\hat{p}_F^m, \hat{p}_I^m)$. We estimate each of these components using time-series variance and covariance for prices on each platform.

Table A6: Sensitivity Matrix in Elasticity Units

	Single-homer average FB use	Multi-homer average FB use	Single-homer average IG use	Multi-homer average IG use	Average diversion ratio	FB bonus response	IG bonus response	Effect of FB ad removal	Effect of IG ad removal	Duplication effect on ln(CTR)	Average ad price	FB FOC	IG FOC
ξ_{sF}	0.505	-0.485	-0.005	-0.015	-0.024	-0.980	-0.020	0.083	0	0	0	0	0
ξ_{mF}	-0.405	0.392	-0.002	0.015	0.015	-0.973	-0.027	0.084	0	0	0	0	0
ξ_{sI}	-0.023	-0.005	0.791	-0.763	-0.129	-0.028	-0.972	0	0.074	0	0	0	0
ξ_{mI}	-0.056	0.056	-0.107	0.108	0.005	-0.124	-0.876	0	0.076	0	0	0	0
ρ	-0.290	-0.518	0.080	-0.271	0.958	-0.808	-0.192	0	0	0	0	0	0
σ_F	-0.450	-0.530	-0.005	-0.015	-0.023	-0.980	-0.020	0	0	0	0	0	0
σ_I	-0.023	-0.005	-0.145	-0.827	-0.128	-0.028	-0.972	0	0	0	0	0	0
γ_F	0.008	0.015	-0.006	-0.016	-0.031	-0.978	-0.022	1.00	0	0	0	0	0
γ_I	-0.023	-0.002	-0.012	0.037	-0.141	-0.025	-0.975	0	1.00	0	0	0	0
κ	0.225	0.256	0.005	0.004	0.001	-0.001	0.001	-0.050	0	-1.11	0.350	-84.5	0
η	0.590	0.702	-0.008	-0.099	0.005	-0.004	0.004	-0.221	0	0	2.28	-377	0
η_0	0.115	0.124	-0.001	-0.034	0.001	-0.001	0.001	-0.052	0	0	0.365	-88.1	0
c_I	-0.176	-1.17	0.317	1.15	0.019	0.006	-0.006	0.153	-0.142	0	0.085	262	-1349

Notes: This table presents the sensitivity matrix defined in [Andrews, Gentzkow, and Shapiro \(2017\)](#) for our estimator described in Section 4. We divide each row by the parameter estimate and multiply each column by the empirical moment, so that each cell can be interpreted as the local elasticity of the parameter in the row with respect to the moment in the column. The Facebook and Instagram FOCs are not empirical moments, so we do not multiply those two columns by anything. Each cell in those two columns can be interpreted as the local percent change in the parameter in the row with respect to the moment in the column.

Table A7: Sensitivity Matrix in Semi-Elasticity Units

	Single-homer average FB use	Multi-homer average FB use	Single-homer average IG use	Multi-homer average IG use	Average diversion ratio	FB bonus response	IG bonus response	Effect of FB ad removal	Effect of IG ad removal	Duplication effect on $\ln(\text{CTR})$	Average ad price	FB FOC	IG FOC
ξ_{sF}	0.701	-0.708	-0.020	-0.067	-0.316	2.35	0.049	0.888	0	0	0	0	0
ξ_{mF}	-0.562	0.572	-0.007	0.067	0.207	2.34	0.066	0.893	0	0	0	0	0
ξ_{sI}	-0.033	-0.007	3.01	-3.46	-1.72	0.067	2.37	0	0.788	0	0	0	0
ξ_{mI}	-0.078	0.081	-0.406	0.488	0.074	0.299	2.13	0	0.813	0	0	0	0
ρ	-0.403	-0.756	0.303	-1.23	12.8	1.94	0.467	0	0	0	0	0	0
σ_F	-0.624	-0.774	-0.020	-0.067	-0.307	2.35	0.048	0	0	0	0	0	0
σ_I	-0.033	-0.007	-0.550	-3.75	-1.71	0.068	2.37	0	0	0	0	0	0
γ_F	0.011	0.021	-0.024	-0.072	-0.416	2.35	0.054	10.6	0	0	0	0	0
γ_I	-0.032	-0.003	-0.046	0.167	-1.88	0.059	2.38	0	10.6	0	0	0	0
κ	0.313	0.374	0.017	0.018	0.016	0.002	-0.002	-0.527	0	3.32	34.4	-84.5	0
η	0.820	1.02	-0.029	-0.449	0.072	0.009	-0.009	-2.35	0	0	224	-377	0
η_0	0.159	0.181	-0.004	-0.153	0.017	0.002	-0.002	-0.549	0	0	35.9	-88.1	0
c_I	-0.245	-1.71	1.21	5.21	0.254	-0.016	0.016	1.63	-1.51	0	8.33	262	-1349

Notes: This table presents the sensitivity matrix defined in [Andrews, Gentzkow, and Shapiro \(2017\)](#) for our estimator described in Section 4. We divide each row by the parameter estimate, so that each cell can be interpreted as the local percent change in the parameter in the row with respect to the moment in the column.

D.4 Aggregate Elasticity of Ad Demand in Merged Equilibrium

We define the aggregate elasticity of ad demand on platform j as

$$\varepsilon_j^D := \frac{\partial Q_j}{\partial P_j} \cdot \frac{P_j}{Q_j}, \quad (119)$$

where

$$P_j := \sum_{i \in \mathcal{U}_j} T_{ij} \cdot p_i, \quad q_i := Am \cdot \left(1 - \frac{p_i}{\eta} + \eta_0\right), \quad Q_j := \sum_{i \in \mathcal{U}_j} T_{ij} \cdot q_i. \quad (120)$$

The aggregate elasticity of ad demand is the elasticity of time-weighted ad demand, given by Q_j , with respect to time-weighted ad price, P_j . Since

$$Q_j = \sum_{i \in \mathcal{U}_j} T_{ij} \cdot Am - \frac{Am}{\eta} T_{ij} \cdot p_i + T_{ij} \cdot Am \cdot \eta_0 \quad (121)$$

$$= \sum_{i \in \mathcal{U}_j} T_{ij} \cdot Am \cdot (1 + \eta_0) - \frac{Am}{\eta} P_j, \quad (122)$$

we have

$$\varepsilon_j^D = -\frac{Am \sum_{i \in \mathcal{U}_j} T_{ij} \cdot p_i}{\eta \sum_{i \in \mathcal{U}_j} T_{ij} \cdot q_i}. \quad (123)$$

We define the elasticity in this way to preserve intuitive properties of the elasticity in the merged equilibrium – namely, that a monopolist sets an aggregate elasticity of demand on each platform weakly above one, strictly so if either costs are positive or users are averse to ad load. To illustrate this property, note the merged equilibrium problem is:

$$\max_{\alpha} \sum_i p_i(\alpha \cdot \mathbf{T}_i(\alpha)) \cdot \alpha \cdot \mathbf{T}_i(\alpha) - c \cdot \alpha \quad (124)$$

In this notation, the FOC with respect to α_j is

$$\begin{aligned} c_j &= \sum_i \frac{\partial}{\partial \alpha_j} (\alpha \cdot \mathbf{T}_i(\alpha)) \cdot \left(p_i + \alpha \cdot \mathbf{T}_i(\alpha) \cdot \frac{\partial p_i}{\partial (\alpha \cdot \mathbf{T}_i(\alpha))} \right) \\ &= \sum_i \left(T_{ij}(\alpha) + \alpha \cdot \frac{\partial \mathbf{T}_i}{\partial \alpha_j} \right) \cdot \left(p_i - \alpha \cdot \mathbf{T}_i(\alpha) \cdot \frac{\eta}{Am} \right). \end{aligned} \quad (125)$$

Rearranging gives

$$c_j - \sum_i \alpha \cdot \frac{\partial \mathbf{T}_i}{\partial \alpha_j} \cdot \left(p_i - \alpha \cdot \mathbf{T}_i(\alpha) \cdot \frac{\eta}{Am} \right) = \sum_i T_{ij}(\alpha) \cdot \left(p_i - \alpha \cdot \mathbf{T}_i(\alpha) \cdot \frac{\eta}{Am} \right). \quad (126)$$

This illustrates the typical two-sided market intuition that the merged platform balances the elasticity of time use (LHS) with the elasticity of demand from advertisers (RHS). Define the effective cost of higher ad load as $\tilde{c}_j := c_j - \sum_i \alpha \cdot \frac{\partial \mathbf{T}_i}{\partial \alpha_j} \cdot \left(p_i - \alpha \cdot \mathbf{T}_i(\alpha) \cdot \frac{\eta}{Am} \right)$, which accounts for both

“physical” costs from higher ad load as well costs from lost infra-marginal revenue due to lower time use. Substitute $q_i = \boldsymbol{\alpha} \cdot \mathbf{T}_i(\boldsymbol{\alpha})$. Rearranging equation (126) gives

$$\frac{\tilde{c}_j - \sum_{i \in \mathcal{U}_j} T_{ij}(\boldsymbol{\alpha}) \cdot p_i}{\sum_{i \in \mathcal{U}_j} T_{ij}(\boldsymbol{\alpha}) \cdot p_i} = -\frac{\eta}{Am} \cdot \frac{\sum_{i \in \mathcal{U}_j} T_{ij}(\boldsymbol{\alpha}) \cdot q_i}{\sum_{i \in \mathcal{U}_j} T_{ij}(\boldsymbol{\alpha}) \cdot p_i} \iff \frac{P_j - \tilde{c}_j}{P_j} = -\frac{1}{\varepsilon_j^D}. \quad (127)$$

This shows that under our definition of ε_j^D , monopoly ad load follows an analogy to the inverse elasticity markup rule. This implies that $\varepsilon_j^D \leq -1$, with greater absolute value indicating higher effective costs.

To compute ε_j^D , the numerator is the same as equation (152), divided through by α_j . The denominator is

$$\begin{aligned} \sum_i \boldsymbol{\alpha} \cdot \mathbf{T}_i(\boldsymbol{\alpha}) \cdot T_{ij}(\boldsymbol{\alpha}) &= M \cdot [\alpha_j \cdot (T_{mj}^2 + \mathcal{E}_{mj}^2) + \alpha_{j'} \cdot (T_{mj}T_{mj'} + \mathcal{E}_{12})] \\ &\quad + (N_j - M) \cdot [\alpha_j \cdot (T_{sj}^2 + \mathcal{E}_{sj}^2)]. \end{aligned} \quad (128)$$

E Counterfactual Simulation Appendix

Throughout this appendix section, we use the notation M and N_j to refer to the number of multi-homers and users on platform j , respectively, satisfying $\mu_j = M/N_j$ and $M + \sum_j (N_j - M) = N$.

E.1 Setup

Social optimum. The social optimum maximizes total surplus given merged equilibrium platform revenue and advertiser surplus that coordinates to avoid wasteful duplication:

$$\alpha^o := \max_{\alpha} CS(\alpha) + AS^m(\alpha) + R^m(\alpha) - c \cdot \alpha \quad (129)$$

where $R^m(\alpha)$ is total platform revenue with no duplication, consumer surplus CS sums utility over all users:

$$CS(\alpha) := \sum_i U_i(T_i(\alpha)) \quad (130)$$

and advertiser surplus with no duplication $AS^m(\alpha)$ is obtained from integrating under the advertiser demand curve for each user and summing across users:

$$AS^m(\alpha^m) = \sum_i Am \cdot \int_{p_i(\alpha^m)}^{(\pi\omega)^{\max}} x dH(x) - R^m(\alpha^m) \quad (131)$$

where $p_i(\alpha)$ is given by Equation (4).

Let α^m represent ad load in the merged equilibrium. The difference in consumer surplus, advertiser surplus, and platform surplus between the social optimum and the merged equilibrium are $\Delta CS^o := CS(\alpha^o) - CS(\alpha^m)$, $\Delta AS^o := AS^m(\alpha^o) - AS^m(\alpha^m)$, and $\Delta PS^o := R^m(\alpha^o) - R^m(\alpha^m)$, respectively.

Counterfactual ad load – no coordination. Under Facebook-Instagram separation where platforms cannot coordinate to avoid duplication, reaction functions are (substituting in advertiser-side parameters):

$$\alpha_j^{*,s}(\alpha_j'; \Theta) := \arg \max_{\alpha_j} (1 - \zeta_j(\alpha) \cdot O'_{aj}(\alpha)) \cdot \eta \left(\sum_i \alpha_j T_{ij}(\alpha) \cdot \left(1 + \eta_0 - \frac{\alpha_j T_{ij}(\alpha)}{A} \right) \right) - c_j \cdot \alpha_j \quad j = 1, 2 \quad (132)$$

The counterfactual equilibrium is (α_1^s, α_2^s) the fixed point where $\alpha_j^{*,s}(\alpha_j^s; \cdot) = \alpha_j^s$ for $j = 1, 2$. Note that evaluating equation (132) requires calculating marginal duplication $O'_{aj}(\alpha)$, which depends on the joint distribution of $T_{iF}(\alpha), T_{iI}(\alpha)$ for multi-homers. We calculate $O'_{aj}(\alpha)$ by numerically integrating under the discretized joint distribution of $\hat{\xi}_{iF}, \hat{\xi}_{iI}$ for multi-homers for each candidate value of α in searching for the equilibrium fixed point.

The change in consumer surplus is $\Delta CS^s := CS(\alpha^s) - CS(\alpha^m)$. The change in platform surplus

is:

$$\Delta PS^s := \left(\sum_j R_j^s(\alpha^s) \right) - R^m(\alpha^m) - \mathbf{c} \cdot (\alpha^s - \alpha^m) \quad (133)$$

Advertiser surplus in the counterfactual equilibrium changes due to both endogenous changes in price, as well as inefficient duplication of ads. In Appendix E.2, we show that in the counterfactual equilibrium:

$$\sum_j AS_j^s(\alpha^s) = \overbrace{\left(\sum_j \sum_{i \in \mathcal{U}_j} Am \cdot \int_{p_{ij}(\alpha^s)}^{(\pi\omega)^{\max}} x dH(x) - R_j^s(\alpha^s) \right)}^{\text{surplus — no inefficient duplication}} - \overbrace{\zeta_j \cdot \sum_i \int_{p_i(\alpha^s)}^{(\pi\omega)^{\max}} x dH(x)}^{\text{inefficient duplication}} \quad (134)$$

where $p_i(\alpha^s) := \max_j H_i^{-1} \left(1 - \frac{\alpha_j T_{ij}(\alpha^s)}{Am} \right)$

The change in advertiser surplus is therefore $\Delta AS^s := \left(\sum_j AS_j^s(\alpha^s) \right) - AS^m(\alpha^m)$. Appendix E.2 provides explicit formulas given our parameterizations.

Counterfactual ad load – coordination. Under Facebook-Instagram separation where platforms coordinate to avoid duplication, reaction functions are:

$$\alpha_j^{*,c}(\alpha_j; \Theta) := \arg \max_{\alpha_j} \eta \left(\sum_i \alpha_j T_{ij}(\alpha) \cdot \left(1 + \eta_0 - \frac{\alpha_j T_{ij}(\alpha)}{A} \right) \right) - c_j \cdot \alpha_j \quad j = 1, 2 \quad (135)$$

The counterfactual equilibrium is (α_1^c, α_2^c) , the fixed point where $\alpha_j^{*,c}(\alpha_j^{*,c}; \cdot) = \alpha_j^{*,c}$ for $j = 1, 2$. Unlike in equation (132), the fact that platforms coordinate to avoid duplication implies the reaction function in equation (135) does not depend on marginal duplication.

Expressions for total consumer, advertiser, and platform surplus are the same as in the merged equilibrium, so this counterfactual only affects surplus by changing equilibrium ad load. In particular, the change in surplus relative to the merged equilibrium is $\Delta CS^c := CS(\alpha^c) - CS(\alpha^m)$, $\Delta AS^c := AS^m(\alpha^c) - AS^m(\alpha^m)$, and $\Delta PS^c := R^m(\alpha^c) - R^m(\alpha^m)$.

E.2 Welfare Formulas

Consumer surplus, as a function of \mathbf{T}_i , is:

$$\begin{aligned} \sum_i U_i(\mathbf{T}_i) = M \cdot & \left[\sum_j (\xi_{mj} - \gamma_j \alpha_j) T_{mj} + E[\varepsilon_{ij} e_{ij} | k = m] - \sigma_j / 2 (T_{mj}^2 + \mathcal{E}_{mj}^2) + \rho (T_{m1} T_{m2} + \mathcal{E}_{m12}) \right] \\ & + \sum_j (N_j - M) \cdot [(\xi_{sj} - \gamma_j \alpha_j) \cdot T_{sj} + E[\varepsilon_{ij} e_{ij} | k = s] - \sigma_j / 2 (T_{sj}^2 + \mathcal{E}_{sj}^2)] \end{aligned} \quad (136)$$

where ε_{ij} are residuals from ξ_{kj} . Since:

$$\varepsilon_{ij} = \sigma_j e_{ij} - \rho e_{i,-j}, \quad i \text{ multi-homer} \quad (137)$$

$$\varepsilon_{ij} = \sigma_j e_{ij}, \quad i \text{ single-homer} \quad (138)$$

we have:

$$\begin{aligned} \sum_i U_i(\mathbf{T}_i) = & M \cdot \left[\left(\sum_j (\xi_{mj} - \gamma_j \alpha_j) T_{mj} + \sigma_j \mathcal{E}_{mj}^2 - \rho \mathcal{E}_{m12} - \sigma_j/2 \cdot (T_{mj}^2 + \mathcal{E}_{mj}^2) \right) + \rho \cdot (T_{m1} T_{m2} + \mathcal{E}_{m12}) \right] \\ & + \sum_j (N_j - M) \cdot [(\xi_{sj} - \gamma_j \alpha_j) \cdot T_{sj} + \sigma_j \mathcal{E}_{sj}^2 - \sigma_j/2 (T_{sj}^2 + \mathcal{E}_{sj}^2)] \end{aligned} \quad (139)$$

Producer surplus in the merged equilibrium is:

$$\begin{aligned} PS^m(\boldsymbol{\alpha}) &= R^m(\boldsymbol{\alpha}) - \mathbf{c} \cdot \boldsymbol{\alpha} \\ &= \eta \cdot \sum_i \boldsymbol{\alpha} \cdot \mathbf{T}_i \cdot \left(1 + \eta_0 - \frac{\boldsymbol{\alpha} \cdot \mathbf{T}_i}{Am} \right) - \mathbf{c} \cdot \boldsymbol{\alpha} \end{aligned} \quad (140)$$

$$\begin{aligned} &= \eta \cdot M \cdot \left[\boldsymbol{\alpha} \cdot \mathbf{T}_m \cdot (1 + \eta_0) - \frac{(\boldsymbol{\alpha} \cdot \mathbf{T}_m)^2 + (\alpha_1^2 \mathcal{E}_{m1}^2 + \alpha_2^2 \mathcal{E}_{m2}^2 + 2 \cdot \alpha_1 \alpha_2 \mathcal{E}_{m12})}{Am} \right] \\ &+ \eta \cdot \sum_j (N_j - M) \cdot \left[\alpha_j T_{sj} \cdot (1 + \eta_0) - \frac{\alpha_j^2 (T_{sj}^2 + \mathcal{E}_{sj}^2)}{Am} \right] - \mathbf{c} \cdot \boldsymbol{\alpha} \end{aligned} \quad (141)$$

Producer surplus in the separated equilibrium is:

$$\begin{aligned} PS_j^s(\boldsymbol{\alpha}) &= R_j^s(\boldsymbol{\alpha}) - c_j \alpha_j \\ &= \eta \cdot (1 - \zeta_j O'_{aj}(\boldsymbol{\alpha})) \cdot \sum_i \alpha_j T_{ij} \cdot \left(1 + \eta_0 - \frac{\alpha_j T_{ij}}{Am} \right) - c_j \alpha_j \\ &= \eta \cdot (1 - \zeta_j O'_{aj}(\boldsymbol{\alpha})) \cdot M \cdot \left[\alpha_j T_{mj} (1 + \eta_0) - \frac{\alpha_j^2 (T_{mj}^2 + \mathcal{E}_{mj}^2)}{Am} \right] \\ &+ \eta \cdot (1 - \zeta_j O'_{aj}(\boldsymbol{\alpha})) \cdot (N_j - M) \cdot \left[\alpha_j T_{sj} (1 + \eta_0) - \frac{\alpha_j^2 (T_{sj}^2 + \mathcal{E}_{sj}^2)}{Am} \right] - c_j \alpha_j \end{aligned} \quad (142)$$

Advertiser surplus in the merged equilibrium is:

$$\begin{aligned}
AS^m(\boldsymbol{\alpha}^m) &= \sum_i Am \cdot \Pr(a \text{ impresses } i) \cdot E[\omega_{ia}\pi_a | \omega_{ia}\pi_a \geq p_i] - \boldsymbol{\alpha} \cdot \mathbf{T}_i \cdot p_i \\
&= \sum_i Am \cdot \int_{p_i(\boldsymbol{\alpha}^m)}^{(\pi\omega)^{\max}} x dH(x) - \boldsymbol{\alpha} \cdot \mathbf{T}_i \cdot p_i \\
&= \sum_i \left[\frac{Am}{2\eta} \eta^2 (1 + \eta_0)^2 - \frac{Am}{2\eta} p_i^2 - \boldsymbol{\alpha} \cdot \mathbf{T}_i \cdot p_i \right]
\end{aligned} \tag{143}$$

We implement this by calculating:

$$\begin{aligned}
\sum_i \frac{Am}{2\eta} \eta^2 (1 + \eta_0)^2 &= N \frac{Am}{2\eta} \eta^2 (1 + \eta_0)^2; \\
\sum_i p_i^2 &= \sum_i \eta^2 \cdot \left(1 + \eta_0 - \frac{\boldsymbol{\alpha} \cdot \mathbf{T}_i}{Am} \right)^2 \\
&= \eta^2 \cdot M \cdot \left[(1 + \eta_0)^2 - 2 \cdot \frac{1 + \eta_0}{Am} \cdot \boldsymbol{\alpha} \cdot \mathbf{T}_m + \frac{(\boldsymbol{\alpha} \cdot \mathbf{T}_m)^2 + (\alpha_1^2 \mathcal{E}_{m1}^2 + \alpha_2^2 \mathcal{E}_{m2}^2 + 2\alpha_1 \alpha_2 \mathcal{E}_{m12})}{(Am)^2} \right] \\
&\quad + \eta^2 \cdot \sum_j (N_j - M) \cdot \left[(1 + \eta_0)^2 - 2 \cdot \frac{1 + \eta_0}{Am} \cdot \alpha_j T_{sj} + \frac{\alpha_j^2 (T_{sj}^2 + \mathcal{E}_{sj}^2)}{(Am)^2} \right]; \\
\sum_i \boldsymbol{\alpha} \cdot \mathbf{T}_i \cdot p_i &= R^m(\boldsymbol{\alpha}).
\end{aligned} \tag{144}$$

where $R^m(\boldsymbol{\alpha})$ is given by Equation (141).

To find advertiser surplus in the separated equilibrium, first calculate advertiser surplus with no inefficient duplication, denoted by $AS'_j(\boldsymbol{\alpha})$, then subtract out lost surplus from inefficient duplication. Advertiser surplus without inefficient duplication is:

$$\begin{aligned}
AS'_j(\boldsymbol{\alpha}) &= \sum_i Am \cdot \Pr(a \text{ impresses } i \text{ on } j) \cdot E[\omega_{ia}\pi_a | \omega_{ia}\pi_a \cdot (1 - \zeta_j \cdot O'_{aj}) \geq p_{ij}] - \alpha_j \cdot T_{ij} \cdot p_i \\
&= \sum_{i \in \mathcal{U}_j} Am \cdot \int_{p_{ij}(\boldsymbol{\alpha})/(1 - \zeta_j \cdot O'_{aj})}^{(\pi\omega)^{\max}} x dH(x) - \alpha_j T_{ij} p_{ij} \\
&= \sum_{i \in \mathcal{U}_j} \left[\frac{Am}{2\eta} \eta^2 (\eta_0 + 1)^2 - \frac{Am}{2\eta} \left(\frac{p_{ij}}{1 - \zeta_j O'_{aj}} \right)^2 - \alpha_j T_{ij} p_{ij} \right]
\end{aligned} \tag{145}$$

We implement this by calculating:

$$\begin{aligned}
\sum_{i \in \mathcal{U}_j} \frac{Am}{2\eta} \eta^2 (\eta_0 + 1)^2 &= N_j \cdot \frac{Am}{2\eta} \eta^2 (\eta_0 + 1)^2 \\
\sum_{i \in \mathcal{U}_j} \frac{p_{ij}^2}{\left(1 - \zeta_j O'_{aj}\right)^2} &= \sum_{i \in \mathcal{U}_j} \eta^2 \cdot \left(1 + \eta_0 - \frac{\tilde{\alpha}_j T_{ij}}{Am}\right)^2 \\
&= \eta^2 \cdot M \cdot \left((1 + \eta_0)^2 - 2 \cdot \frac{1 + \eta_0}{Am} \alpha_j T_{mj} + \frac{\alpha_j^2 \cdot (T_{mj}^2 + \mathcal{E}_{mj}^2)}{(Am)^2} \right) \\
&\quad + \eta^2 \cdot (N_j - M) \cdot \left((1 + \eta_0)^2 - 2 \cdot \frac{1 + \eta_0}{Am} \alpha_j T_{sj} + \frac{\alpha_j^2 \cdot (T_{sj}^2 + \mathcal{E}_{sj}^2)}{(Am)^2} \right) \\
\sum_{i \in \mathcal{U}_j} \alpha_j T_{ij} p_{ij} &= R_j^s(\boldsymbol{\alpha})
\end{aligned} \tag{146}$$

where $R_j^s(\boldsymbol{\alpha})$ is given in Equation (142).

To compute advertiser surplus given inefficient duplication, first note that an advertiser buys enough clicks on j so that they will serve an ad to all i where:

$$p_{ij} \leq \pi_a \omega_{ia} (1 - \zeta_j O'_{aj}) \iff H_i^{-1} \left(1 - \frac{\alpha_j T_{ij}(\boldsymbol{\alpha})}{A} \right) \leq \pi_a \omega_{ia} \tag{147}$$

Inefficient duplication occurs if the advertiser would buy enough clicks to serve i on both j and $-j$. Define $\underline{p}_i(\boldsymbol{\alpha}) = \max_j H_i^{-1} \left(1 - \frac{\alpha_j T_{ij}(\boldsymbol{\alpha})}{A} \right)$. The surplus lost due to inefficient duplication for person i is

$$\begin{aligned}
AS^L(\boldsymbol{\alpha}) &= \sum_{i \in \mathcal{U}_m} Am \cdot \Pr(\text{a impresses } i \text{ on } j, j') \cdot E \left[\zeta_i \pi_a \omega_{ia} | \pi_a \omega_{ia} \geq \underline{p}_i(\boldsymbol{\alpha}) \right] \\
&= \sum_{i \in \mathcal{U}_m} Am \cdot \Pr \left(\pi_a \omega_{ia} \geq \underline{p}_i(\boldsymbol{\alpha}) \right) \cdot E \left[\zeta_i \cdot \pi_a \omega_{ia} | \pi_a \omega_{ia} \geq \underline{p}_i(\boldsymbol{\alpha}) \right] \\
&= \left(1 - \frac{\kappa}{\eta \cdot (1 + \eta_0)} \cdot E \left[p_i(\boldsymbol{\alpha}^m) | \pi_a \omega_{ia} \geq \underline{p}_i(\boldsymbol{\alpha}) \right] \right) \cdot \sum_{i \in \mathcal{U}_m} Am \cdot \int_{\underline{p}_i(\boldsymbol{\alpha})}^{(\pi\omega)^{\max}} x dH(x) \\
&= \frac{Am}{2\eta} \cdot \left(1 - \frac{\kappa}{\eta \cdot (1 + \eta_0)} \cdot E[p_i(\boldsymbol{\alpha}^m)] \right) \cdot \left[\eta^2 (1 + \eta_0)^2 - \left(\underline{p}_i(\boldsymbol{\alpha}) \right)^2 \right].
\end{aligned} \tag{148}$$

In this derivation, the fourth line follows from the third because $p_i^m = H_i^{-1} \left(1 - \frac{\boldsymbol{\alpha} \cdot \mathbf{T}_i(\boldsymbol{\alpha}^m)}{Am} \right)$ is uncorrelated with $\pi_a \omega_{ia}$ by Assumptions 1 and 2, so conditioning on $\pi_a \omega_{ia} \geq \underline{p}_i(\boldsymbol{\alpha})$ does not change the expectation of p_i^m .

Total inefficient duplication becomes:

$$AS^L(\boldsymbol{\alpha}) = \left(1 - \frac{\kappa}{\eta \cdot (1 + \eta_0)} \cdot E[p_i(\boldsymbol{\alpha}^m)]\right) \cdot \sum_{i \in \mathcal{U}_m} \frac{Am}{2\eta} \left[\eta^2(1 + \eta_0)^2 - \left(\max_j \eta \cdot \left(1 + \eta_0 - \frac{\alpha_j T_{ij}(\boldsymbol{\alpha})}{A}\right) \right)^2 \right] \quad (149)$$

where:

$$\frac{E[p_i(\boldsymbol{\alpha}^m)]}{\eta \cdot (1 + \eta_0)} = \frac{1}{(1 + \eta_0)} \cdot \left(1 + \eta_0 - \frac{\boldsymbol{\alpha} \cdot \mathbf{T}_m(\boldsymbol{\alpha}^m)}{Am}\right). \quad (150)$$

Given heterogeneous time use among multi-homers, it is challenging to get an analytical expression for the above. Instead, we directly integrate by following these steps (where the distribution of $\hat{\xi}_{ij}$ for $i \in \mathcal{U}_{kj}$ is denoted with Ξ_{kj} , with Ξ collecting all distributions):

1. Write a function mapping from parameters of time use heterogeneity to $p_i(\boldsymbol{\alpha}; \Xi)$.
2. Numerically integrate under this function using a grid describing the distribution of Ξ .
3. Use Equation (149) to calculate $AS^L(\boldsymbol{\alpha})$.

Finally, we calculate $\sum_j AS_j^s(\boldsymbol{\alpha}) = \left(\sum_j AS_j'(\boldsymbol{\alpha})\right) - AS^L(\boldsymbol{\alpha})$.

E.3 Miscellaneous Formulas

E.3.1 Average Price per Impression

Average price per actual impression on platform j is:

$$\bar{p}_j = \frac{\sum_{i \in \mathcal{U}_j} p_{ij} \cdot \alpha_j T_{ij}}{\sum_{i \in \mathcal{U}_j} \alpha_j T_{ij}} \quad (151)$$

The denominator is straightforward to calculate. In the merged equilibrium, the numerator is:

$$\begin{aligned} \sum_{i \in \mathcal{U}_j} p_i \alpha_j T_{ij} &= \sum_{i \in \mathcal{U}_j} \eta \cdot \left(1 + \eta_0 - \frac{\boldsymbol{\alpha} \cdot \mathbf{T}_i}{Am}\right) \alpha_j T_{ij} \\ &= M \cdot \eta \cdot \left[(1 + \eta_0) \alpha_j T_{mj} - \frac{\alpha_j^2 (T_{mj}^2 + \mathcal{E}_{mj}^2) + \alpha_j \alpha_{-j} (T_{mj} T_{m,-j} + \mathcal{E}_{12})}{Am} \right] \\ &\quad + (N_j - M) \cdot \eta \cdot \left[(1 + \eta_0) \alpha_j T_{sj} - \frac{\alpha_j^2 (T_{sj}^2 + \mathcal{E}_{sj}^2)}{Am} \right] \end{aligned} \quad (152)$$

In the separated equilibrium, the numerator is:

$$\begin{aligned}
\sum_{i \in \mathcal{U}_j} p_{ij} \alpha_j T_{ij} &= (1 - \zeta O'_{aj}) \cdot \eta \cdot \sum_{i \in \mathcal{U}_j} \left(1 + \eta_0 - \frac{\alpha_j T_{ij}}{Am} \right) \alpha_j T_{ij} \\
&= (1 - \zeta O'_{aj}) \cdot \eta \cdot M \cdot \left((1 + \eta_0) \alpha_j T_{mj} - \frac{\alpha_j^2 (T_{mj}^2 + \mathcal{E}_{mj}^2)}{Am} \right) \\
&\quad + (1 - \zeta O'_{aj}) \cdot \eta \cdot (N_j - M) \cdot \left((1 + \eta_0) \alpha_j T_{sj} - \frac{\alpha_j^2 (T_{sj}^2 + \mathcal{E}_{sj}^2)}{Am} \right) \quad (153)
\end{aligned}$$

E.3.2 Formula for $\zeta_j(\alpha)$

By definition:

$$\zeta_j(\alpha) = 1 - \frac{\kappa}{\eta \cdot (1 + \eta_0)} \frac{E_i [T_{ij}(\alpha) \cdot p_i^m | i \in \mathcal{U}_m]}{T_{mj}(\alpha)} \quad (154)$$

Since:

$$E_i [T_{ij}(\alpha) \cdot p_i^m | i \in \mathcal{U}_m] = M^{-1} \sum_{i \in \mathcal{U}_m} T_{ij}(\alpha) \cdot p_i^m \quad (155)$$

$$M^{-1} \sum_{i \in \mathcal{U}_m} \left[\eta \cdot \left(1 + \eta_0 - \frac{\alpha^m \cdot T_i(\alpha^m)}{Am} \right) \cdot T_{ij}(\alpha) \right] \quad (156)$$

$$= \eta \cdot \left[(1 + \eta_0) \cdot T_{mj}(\alpha) - \frac{\alpha_j^m (T_{mj}(\alpha^m) T_{mj}(\alpha) + \mathcal{E}_{mj}^2) + \alpha_{-j}^m (T_{m,-j}(\alpha^m) T_{mj}(\alpha) + \mathcal{E}_{12})}{Am} \right] \quad (157)$$

the formula for $\zeta_j(\alpha)$ is

$$\zeta_j(\alpha) = 1 - \frac{\kappa}{1 + \eta_0} \cdot T_{mj}^{-1}(\alpha) \cdot \left((1 + \eta_0) \cdot T_{mj}(\alpha) - \frac{\alpha_j^m (T_{mj}(\alpha^m) T_{mj}(\alpha) + \mathcal{E}_{mj}^2) + \alpha_{-j}^m (T_{m,-j}(\alpha^m) T_{mj}(\alpha) + \mathcal{E}_{12})}{Am} \right) \quad (158)$$

E.4 Overlap Sensitivity Analysis Implementation Details

In this appendix, we describe how we convert users between being single-homers and multi-homers for the purpose of constructing Figure 9.

We first describe how we convert multi-homers into single-homers. Setting $n_i = 0$, the original utility functions for multi-homers are:

$$U_i(\mathbf{T}_i, n_i; \alpha) = \sum_j [(\xi_{ij} - \gamma_j \alpha_j) T_{ij} - \sigma_j T_{ij}^2 / 2] + \rho T_{i1} T_{i2}. \quad (159)$$

To increase the share of single-homers, we separate multi-homers into two single-homers, with one on each platform, such that T_{ij} and total U_i are unchanged at baseline ad load. The utility functions for new single-homers i on j who were previously multi-homers is:

$$U_{ij} = \left(\xi_{ij} + \rho \hat{T}_{i,-j}^m - \gamma_j \alpha_j \right) T_{ij} - \sigma_j T_{ij}^2 / 2 - \rho \hat{T}_{i1}^m \hat{T}_{i2}^m / 2 \quad (160)$$

where \hat{T}_{ij}^m is person i 's time use observed in the merged equilibrium. Differentiating with respect to T_{ij} and solving delivers:

$$T_{ij}(\alpha) = \frac{\xi_{ij} - \gamma_j \alpha_j + \rho \hat{T}_{i,-j}^m}{\sigma_j} \quad (161)$$

When evaluated at the merged equilibrium α^m , equation (161) aligns with equation (22) for time use on platform j for single-homers who were formerly multi-homers. This implies the sum of merged equilibrium average time use \mathbf{T}_m for the new single-homers equals \mathbf{T}_m for the original multi-homer. Utility also aligns because the combined users have total utility in the merged equilibrium equal to:

$$\sum_j U_{ij} = \sum_j \left(\xi_{ij} + \rho \hat{T}_{i,-j}^m - \gamma_j \alpha_j^m \right) \hat{T}_{ij}^m - \sigma_j \left(\hat{T}_{ij}^m \right)^2 / 2 - \rho \hat{T}_{i1}^m \hat{T}_{i2}^m \quad (162)$$

$$= \sum_j \left(\xi_{ij} - \gamma_j \alpha_j^m \right) \hat{T}_{ij}^m - \sigma_j \left(\hat{T}_{ij}^m \right)^2 / 2 + \rho \hat{T}_{i1}^m \hat{T}_{i2}^m = U_i(\hat{\mathbf{T}}^m, n_i; \alpha^m) \quad (163)$$

We now describe how we convert single-homers into multi-homers. Again setting $n_i = 0$, the original utility functions for single-homers can be written as

$$U_{ij}(T_{ij}, n_i; \alpha_j) = (\xi_{ij} - \gamma_j \alpha_j) T_{ij} - \sigma_j T_{ij}^2 / 2. \quad (164)$$

To increase the share of multi-homers, we combine two randomly-drawn single-homers into one multi-homer, such that T_{ij} and total U_i are again unchanged at baseline ad load. The new utility functions for multi-homers are

$$U_i = \sum_j \left[\left(\xi_{ij} - \rho \hat{T}_{i,-j}^m - \gamma_j \alpha_j \right) T_{ij} - \sigma_j T_{ij}^2 / 2 \right] + \rho T_{i1} T_{i2} + \rho \hat{T}_{i1}^m \hat{T}_{i2}^m. \quad (165)$$

Differentiating with respect to T_{ij} yields:

$$T_{ij}(\alpha) = \frac{\xi_{ij} - \gamma_j \alpha_j + \rho \left(T_{i,-j} - \hat{T}_{i,-j}^m \right)}{\sigma_j} \quad (166)$$

Equation (166) aligns with equation (22) for time use on platform j for multi-homers who were formerly single-homers when evaluated at merged equilibrium α^m . Utility also aligns because

combined users have total utility in the merged equilibrium equal to:

$$U_i = \sum_j \left(\xi_{ij} - \rho \hat{T}_{i,-j}^m - \gamma_j \alpha_j^m \right) \hat{T}_{ij}^m - \sigma_j \left(\hat{T}_{ij}^m \right)^2 / 2 + \rho \hat{T}_{i1}^m \hat{T}_{i2}^m + \rho \hat{T}_{i1}^m \hat{T}_{i2}^m \quad (167)$$

$$= \sum_j \left(\xi_{ij} - \gamma_j \alpha_j^m \right) \hat{T}_{ij}^m - \sigma_j \left(\hat{T}_{ij}^m \right)^2 / 2 = U_{i1}(\hat{\mathbf{T}}^m, n_i; \boldsymbol{\alpha}^m) + U_{i2}(\hat{\mathbf{T}}^m, n_i; \boldsymbol{\alpha}^m) \quad (168)$$

where U_{ij} here represents the utility of the single-homing user on platform j combined with another user on $-j$ to create multi-homer i .

Equations (160) and (165) introduce three new user types: single-homers on Facebook converted from multi-homers, single-homers on Instagram converted from multi-homers, and multi-homers converted from one single-homer on Facebook and one single-homer on Instagram. The modeled averages of time on platform j for these groups are, respectively:

$$T_{s'j} = \frac{\xi_{mj} + \rho \hat{T}_{m,-j}^m - \gamma_j \alpha_j}{\sigma_j} \quad (169)$$

$$T_{m'j} = \frac{\xi_{sj} - \rho \hat{T}_{s,-j}^m - \gamma_j \alpha_j + \rho T_{m',-j}}{\sigma_j} = \frac{\left(\xi_{sj} - \rho \hat{T}_{s,-j}^m - \gamma_j \alpha_j \right) + \left(\xi_{s,-j} - \rho \hat{T}_{sj}^m - \gamma_{-j} \alpha_{-j} \right) \cdot \rho / \sigma_{-j}}{\sigma_j - \rho^2 / \sigma_{-j}} \quad (170)$$

where we use the subscript $s'j$ to denote single-homers on j converted from multi-homers, and the subscript $m'j$ to denote multi-homers on j converted from one single-homer on Facebook and one single-homer on Instagram. Average time use for single-homers, multi-homers, and all users is given by:

$$T_{Sj} = (1 - \mu'_{sj})T_{sj} + \mu'_{sj}T_{s'j} \quad (171)$$

$$T_{Mj} = (1 - \mu'_{mj})T_{mj} + \mu'_{mj}T_{m'j} \quad (172)$$

$$T_j = (1 - \mu_j)T_{Sj} + \mu_j T_{Mj} \quad (173)$$

where μ'_{sj} is the share of single-homers on j converted from multi-homers; μ'_{mj} is the share of multi-homers on j converted from single-homers; and μ_j is the total platform share of multi-homers.

When we change the overlap share to be below overlap in the merged equilibrium, we convert multi-homers into single-homers. The new number of multi-homers and single-homers becomes $M' = M - \Delta$, $N'_j = N_j + \Delta$. The overlap share becomes $\mu_j = M'/N'_j$, the share of single-homers converted from multi-homers becomes $\mu'_{sj} = \Delta/(N'_n - M')$, and the share of multi-homers converted from single-homers is $\mu'_{mj} = 0$.

When we change the overlap share to be above overlap in the merged equilibrium, we convert single-homers into multi-homers. The new number of multi-homers and single-homers becomes $M' = M + \Delta$, $N'_j = N_j - \Delta$. The overlap share becomes $\mu_j = M'/N'_j$, the share of single-homers converted from multi-homers is $\mu'_{sj} = 0$, and the share of single-homers converted from multi-homers

is $\mu'_{mj} = \Delta/M'$.

Finally, equations (161) and (166) show that conversions affect the distribution of ξ_{ij} for multi-homers and single-homers, meaning conversions also affect the variance of time use residuals on each platform. Letting i' denote users subject to conversions, we have, for $K \in S, M$:

$$\text{Var}(T_{iKj}) = \text{Var}((1 - \mu'_{kj})T_{ikj} + \mu'_{kj}T_{ik'j}) \quad (174)$$

$$= (1 - \mu'_{kj})^2 \cdot \text{Var}(T_{ikj}) + (\mu'_{kj})^2 \cdot \text{Var}(T_{ik'j}) \quad (175)$$

Hence:

$$\text{Var}(T_{iSj}) = (1 - \mu'_{sj})^2 \cdot \mathcal{E}_{sj}^2 + (\mu'_{sj})^2 \cdot \mathcal{E}_{mj}^2 \quad (176)$$

$$\text{Var}(T_{iMj}) = (1 - \mu'_{mj})^2 \cdot \mathcal{E}_{mj}^2 + (\mu'_{mj})^2 \cdot \mathcal{E}_{sj}^2 \quad (177)$$

Since conversions impact the marginal distribution of residual time use, they also potentially impact the joint distribution of residual time use. For parsimony, we leave the joint distribution of residual time use, and the joint distribution used to calculate the marginal overlap function, fixed as we vary the multi-homer share.

E.5 Structural Estimates and Counterfactuals with Alternative Parameter Values

E.5.1 Alternative Time Use

In this appendix, we present parameter estimates and counterfactual simulations under alternative assumptions for user time on platform. [eMarketer \(2025\)](#) estimates that the average Facebook user spends 33 minutes per day on Facebook, while the average Instagram user spends 29 minutes on Instagram. We rescale the FIES time use moments \hat{T}_{kj}^C and standard errors to match the [eMarketer \(2025\)](#) estimates. This decreases the Facebook time use moments and increases the Instagram time use moments. Lacking alternative data on the distributions around these time use means, we maintain our baseline estimates of the distributions of e_{ij} and ξ_{ij} .

Table [A8](#) summarizes the updated empirical moments. Tables [A9](#) and [A10](#) present the updated parameter estimates and counterfactual simulation results.

Table A8: **Alternative Time Use Specification: Changes to Empirical Moments**

Parameter	Description	Primary Value	Alternative value	Alternative source
\hat{T}_{sF}^C	Single-homer average FB use (hours/day)	0.720	0.565	FIES, eMarketer (2025)
\hat{T}_{mF}^C	Multi-homer average FB use (hours/day)	0.685	0.538	FIES, eMarketer (2025)
\hat{T}_{sI}^C	Single-homer average IG use (hours/day)	0.263	0.564	FIES, eMarketer (2025)
\hat{T}_{mI}^C	Multi-homer average IG use (hours/day)	0.220	0.473	FIES, eMarketer (2025)

Notes: This table summarizes the updated empirical moments in this alternative specification. Standard errors are similarly rescaled relative to the values in Table 5. “FIES” refers to the Facebook and Instagram Election Study.

Table A9: **Alternative Time Use Specification: Parameter Estimates**

Parameter	Description	Units	Estimate	SE
ξ_{sF}	FB single-homer demand intercept	\$/hour	6.4	0.76
ξ_{mF}	FB multi-homer demand intercept	\$/hour	6.7	0.73
ξ_{sI}	IG single-homer demand intercept	\$/hour	7.0	1.29
ξ_{mI}	IG multi-homer demand intercept	\$/hour	6.6	1.02
ρ	Platform substitution	\$/hour ²	-1.14	0.72
σ_F	FB curvature	\$/hour ²	10.4	1.20
σ_I	IG curvature	\$/hour ²	11.5	2.00
γ_F	FB ad load disutility	\$/ad	0.0076	0.0018
γ_I	IG ad load disutility	\$/ad	0.0090	0.0024
κ	Return to duplication		0.537	0.10
η	Advertiser demand slope	$\frac{\text{share of } A}{\$/\text{impression}}$	0.066	0.01
η_0	Advertiser demand intercept	share of A	-0.737	0.05
c_I	IG ad load cost	\$/ (ad/hour)	0.0020	0.0003

Notes: This table presents the parameter estimates from the estimation procedure described in Section 4 using the updated time use moments from Table A8.

Table A10: Alternative Time Use Specification: Counterfactual Simulations

	Baseline	Social optimum		FB-IG separation coordinated ads		FB-IG separation uncoordinated ads	
	(1)	(2)	(3)	(4)	(5)	(6)	(7)
	Δ from baseline	Δ from baseline	% Δ from baseline	Δ from baseline	% Δ from baseline	Δ from baseline	% Δ from baseline
Panel (a): Market Outcomes							
FB ad load (ads/hour)	69.9	11.3	16.2%	2.8	4.0%	11.8	16.9%
IG ad load (ads/hour)	57.6	-55.4	-96.1%	16.3	28.3%	24.0	41.6%
Average time on FB (hours/day)	0.55	-0.01	-2.0%	-0.00	-0.2%	-0.01	-1.4%
Average time on IG (hours/day)	0.48	0.04	9.2%	-0.01	-2.6%	-0.02	-3.8%
Average FB ad price (\$/1000 impressions)	9.1	-0.27	-3.0%	-0.54	-5.9%	-1.7	-19.2%
Average IG ad price (\$/1000 impressions)	12.6	2.1	16.7%	-0.75	-6.0%	-3.0	-23.8%
Panel (b): Surplus							
Consumer surplus (\$/user-year)	1,911	33.9	1.8%	-17.4	-0.9%	-35.8	-1.9%
Advertiser surplus (\$/user-year)	67.4	-4.1	-6.1%	12.0	17.8%	21.6	32.1%
if no duplication loss (\$/user-year)	67.4	-4.1	-6.1%	12.0	17.8%	66.6	98.9%
duplication loss (\$/user-year)	0.00	0.00	0.0%	0.00	0.0%	45.0	66.9%
Advertiser + consumer surplus (\$/user-year)	1,978	29.9	1.5%	-5.4	-0.3%	-14.2	-0.7%
Platform surplus: FB (\$/user-year)	119	12.4	10.4%	-2.8	-2.4%	-8.6	-7.2%
Platform surplus: IG (\$/user-year)	32.3	-30.3	-93.6%	1.0	3.2%	-15.5	-48.1%
Total surplus (\$/user-year)	2,130	12.0	0.6%	-7.2	-0.3%	-38.3	-1.8%

Notes: This table presents the counterfactual simulation results using the updated parameter estimates from Table A9. Column (1) presents the merged equilibrium, which we label as the “baseline.” Columns (2) and (3) present the social optimum, columns (4) and (5) present the separated equilibrium with uncoordinated ad delivery, and columns (6) and (7) present the separated equilibrium with coordinated ad delivery.

E.5.2 Alternative Ad Disutility, with Network Effects Interpretation

In this appendix, we present alternative parameter estimates and counterfactual results under an alternative estimation strategy. Instead of identifying Instagram users' ad disutility γ_I using the Instagram ad response moment h_I^A in equation (32), we instead drop h_I^A , impose $c_I = 0$, and identify γ_I using the Instagram FOC. This identifies γ_I as an implicit "cost" of higher ad load from reduced time use. Unlike the ad response moment, which only captures the effect of changes in α_j from the Brynjolfsson et al. (2024) individual-level randomized ad holdout experiment, γ_I identified from the Instagram FOC could capture the merged platform's belief about the effect on time use due to a change in α_j for *all* platform users, inclusive of any network effects.

Table A11 presents alternative parameter estimates. The FOC-implied Instagram ad load disutility $\hat{\gamma}_I$ is about nine times higher than in the primary specification. Instagram utility intercepts are higher than at baseline, and other parameter estimates are essentially unchanged.

These results imply that given the empirical moments and model structure, the merged platform would set Instagram ad load higher than is observed in the data if users had the low aversion to ad load implied by the Brynjolfsson et al. (2024) experiment. That Instagram sets ad load lower is consistent with user network effects.

To quantify implications for network effects, we interpret the reduced-form $\hat{\gamma}_I$ through the lens of an alternative utility specification with explicit network effects. This exercise holds fixed other parameters at their estimated values, although some estimates might change if estimated using the form for utility specified below. Given this caveat, we view these results as illustrative.

Suppose utility were:

$$U_i(\mathbf{T}_i, n_i; \boldsymbol{\alpha}) = \sum_j [(\xi_{ij} + \omega_j T_j - \gamma_j \alpha_j) T_{ij} - \sigma_j T_{ij}^2 / 2] + \rho T_{i1} T_{i2} + n_i, \quad (178)$$

where ω_j is the "network effect": the effect on individual utility of other users' time on platform. Maximizing utility gives

$$T_{sj} = \frac{\xi_{sj} + \omega_j T_j - \gamma_j \alpha_j}{\sigma_j} \quad (179)$$

$$T_{mj} = \frac{(\xi_{mj} + \omega_j T_j - \gamma_j \alpha_j) + (\xi_{m,-j} + \omega_{-j} T_{-j} - \gamma_{-j} \alpha_{-j}) \cdot \rho / \sigma_{-j}}{\sigma_j - \rho^2 / \sigma_{-j}} \quad (180)$$

$$T_j = (1 - \mu_j) T_{sj} + \mu_j T_{mj}. \quad (181)$$

Closed forms for these expressions require solving for T_j . Assuming that $\omega_F = 0$, T_j is given by

$$T_j = \frac{(1 - \mu_j)}{S_j(\omega_j)} \cdot \frac{\xi_{sj} - \gamma_j \alpha_j}{\sigma_j} + \frac{\mu_j}{S_j(\omega_j)} \cdot \frac{(\xi_{mj} - \gamma_j \alpha_j) + (\xi_{m,-j} - \gamma_{-j} \alpha_{-j}) \cdot \rho / \sigma_{-j}}{\sigma_j - \rho^2 / \sigma_{-j}}, \quad (182)$$

where

$$S_j(\omega_j) := \left(1 - \left[\frac{(1 - \mu_j)}{\sigma_j} + \frac{\mu_j}{\sigma_j - \rho^2/\sigma_{-j}} \right] \omega_j \right). \quad (183)$$

In the reduced-form specification we estimate in this subsection, we have:

$$\frac{\partial T_I}{\partial \alpha_I} = -\hat{\gamma}_I \cdot \left(\frac{1 - \mu_I}{\sigma_I} + \frac{\mu_I}{\sigma_I - \rho^2/\sigma_F} \right) \quad (184)$$

In the network effects model, we would have:

$$\frac{\partial T_I}{\partial \alpha_I} = -\gamma_I \cdot \frac{1 - S_I(\omega_I)}{S_I(\omega_I)} \quad (185)$$

To interpret our estimate of $\hat{\gamma}_I$ through the lens of a network effects model, we solve for ω_I so that:

$$-\hat{\gamma}_I \cdot \left(\frac{1 - \mu_I}{\sigma_I} + \frac{\mu_I}{\sigma_I - \rho^2/\sigma_F} \right) = -\hat{\gamma}_{I0} \cdot \frac{1 - S_I(\omega_I)}{S_I(\omega_I)} \quad (186)$$

where $\hat{\gamma}_{I0}$ is what we would estimate for γ_I in a full network effects model. We approximate this with our estimate for γ_I from the baseline model identified using the [Brynjolfsson et al. \(2024\)](#) experiment. We have

$$\omega_I = \frac{\hat{\gamma}_I}{\hat{\gamma}_{I0} + \hat{\gamma}_I \cdot \left(\frac{1 - \mu_I}{\sigma_I} + \frac{\mu_I}{\sigma_I - \rho^2/\sigma_F} \right)}. \quad (187)$$

Applying $\hat{\gamma}_I$ and estimates of σ_j, ρ from Table [A11](#)¹⁷ with an estimate of $\hat{\gamma}_{I0}$ from Table [6](#) implies $\omega_I = 6.01$ \$/hour². Thus, our estimates imply that average Instagram time use of 0.225 hours/day increases the demand intercept by 1.35 \$/hour. This is about one-fifth of the estimated demand intercepts, and means the estimate γ_I from the FOC is consistent with reasonably large network effects.

Table [A12](#) presents counterfactual results. There are three qualitative differences relative to the baseline counterfactual results, all driven by the higher estimated ad aversion on Instagram. First, the social optimum is a corner solution with zero ads on Instagram. Second, Instagram competes harder for users in the separated equilibrium and hence lowers ad load. Third, Instagram surplus, and hence total surplus, is much more sensitive to ad load changes. Total surplus increases by about 9.5 percent in the social optimum relative to the merged equilibrium. Instagram's competition for users, and the resulting decrease in Instagram ad load, raises total surplus in the separated equilibrium with coordinated ad delivery, relative to the merged equilibrium. However, the welfare loss from inefficient duplication reduces total surplus in the separated equilibrium with uncoordinated ads, relative to the merged equilibrium.

¹⁷In principle, estimates of σ_j and ρ may change in a fully-estimated network effects model. In practice, as shown in Table [A6](#), σ_j and ρ are only sensitive to h^C, h^D , and h^B , all of which would not change in the fully-estimated network effects model.

Table A11: **Alternative Ad Disutility Specification: Parameter Estimates**

Parameter	Description	Units	Estimate	SE
ξ_{sF}	FB single-homer demand intercept	\$/hour	6.6	0.74
ξ_{mF}	FB multi-homer demand intercept	\$/hour	6.5	0.72
ξ_{sI}	IG single-homer demand intercept	\$/hour	10.3	2.08
ξ_{mI}	IG multi-homer demand intercept	\$/hour	10.1	1.66
ρ	Platform substitution	\$/hour ²	-1.18	0.77
σ_F	FB curvature	\$/hour ²	8.4	0.93
σ_I	IG curvature	\$/hour ²	23.8	4.53
γ_F	FB ad load disutility	\$/ad	0.0078	0.0018
γ_I	IG ad load disutility	\$/ad	0.070	0.01
κ	Return to duplication		0.557	0.10
η	Advertiser demand slope	$\frac{\text{share of } A}{\$/\text{impression}}$	0.080	0.01
η_0	Advertiser demand intercept	share of A	-0.765	0.03

Notes: This table presents the parameter estimates using the alternative estimation procedure described in Section [E.5.2](#).

Table A12: Alternative Ad Disutility Specification: Counterfactual Simulations

Baseline	Social optimum		FB-IG separation coordinated ads		FB-IG separation uncoordinated ads		
	(1)	(2)	(3)	(4)	(5)	(6)	(7)
		Δ from baseline	$\% \Delta$ from baseline	Δ from baseline	$\% \Delta$ from baseline	Δ from baseline	$\% \Delta$ from baseline
Panel (a): Market Outcomes							
FB ad load (ads/hour)	69.9	10.1	14.4%	2.0	2.8%	6.1	8.7%
IG ad load (ads/hour)	57.6	-57.6	-100.0%	-0.90	-1.6%	1.2	2.0%
Average time on FB (hours/day)	0.70	-0.02	-3.3%	-0.00	-0.3%	-0.01	-0.8%
Average time on IG (hours/day)	0.23	0.17	75.9%	0.00	1.2%	-0.00	-1.4%
Average FB ad price (\$/1000 impressions)	9.8	-0.67	-6.9%	-0.23	-2.4%	-0.72	-7.4%
Average IG ad price (\$/1000 impressions)	12.5	-	-	-0.03	-0.3%	-4.2	-33.7%
Panel (b): Surplus							
Consumer surplus (\$/user-year)	1,839	226	12.3%	-0.90	-0.0%	-14.5	-0.8%
Advertiser surplus (\$/user-year)	82.7	5.6	6.8%	3.8	4.7%	6.8	8.2%
if no duplication loss (\$/user-year)	82.7	5.6	6.8%	3.8	4.7%	33.7	40.8%
duplication loss (\$/user-year)	0.00	0.00	0.0%	0.00	0.0%	26.9	32.5%
Advertiser + consumer surplus (\$/user-year)	1,922	232	12.1%	2.9	0.2%	-7.6	-0.4%
Platform surplus: FB (\$/user-year)	163	5.0	3.1%	0.10	0.1%	-1.1	-0.7%
Platform surplus: IG (\$/user-year)	34.8	-34.8	-100.0%	-0.21	-0.6%	-11.7	-33.7%
Total surplus (\$/user-year)	2,120	202	9.5%	2.8	0.1%	-20.5	-1.0%

Notes: This table presents the counterfactual simulation results using the alternative estimation procedure described in Section E.5.2. Column (1) presents the merged equilibrium, which we label as the “baseline.” Columns (2) and (3) present the social optimum, columns (4) and (5) present the separated equilibrium with uncoordinated ad delivery, and columns (6) and (7) present the separated equilibrium with coordinated ad delivery.

